University of Alberta

Patterning the zebrafish visual system requires the actions of Pbx transcription factors, and a downstream growth factor, Gdf6a

by

Curtis Robert French

A thesis submitted to the Faculty of Graduate Studies and Research
in partial fulfillment of the requirements for the degree of

Doctor of Philosophy
in
Molecular Biology and Genetics

Department of Biological Sciences

Fall 2010
Edmonton, Alberta

Examining Committee

Dr. Andrew Waskiewicz, Department of Biological Sciences, University of Alberta (supervisor)

Dr. Ted Allison, Department of Biological Sciences, University of Alberta

Dr. Shelagh Campbell, Department of Biological Sciences, University of Alberta

Dr. Ordan Lehmann, Department of Ophthalmology, University of Aberta

Dr. James Fadool, Department of Biological Sciences, Florida State University

Abstract

The zebrafish visual system relies on positional information in the retina and optic tectum, so that the spatial fidelity of light signals that enter the eye are preserved for visual processing. This positional information is essential for ordered topographic mapping of retinal ganglion cell axons. Spatial information in the retina and tectum relies on discrete signaling pathways that regulate polarized expression of axon guidance molecules in distinct domains in both the retina and tectum, thereby ensuring that accurate topographic maps are created.

In this thesis, I have investigated the function of two families of transcription factors, Pbx and Meis, as well as a growth factor of the Bmp family, Gdf6a, in specifying positional identity in the zebrafish visual system. I demonstrate that two partially redundant *pbx* genes, *pbx2* and *pbx4*, along with members of the *meis* family, are required for patterning of the dorsal retina and tectum in zebrafish. Embryos lacking these critical transcription factors exhibit retinal ganglion cell axon outgrowth errors, which are likely the result of tectal mis-patterning.

Bone morphogenetic protein (Bmp) growth factors regulate dorsal retinal identity in vertebrate models, but the developmental timing of this signaling remains unclear. In this thesis, I investigate the functions of two zebrafish Bmps, Gdf6a and Bmp4, during initiation of dorsal retinal identity. Knockdown of zebrafish Gdf6a blocks initiation of dorsal marker expression, while knockdown of Bmp4 produces no discernable retinal phenotype. These data, combined with analyses of embryos ectopically expressing Bmps, demonstrate that Gdf6a is

necessary and sufficient for initiation of dorsal retinal identity, and loss of such identity leads to errors in retinal ganglion cell topographic mapping.

Finally, I demonstrate that *gdf6a* is required for numerous embryonic processes in addition to dorsal retina specification. Gdf6a in required for eye growth, as loss of Gdf6a function leads to microphthalmia. I have obtained preliminary evidence that this growth factor is also required for development of the lens and axial skeleton. Furthermore, many of these phenotypes are similar to those seen in human patients with mutations in *GDF6*, highlighting the importance of understanding the function of this growth factor in model organisms.

Table of Contents

List of Tables

List of figures

Appendix E

List of Abbreviations

Aldh -aldehyde dehydrogenase

Ascl- Achaete/scute like

Atoh- Atonal homolog

AV- Atrioventricular

ATP- Adenosine Tri-phosphate

Bambi- Bmp and activin membrane bound inhibitor

BCIP- Bromo-chloro-indoyl phosphate

bHLH- Basic helix-loop-helix

Bmp- Bone morphogenetic protein

Bp- Base pair

BSA- Bovine serum albumin

Cad- Carbamoylphosphate synthetase aspartate carbamyltransferase/ dihydroorotase

caBMPR- Constituatively active Bmp receptor

Ccn- Cyclin

cDNA- Complementary Deoxyribonucleic acid

CMZ- Ciliary Marginal Zone

Crx- Cone-rod homeobox

Cry- Crystallin

Cx- Connexin

DMSO- Dimethyl sulfoxide

Dkk- Dikkof

DN- Dominant negative

Dpf- Days post fertilization

Efn- Ephrin receptor

Eph- Eph receptor tyrosine kinase

Exd- Extradenticle

Fabp- Fatty acid Binding protein

FGF- Fibroblast growth factor

Flk- Fetal liver kinase

Flh- Floating head

GCL- Ganglion cell layer

Gdf- Growth and differentiation factor

H_20_2- Hydrogen peroxide

Hmx- H6 homeobox

Hox- Homeotic complex

Hpf- Hours post fertilization

Hsp- Heat shock protein

Hth- Homothorax

INL- Inner nuclear layer

IPF- Insulin promoting factor

KOH- Potassium hydroxide

LGN- Lateral geniculate nucleus

Lim- Lens intrinsic membrane protein

LRP- lipoprotein-receptor related protein

Lzr- Lazarus

Meinox- Meis/pKnox

Meis- Myeloid ecotropic viral integration site

MO- morpholino

mRNA- Messenger ribonucleic acid

Myc- myelocytomatosis oncogene

MyoD- Myogenic differentiation factor

MZ- Maternal zygotic

Nat- N-acetyl transferase

NBT- nitroblue tetrazolium

Ngn- Neurogenin

Nog- Noggin

Odc- ornithine decarboxylase

ONL- Outer nuclear layer

ORF- Open reading frame

Otx- Orthodenticle homolog

PAP- PIM1 -associated protein

Pax- Paired box homeobox

PBSDTT- Phosphate buffered saline with 0.1% Tween-20, 1 % DMSO, 0.1%, Triton X-100

PBST- Phosphate buffered saline with 0.1% Tween-20

Pbx- Pre-B Cell Leukemia Transcription Factor

PCR- Polymerase chain reaction

Pdx- Pancreatic transcription factor

PFA- Paraformaldhyde

PTU- Phenylthiourea

qRTPCR- Quantitative real-time polymerase chain reaction

RA- retinoic acid

RGC- Retinal ganglion cell

RNA- ribonucleic acid

Rp9- retinitis pigmentosa homolog

RPE- retinal pigmented epithelium

Rx- retinal homeobox

SC- superior colliculus

Scl - Stem cell leukemia

Shh- Sonic hedgehog

Six- Sin oculis homeobox homolog

SnRNA- Small nuclear ribonucleic acid

So- sin oculus

Soho- sensory organ homeobox

Sox- sex determining region Y -box

TALE- Three amino acid loop extension

Tbx- T-box transcription factor

Tgf- transforming growth factor

Uhrf- Ubiquitin-like, containing PHD
and RING finger domains

UTR- Untranslated region

Vax- ventral anterior homeobox

VAD- vitamin A deficient diet

Vsx- Visual system homeobox

Wnt- wingless-type MMTV integration site

Chapter 1

Introduction

Zebrafish eye development

Development of the eye is well conserved among vertebrate species, including the well-studied teleost (ray-finned fish) model organism zebrafish. The combination of forward and reverse genetics together with robust methods for evaluating embryonic gene expression have made zebrafish a very powerful model to study the basic processes of eye development and the molecular mechanisms that are perturbed in human ocular disorders.

Eye development in zebrafish begins with the regionalization of the anterior forebrain, whereby a subset of cells are sequestered to give rise to an optic fate (Bailey et al., 2004). These cells can be identified by the expression of eye specific markers that can be detected by late gastrulation (Carl et al., 2002; Seo et al., 1998). This set of sequestered cells comprises the neuroectodermal retina anlage and the abutting ectodermal lens-competence regions (Loosli et al., 2003). A few hours later (6-7 somite stage), cells of newly separated optic primordia evaginate from the forebrain, producing bilateral optic vesicles (Schmitt and Dowling, 1994). Further morphoghenetic movements allow for the invagination of the cells of the optic vesicle, forming the optic cup, which is well defined by 24 hpf (Schmitt and Dowling, 1994). Induction of lens tissue occurs via contact of the surface ectoderm with the optic cup, resulting in the invagination of the lens placode (Dahm et al., 2007).

Specification of retinal progenitor cells

Experiments in several model organisms have identified a network of transcription factors that are required for the early regionalization of forebrain tissue to produce the optic primordium, and subsequent growth and morphogenesis to produce the optic vesicles. In Drosophila, for example, the development of the larval and adult visual system requires the activity of the homeobox-containing transcription factor *sine oculis* (*so*) (Cheyette et al., 1994). Over-expression of the vertebrate ortholog, *six3*, can cause ectopic eye formation within the midbrain and cerebellum (Loosli et al., 1999), indicating that *six3* likely functions very early in the eye development pathway. In Medaka, a distinct teleost fish model, loss of function experiments removing *six3* activity result in a complete lack of eye formation (Carl et al., 2002), providing support for this hypothesis.

Further research has indicated that *six3* cooperates with another transcription factor early in eye development, known as *paired box gene 6a* (*pax6*). Loss of *pax6* can cause a host of ocular abnormalities, including microphthalmia in mice (Graw et al., 2005), Anirida in humans (Chien et al., 2009; Glaser et al., 1992; Jordan et al., 1992), and an eyeless phenotype in flies (Quiring et al., 1994). The expression domains of *pax6* and *six3* partially overlap during the late gastrula stage (Loosli et al., 1998; Oliver et al., 1995) and over-expression experiments indicate that each transcription factor activates transcription of the other during early eye development (Chow et al., 1999; Loosli et al., 1999; Wargelius et al., 2003). Loss of either gene in zebrafish results in

increased apoptosis of retinal progenitor cells. This apoptotic phenotype is not enhanced in double mutants, indicating that *six3* and *pax6* act in the same genetic pathway, leading to absent or reduced eye size (Wargelius et al., 2003).

Subsequent to specification of the retinal anlage, eye formation requires the evagination of these cells to form distinct eye vesicles. The homoeobox transription factor *retinal homeobox 3* (*rx3*) is necessary for this process in teleost fishes (Loosli et al., 2003; Loosli et al., 2001). *rx3* is expressed in the early eye field in all vertebrate models tested, with loss of function alleles being reported in zebrafish and Medaka (Loosli et al., 2003; Loosli et al., 2001). Zebrafish *rx3* (*chokh*), and medaka *rx3* (*eyeless*) mutants display anophthalmia phenotypes, however expression of *six3* and *pax6* is unaffected, indicating that *rx3* is not required for specification of retinal progenitors from forebrain tissue. Furthermore, over-expression of *six3* cannot rescue the eyeless phenotype in *rx3* mutants (Loosli et al., 2001), suggesting that *rx3* functions either downstream or parallel to that of *six3*. Additional experiments showing that over-expression of *six3* induces ectopic *rx3* expression confirms that *rx3* acts genetically downstream of *six3*. As early specification of retinal progenitors in the forebrain is normal in *rx3* mutants, it is likely that the eyeless phenotype results form failure of retinal progenitors to evaginate form the forebrain to form optic distinct vesicles. Additionally, over-expression of *rx3* results in larger optic vesicles, pointing to a role for *rx3* in the control of proliferation of retinal progenitor cells (Loosli et al., 2001)

Function of zebrafish retinal neurons.

The mature zebrafish retina contains seven distinct retinal cell types, including six neural, and one glial (Müller glia) cell type. Retinal neurons are organized into three nuclear and two plexiform layers, and function to receive light signals from the environment and relay such information to visual processing centers in the brain. The outer most nuclear layer contains rod and cone photoreceptors. While rod photoreceptors function to detect dim light (can detect a single photon), cone photoreceptors detect light intensities up to eleven orders of magnitude higher (Pugh et al., 1999). Photoreceptors contain pigment proteins known as opsins, which undergo a conformational change upon photic activation. This photoisomerization induces a chain of events that results in a change of membrane potential (Tsujikawa and Malicki, 2004), which is then relayed to interneurons via synapses in the outer plexiform layer.

The cell bodies of the zebrafish retinal interneurons are found in the inner nuclear layer (INL), and function to relay chemical signals produced at the photoreceptor synapse to the retinal ganglion cells (RGCs). Zebrafish retinal interneurons include the horizontal, amacrine, and bipolar cells, however each of these populations can be subdivided into multiple subtypes on the basis of distinct morphology and neurotransmitter production (Connaughton et al., 2004). This complexity is required to preserve the spatial fidelity of chemical signals produced by the photoreceptors, and also functions in visual adaptation to different magnitudes of light intensities (Beaudoin et al., 2008; Demb, 2008).

The retinal interneurons synapse with retinal ganglion cells in the inner plexiform layer. Retinal ganglion cells (found in the ganglion cell layer) extend their axons to the optic tectum (primary visual processing center in zebrafish). RGC axons arborize in a distinct spatial pattern within the tectum on the basis of the axial position of RGC cell body in the ganglion cell layer, ensuring that spatial information is preserved for visual processing. At least eleven morphological subtypes of ganglion cells have been identified (Beaudoin et al., 2008), allowing for response to excitatory and inhibitory nuertrotransmitter signals from distinct subtypes of retinal interneurons.

Specification of zebrafish retinal neurons

Retinal progenitor cells in the optic cup continue to proliferate until about 32 hpf, in which a wave of differentiation occurs, beginning in the ventral-nasal portion of the retina (Hu and Easter, 1999) In zebrafish, this wave of differentiation requires the actions of two peptide growth factors, Sonic hedgehog (Shh) and fibroblast growth factor (Fgf) (Beaudoin et al., 2008), emanating from the optic stalk. This wave of neurogenic differentiation is highly ordered, with specific retinal cell types exiting the cell cycle at distinct times. In all vertebrates tested, the retinal ganglion cells are the first identifiable post mitotic neurons (Beaudoin et al., 2008; Hu and Easter, 1999; Stiemke and Hollyfield, 1995; Young, 1985). Soon after the differentiation of RGCs, cells of the inner nuclear layer exit the cell cycle, while the photoreceptors and müller glia are specified last (Hu and Easter, 1999; Morris and Fadool, 2005). Photoreceptors are initially

specified from a small patch of cells in the ventral-nasal domain of the retina, giving rise to both rods and cones. Propagation of the wave of neurogenesis produces additional cone photoreceptors, while additional rod photoreceptors are only produced subsequent to cone photoreceptor differentiation. These rods appear sporadically throughout the retina as opposed to following a wave-like pattern (Fadool, 2003; Morris and Fadool, 2005; Raymond et al., 1995; Schmitt and Dowling, 1996), implying differential mechanisms for rod and cone photoreceptor specification in zebrafish. Birth dating experiments indicate that retinal progenitor cells can only give rise to a subset of retinal neuron types at any given time during the neurogenic wave (Belliveau et al., 2000), implying that both intrinsic and extrinsic factors control the timing of cell cycle exit and differentiation in the retina. These observations support a model whereby progenitors pass through a series of competence states, during each of which the progenitors are competent to produce only a subset of retinal cell types (Cepko et al., 1996).

Of importance to the timing of cell cycle exit and neurogenesis in the zebrafish retina is *atonal7* (*atoh7*), an ortholog of Drosophila *atonal* gene. *atonal* encodes a basic helix-loop-helix transcription factor is required for the development of the Drosophila R8 photoreceptor, the earliest post mitotic cell type of the Drosophila compound eye (Jarman et al., 1993). Identification of a zebrafish mutant, *lakritz*, which contains an *atoh7* null mutation, confirms that zebrafish *atoh7* is required for the earliest born neurons in the vertebrate eye as *lakritz* mutants lack retinal ganglion cells (Kay et al., 2001). Over-expression of

Xenopus ortholog, *xath5,* biases retinal neurogenesis toward a RGC fate at the expense of later born retinal neurons (Kanekar et al., 1997), further supporting this model.

Analysis of zebrafish mutants with disrupted aspects of the Sonic hedgehog (Shh) pathway revealed that retinal neurogenesis is under the control of the *shh* pathway, and many of these mutants fail to make the transition from proliferating neuroepithelium to post mitotic neurons (Stenkamp et al., 2002). Like *atoh7,* expression is induced in the ventral-nasal patch of the retina and expands in a wave like fashion during neurogenesis (Neumann and Nuesslein-Volhard, 2000; Vinothkumar et al., 2008). This initial expression of *shh* is under the transcriptional control of the FGF signaling pathway, which is active in the optic stalk adjacent to the ventral-nasal domain of *shh* expression. The subsequent propagation of *shh* expression throughout the retina appears to be dependent on its own signaling output, as blocking Shh function after initiation of *shh* expression inhibits further *shh* expression and neural differentiation (Neumann and Nuesslein-Volhard, 2000).

It has been noted that differentiated RGCs secrete Shh ligand, and this source has been postulated to help in the propagation of the neurogenic wave of *atoh7* to induce later born neural types. Although many Shh signaling mutants are unable to propagate *atoh7* expression throughout the retina, these phenotypes are not fully penetrant, with some mutant embryos expressing *atoh7* at wildtype levels (Stenkamp et al., 2002). Thus, it is likely that at least one other signal is involved in the spread of *atoh7* expression during retinal neurogenesis. Shh has

been shown to initiate a second wave of neurogenesis, that occurs almost simultaneously with the first wave, and gives rise to a subset of amacrine cells that, in turn, secrete Shh ligand. This Shh signal is independent of *atoh7*, and is required for differentiation of cells in both the inner and outer nuclear layers (Shkumatava et al., 2004).

The latest born neurons of the vertebrate retina, the photoreceptors, are also dependent on Shh signaling for their differentiation. Evidence indicates that Shh ligand, secreted from the retinal pigmented epithelium (RPE) is required for the earliest stages of photoreceptor differentiation. Specific knockdown of Shh ligand translation at later stages of development results in reduced opsin expression, which was confirmed in a *shh* (*sonic-you*) mutant (Stenkamp and Frey, 2003; Stenkamp et al., 2002; Stenkamp et al., 2000). These experiments were conducted by injecting morpholino antisense oligonucleotides into embryonic zebrafish between 51-58 hpf, thus specifically targeting the RPE source of Shh ligand which is active at this developmental stage (Stenkamp and Frey, 2003; Stenkamp et al., 2000).

Over-expression studies have indicated that the neurogenic wave of *atoh7* expression is also required for the development of photoreceptors, as retroviral mis-expression of *atoh7* in chicken embryos leads to ectopic photoreceptor development while ectopic expression of *atoh7* in cultured RPE cells induced transdifferentiation into cells that morphologically resemble photoreceptors and express *opsin* genes (Ma et al., 2004). This ability of *atoh7* to induce photoreceptor differentiation is developmental stage-dependent and lags behind

the ganglion cell-promoting activity (Ma et al., 2004), which is in agreement with the competency state model of retinal differentiation whereby retinal progenitors are competent to give rise to distinct subsets of retinal neurons at specific times during development.

A number of transcription factors have been identified downstream of both Atoh7 and Shh for the development of photoreceptors. One such transcription factor is *retinal homeobox* 1 (*rx1*), as morpholino inhibition of hedgehog ligands leads to reduced *rx1* expression in the photoreceptor layer of zebrafish (Nelson et al., 2009). It has been demonstrated in Xenopus that the Rx protein binds to conserved elements in the promoter regions of photoreceptor specific genes such as *rhodopsin* and *red cone opsin* (Pan et al., 2006). Loss of function studies in zebrafish and Xenopus demonstrate that photoreceptor gene expression is inhibited without *rx1* (and to a milder extent, *retinal homeobox gene 2, rx2*), gene function (Nelson et al., 2009; Pan et al., 2010), supporting a role for retinal homeobox genes in photoreceptor differentiation and survival. Further support for this hypothesis is gained through experiments showing a synergistic relationship between the Xenopus *rx* gene and another critical transcription factor, *cone rod homeobox* (*crx*) (Pan et al., 2010). Mutations in the *crx* gene in humans can lead to loss of vision through the degeneration of photoreceptors, again suggesting a role in photoreceptor survival and function (Rivolta et al., 2001; Swain et al., 1997; Swaroop et al., 1999).

Topographic mapping of retinal ganglion cells

Development of the visual system in vertebrates requires not only a functional eye, but also involves making the correct neural connections between the retinal ganglion cell axons and visual processing centers. RGC axons exit the eye through the optic nerve, and in zebrafish, project contralaterally toward the optic tectum. In higher vertebrates, such as mammals, axons map to the superior colilicus (SC), a structure analogous to the teleost optic tectum, and the lateral geniculate nucleus (LGN). In mice, ipsilateral projections are also observed in addition to contralateral projections. Despite these differences, all vertebrates display precise topographic mapping or retinal ganglion cell axons onto visual processing centers in order to preserve the spatial fidelity of light signals that enter the eye.

Topographic mapping relies on gradients of ligand and receptors that offer either attractive or repulsive cues between retinal ganglion cell axons and the tissue in which they migrate. This chemoaffinity hypothesis was first described by Sperry decades ago (Sperry, 1963), and recent work has demonstrated that the Eph receptors (Eph) and their counterpart Ephrin (Efn) ligands influence topographic mapping in vertebrates. The Ephs are a family of widely expressed receptor tyrosine kinases comprising ten EphA and six EphB members in vertebrates (Murai and Pasquale, 2003; Palmer and Klein, 2003), which bind promiscuously to their counterpart EphrinA and EphrinB ligands (Noren and Pasquale, 2004). Interactions between Eph receptor tyrosine kinases and Ephrin ligands result in cytoskeletal rearrangments and changes in cell adhesion, thereby

eliciting either attractive or repulsive responses that result in the collapse or spreading of RGC axon growth cones, respectively (Scicolone et al., 2009; Woo et al., 2009). Thus, by interpreting the molecular Eph and Ephrin code, RGC axons form a precise topographic map within the optic tectum.

Topographic mapping in zebrafish occurs along two orthogonally oriented axes: the nasal-temporal and dorsal-ventral axes. Inverse maps are created, whereby axons from the temporal retina map to the anterior tectum, while axons from the nasal retina map to the posterior tectum. Similarly, axons that originate from RGCs in the dorsal retina map to the lateral tectum, while ventral RGC axons map to the medial tectum. It has been demonstrated that EphrinA ligands and the EphA receptors provide repulsive cues that are required for growth cone decisions during RGC mapping along the anterior-posterior tectal axis (Roskies and O'Leary, 1994). In vertebrates, *ephrinA* ligands are expressed in a posterior high/anterior low gradient across the optic tectum (or SC), while *ephA* receptors are expressed in an anterior high/posterior low gradient. (Rashid et al., 2005; Stubbs et al., 2000). As nasal RGCs express high levels of *ephrinA* ligands, growth cones avoid the anterior tectum where expression of its counterpart *ephA* receptor is highest, and thus continue to grow toward the posterior tectum. Similarly, temporal RGCs express high levels of *ephA* receptors, and thus receive repulsive cues from the posterior tectum, where expression of *ephrinA* ligands is greatest. Thus, graded expression of *ephA* receptors and *ephrinA* ligands in both the retina and optic tectum are required to sort RGC axons along the anterior-

posterior tectal axis, thus preserving spatial information during visual processing. This model is summarized in figure 1-1.

Of critical importance topographic mapping along the medial-lateral tectal axis are the EphrinB/EphB ligands and receptors. In contrast to EphA/EphrinA signaling, ephB receptor and EphrinB ligand interaction results in attractive cues and thus growth cone collapse (Hindges et al., 2002; Mann et al., 2002). Expression of *ephB* molecules is detected in the ventral retina, while expression of *ephrinB* ligands are observed in the dorsal retina (Hindges et al., 2002; Mann et al., 2002; Scicolone et al., 2009; Wagle et al., 2004). Loss of two *EphB* genes (*EphB2* and *EphB3*) in mice results in ectopic lateral branching of retinal ganglion cell from the ventral retina, suggesting that these receptors are required for the proper extension of branches medially (Hindges et al., 2002). This model is summarized in Figure 1-2.

The function of ephrinB ligands is currently less well understood. Although some *ephrinB* ligands are expressed in distinct domains in the eye and tectum (for example *EphrinB1* in the mouse medial SC and *ephrinB2a* in the zebrafish dorsal retina), others do not display restricted expression patterns (Mann et al., 2002). Furthermore, mice RGCs axons arising from the same dorsoventral retinal location, and therefore having similar levels of EphB receptors, extend axon branches both medially and laterally despite a lateral high/medial low gradient of the *EphrinB1* expression in the mouse SC (Hindges et al., 2002). This suggests that an additional mechanism for topographic mapping along the medial-lateral axis is required in addition to the attractive cues resulting from

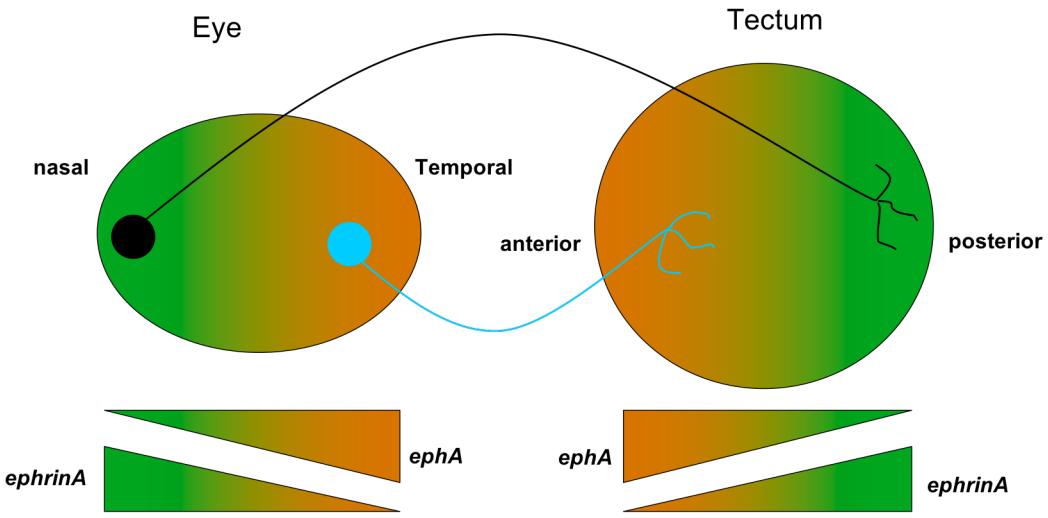

Figure 1-1. Model of topographic mapping along the anterior-posterior axis of the optic tectum. *ephrinA* ligands, found at highest concentrations in the nasal retina, receive repulsive cues from high levels of *ephA3* expression in the anterior tectum, and thus continue grow toward posterior tectum where *ephA3* expression is lowest. Similarly, Axons from the temporal tectum where *ephA* expression is highest, are repulsed by high levels of *ephrinA* expression in the posterior tectum, resulting in arborization in the anterior tectum only.

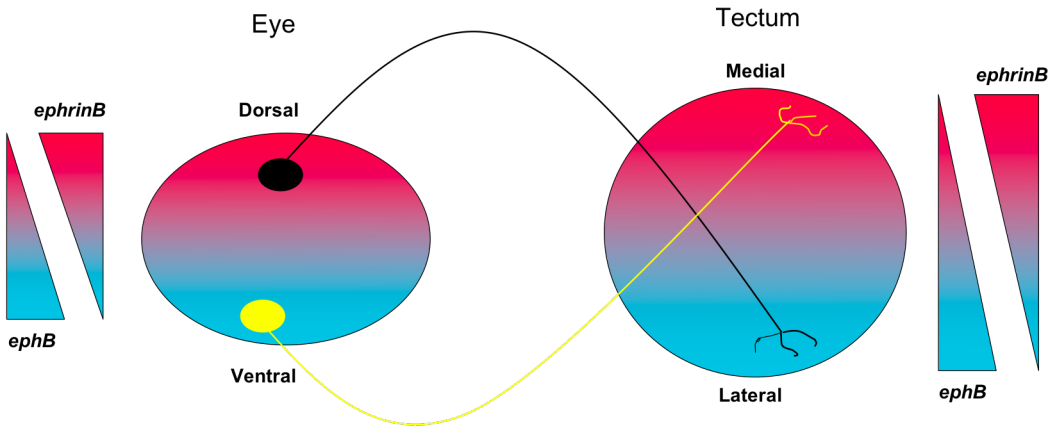

Figure 1-2. Topographic mapping of retinal ganglion cell axons along the medial-lateral axis of the optic tectum. RGCs from the dorsal retina, where expression of *ephrinB* ligands is highest, receive attractive cues from high levels of *ephB* receptors in the lateral tectum. Similarly, RGC axons from the ventral retina, where expression of *ephB* receptors is highest receive attractive cues from high levels of *ephrinB* expression in the medial tectum.

ephrinB1/ephB2/3 interactions.

Establishing the nasal-temporal pattern in the early retina

Although it has been clearly demonstrated that graded expression of *ephrin* and *eph* genes is required for topographic RGC mapping, both the nasal-temporal and dorsal-ventral retinal axes are molecularly defined at earlier stages of development. In zebrafish, as well as in other vertebrates, polarized expression along both axes can be observed in the early proliferating cells of the optic cup, long before retinal ganglion cells have differentiated. Signaling through the Fibroblast growth factor (Fgf) pathway is required for specifying the nasal cell fate, as loss of Fgf3, Fgf8, and Fgf24 function from sources juxtaposed next to the retina expand temporal gene expression at the expense of nasal gene expression (Picker and Brand, 2005; Picker et al., 2009). Resulting RGC projections are shifted to the anterior tectum upon inhibition of Fgf signaling (area normally occupied by temporal RGC axons only), supporting the model that Fgf signaling specifies nasal identity (Picker and Brand, 2005). Fgf signaling in the nasal retina promotes the expression of a forkhead box transcription factor, *foxg1*, which in turn controls the expression of *ephrinA* ligands in the nasal retina (Picker et al., 2009; Takahashi et al., 2009). A second forkhead transcription factor, *foxd1*, defines the temporal domain of the retina (Picker et al., 2009; Takahashi et al., 2003), and is required for expression of *ephA* receptors (Takahashi et al., 2009). Mis-expression of *foxg1* in chick retinas induces and expands the expression of *ephrinA5* and *ephrin A2*, normally confined to the nasal retina, while repressing

the expression of the temporal specific *EphA3* (Takahashi et al., 2003). These experiments have helped to define a model whereby antagonistic relationships between spatially restricted transcription factors, under the control of Fgf signaling, establish both nasal and temporal retinal cell fates.

Establishing the dorsal-ventral pattern in the early retina

Data from vertebrate models indicate that Bone morphogenetic protein (Bmp) signaling is required for specifying dorsal identity within the retina. Bmp ligands function by binding to transmembrane serine/threonine kinase heteromeric complexes of type I and type II Bmp receptors (Sieber et al., 2009). Such interactions promote the phosphorylation and activation of Smads 1, 5, and 8 transcription factors, which in turn associate with another Smad protein, Smad 4, and enter the nucleus to regulate gene transcription. Bmp signaling is tightly regulated during embryonic development, as evidenced by the expression of numerous Bmp antagonists that are often expressed in similar domains to the Bmp ligands and receptors. BMP antagonists can be broadly categorized on the basis of subcellular localization, with classes including: (1) extracellular antagonists, such as Follistatin, Chordin, and Noggin; (2) transmembrane pseudoreceptors, such as Bambi (Bmp and activin membrane bound inhibitor), which prevents function association of type I and type II receptors (Onichtchouk et al., 1999); and (3) intracellular proteins, such as the inhibitory Smad protein Smad 7, that acts by interacting with activated BMP type I receptors and preventing the phosphorylation of Smads 1, 5, and 8 (Hayashi et al., 1997; Souchelnytskyi et al.,

1998) as well as targeting Bmp receptors for degradation (Ebisawa et al., 2001; Kavsak et al., 2000). A model for Bmp signaling is illustrated in Figure 1-3.

In both chick and zebrafish embryos, *bmp2* and *bmp4* are expressed at highest levels in the dorsal retina (Behesti et al., 2006; Hocking and McFarlane, 2007; Sakuta et al., 2006). Expression of the extracellular Bmp antagonist *ventroptin* in the ventral retina of mice and chickens limits Bmp signaling in this domain (Sakuta et al., 2001; Takahashi et al., 2003), although there is no report of a *ventroptin* gene in zebrafish to date. This results in polarized Bmp signaling along the dorsal-ventral retinal axis which is required for downstream expression of transcription factors, believed to be responsible for transcriptional regulation of *ephB* and *ephrinB* axon guidance molecules. The T-box transcription factor *tbx5* is expressed in the dorsal retina where levels of Bmp signaling are the highest (Behesti et al., 2006). The ventral specific *ventral homeobox 2* (*vax2*), is expressed where Bmp signaling levels are lowest, and is likely under the transcriptional regulation of the Hedgehog signaling pathway (Take-uchi et al., 2003). Loss of *Vax2* in mice results in the ectopic expression of late dorsal markers, such as *ephrinB* ligands, in the ventral retina (Barbieri et al., 2002). Thus, Vax2 is required not only for the expression of ventral specific axon guidance molecules, but also to limit the expression of dorsal axon guidance molecules to the dorsal retina. Moreover, mis-expression of *vax2* results in ventralization of the retina, as loss of *tbx5* is observed (Schulte et al., 1999). This again demonstrates that *vax2* can inhibit dorsal retinal gene expression, supporting a model (similar to that seen in the nasal-temporal axis) where

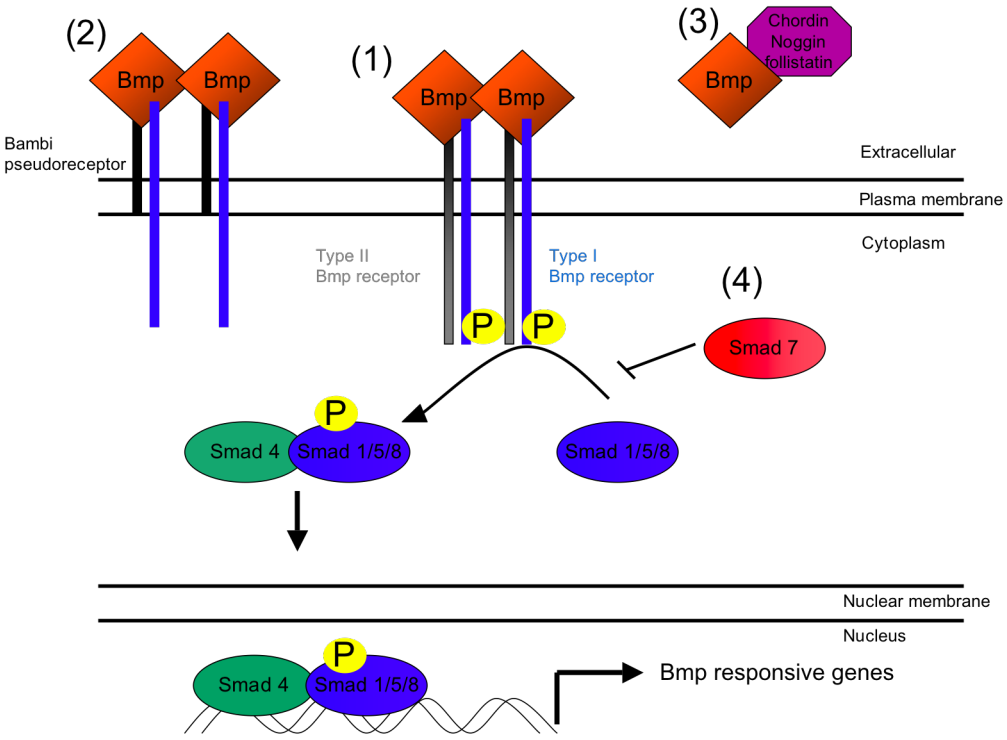
(2)
Bmp
Bmp
(1)
Bmp
Bmp
(3)
Bmp
Chordin
Noggin
follistatin
Bambi
pseudoreceptor
Extracellular
Plasma membrane
Cytoplasm
Type II
Bmp receptor
Type I
Bmp receptor
(4)
P
P
Smad 7
P
Smad 4
Smad 1/5/8
Smad 1/5/8
Nuclear membrane
Nucleus
P
Smad 4
Smad 1/5/8
Bmp responsive genes

Figure 1-3: A model for Bmp signaling in vertebrates. (1) Bmp ligands signal as dimers via a quadramer receptor, composed of type I and Type II heterodimers. Binding of Bmp ligands to this receptor complex induces transphosphorylation of the type I receptor by the type II receptor, leading to the phosphorylation of Smad 1/5/8 proteins through the physical interaction with the Type I receptor. Phosphorylated Smads 1/5/8 interact with Smad 4, and translocate to the nucleus to regulate transcription of Bmp responsive genes. (2) Inhibition of Bmp signaling can be accomplished via binding of the pseudoreceptor Bambi, to Type I Bmp receptors thereby preventing the transphosphorylation event. (3) Bmp inhibition is also accomplished via binding of extracellular inhibitors, such as Chordin, Noggin, and Follistatin to Bmp ligands, thereby preventing their association with Bmp receptors. (4) Smad 7 can inhibit Bmp signaling through prevention of the physical interaction of Smad 1/5/8 proteins with the Type I Bmp receptor, thereby preventing their activation by phosphorylation.

antagonizing activity of spatial restricted transcription factors ensure that both dorsal and ventral cell fates are specified. Before the work contained in this thesis, there was only one report detailing loss of Bmp function and resulting early dorsal-ventral retinal patterning, whereby *ventroptin* was mis-expressed in the dorsal retina, thereby inhibiting Bmp signaling. This resulted in a ventralization of the eye, with expansion of *vax2* expression to the dorsal retina coupled with loss of *tbx5* expression being observed (Sakuta et al., 2001).

Development of coloboma and microphthalmia

During early development, the vertebrate eye contains a transient ventral fissure that is essential for the entry of mesenchymal cells into the retina, where they will eventually form blood vessels that will nourish the eye throughout the life of the organism (Barishak, 1992). Failure of the optic fissure to close results in a loss of ventral tissue, referred to as coloboma. Coloboma, depending on the size and location, can lead to blind spots, lazy eye, and overall reduced visual acuity in patients (Taylor, 2007).

The vertebrate eye is patterned along the proximal-distal axis early in development. The distal eye cells give rise to neural retina and retinal pigmented epithelium, while more proximal cells give rise to the optic stalk and choroid. Before the onset of cellular differentiation in the retina, the fissure begins to close using a contact dependent dissolution of the basal lamina at the contacting neuroepithelium on each side of the optic fissure (Torres et al., 1996).

A number of genes involved in axial eye patterning have been identified that, when mutated, give rise to coloboma. For example, the secreted morphogen Sonic Hedgehog, required for patterning the ventral retina and optic stalk, results in coloboma in human patients when mutated (Schimmenti et al., 2003). Sonic hedgehog is required for the transcription of spatially restricted transcription factors, including both *ventral-anterior homeobox 1* and *2* (*vax1* and *vax2*), which delineate the optic stalk and ventral neural retina regions (Takahashi et al., 2003). Inactivation of both *vax* genes in zebrafish results in severe coloboma (Takahashi et al., 2003). Loss of *shh* in zebrafish leads to severe coloboma and loss of *vax* gene expression, supporting the idea that *shh* acts genetically upstream of *vax* gene expression for closure of the optic fissure.

In addition to Shh and its downstream transcription factors, other signaling molecules have been implicated in the development of coloboma. Of importance is retinoic acid (RA), a secreted morphogen that is required for development of the ventral retina (Hyatt et al., 1996). Mutations in Retinal Binding Protein (*RBP*), for example, have been described in a sibling-pair that presented with iris coloboma (Seeliger et al., 1999). Furthermore, there is suggestive evidence that vitamin A deficient (VAD) diets are correlated with the incidence of coloboma (Hornby et al., 2003). Vitamin A is a precursor for retinoic acid synthesis, thus linking retinoic acid to the development of coloboma.

Animal models have proven invaluable in the field of retinoic acid research. For example, pregnant mice that receive teratogenic doses of retinoic acid give birth to pups with eye defects that include coloboma (Stull and Wikler,

2000). In zebrafish, local delivery of RA to the eye via implanted RA soaked beads not only results in coloboma, but can also induce ectopic fissure formation anywhere in the retina (Hyatt et al., 1996). Furthermore, failure to close the optic fissure in RA treated mice correlates with changes in gene expression along the dorsal-ventral axis of the developing eye (Stull and Wikler, 2000) in a manner similar to that seen with a loss of Sonic Hedgehog signaling.

Work in chickens and mice provides supporting evidence for other signaling pathways, in addition to the Shh and RA signaling pathways, in the development of coloboma. Specifically, the Bmp signaling pathway can give rise to coloboma when inhibited. For example, mis-expression of the Bmp antagonist, *gremlin*, in chick optic vesicles results in coloboma (Huillard et al., 2005), although no mechanism has been defined. Canonical wingless-type MMTV integration site family (Wnt) signaling can also lead to coloboma when perturbed. Loss of *Lrp6* in mice, a receptor required for canonical Wnt signaling, leads to retinal coloboma (Zhou et al., 2008). In this model, Bmp signaling was attenuated, leading to a loss of dorsal patterning genes such as *Tbx5* and increase of ventral specific *Vax2*. Similar retinal mis-patterning was observed in zebrafish embryos over-expressing *dikkof1* (*dkk1*), an inhibitor of Wnt signaling (Veien et al., 2008). Thus, like the Shh pathway, Bmp and Wnt signaling appear to affect the closure of the optic fissure through the regulation of genes required to pattern the dorsal-ventral retinal axis.

In patients, as well as in model organisms, coloboma is often observed in combination with microphthalmia, indicating that closure of the optic fissure may

be linked the overall growth of the eye *in utero*. Indeed it has been shown that mutations in Bmp ligands and antagonists (Huillard et al., 2005; Ye et al., 2010; Zhang et al., 2009), and retinoic acid binding proteins (Golzio et al., 2007) can result in both coloboma and microphthalmia, often in the same patient or animal. Microphthalmia can result due to decreased proliferation and/or increased cell death rates in the early progenitor cells in the retina. As closure of the optic fissure requires contact between the epithelial cells on either side of the fissure, it is logical that reduced rates of proliferation, or increased death rates may prevent this contact dependent closure mechanism. The Bmp pathway has been linked with microphthalmia through regulation of both cell proliferation and apoptosis in the developing eye (Behesti et al., 2006; Hanel and Hensey, 2006; Liu et al., 2003; Trousse et al., 2001).

The zebrafish eye, unlike that of mammals, continues to grow throughout the life of the animal. Thus, there is a requirement for the production of new retinal neurons at times other than embryonic development. For this purpose, a population of self-renewing stem cells in maintained in the ciliary marginal zone (CMZ) of the zebrafish eye. This provides another mechanism for the development of microphthalmia, whereby failure to maintain this stem cell population leads to reduced rates of retinal growth over time. To date, only six strains of zebrafish mutants have been published which have a microphthalmic phenotype attributed to reduced rates of proliferation in the ciliary marginal zone. These six fish lines contain mutations for genes encoding subunits of the vacuolar

-ATPase complex (Behesti et al., 2006), highlighting the importance of this complex for maintaining stem cell populations in the CMZ.

Growth and Differentiation Factor 6a (Gdf6a) signaling in early embryonic development

During vertebrate embryonic development, polarity along the dorsal-ventral axis must be achieved to subsequently produce a phenotypically normal embryo. The early dorsal-ventral axis is characterized by a large ventro-lateral region and a smaller dorsal region, the organizer, which is initially established by maternal components. Gdf6a is a maternally expressed bone morphogenetic protein in zebrafish embryos, and was originally described for its ability to induce ventral embryonic cell fates during early development (Goutel et al., 2000; Sidi et al., 2003). In Xenopus, β-catenin signaling is essential for dorsal specification, through the transcriptional regulation of BMP antagonist genes such as *chordin* (Wessely et al., 2001). Loss of these Bmp inhibitory genes results in a ventralized phenotype that can thus be attributed to increased Gdf6a signaling (Sidi et al., 2003). In addition to Gdf6, other Bmp molecules, such as Bmp2 (Clement et al., 1995; Schmid et al., 2000), Bmp4 (Dale et al., 1992; Schmidt et al., 1995) and Bmp7 (Schmid et al., 2000), have been implicated in the production of ventral cell fates, as loss of these genes eliminates ventral specific structures such as the ventral tail fin and vein. Further epistatic analyses revealed that zygotic transcription of these ventralizing *bmp* genes requires maternal Gdf6a. This model is supported by experiments in which over-expression of *bmp2*, *bmp4*, or *bmp7*

rescues the dorsalized phenotype produced in *gdf6a* (translation blocking) morphants. In contrast, mis-expression of *gdf6a* cannot rescue phenotypes due to *bmp2*, *bmp4*, or *bmp7* loss of function (Goutel et al., 2000; Sidi et al., 2003). Together, these data support a model whereby a hierarchy of Bmp expression is required for specification of the dorsal-ventral embryonic axis, beginning with the maternally expressed *gdf6a*.

In addition to dorsal-ventral embryonic patterning, *gdf6a* has also been implicated in the production and maintenance of specific cell and tissue types in the zebrafish embryo. For example, embryos with reduced Gdf6a function begin to hemorrhage beginning at about 2 dpf. The expression of *gdf6a* partially overlaps with *stem cell leukemia* gene (*scl*) (Hall et al., 2002), a gene required for the production of blood cells and vasculature, indicating that the later hemorrhaging phenotype may result from earlier aberrant development of the zebrafish vascular network.

Research using both mice and zebrafish has uncovered yet another role for *gdf6a* during development. In zebrafish, knockdown of *gdf6a* causes axial defects, producing curled or kinked tails (this work), while *Gdf6* knockout mice display vertebral spine fusions (Asai-Coakwell et al., 2009; Settle et al., 2003). Studies using cell culture have shown that osteogenic differentiation of human bone marrow multipotent mesenchymal stromal cells was reduced upon incubation with Gdf6 (Shen et al., 2009), implying that Gdf6 may be able to inhibit bone formation. This points toward a possible mechanism for vertebral fusions in *Gdf6*

mutants whereby osteoblast differentiation occurs ectopically between vertebral discs.

The identification of a role in bone formation for Gdf6a has sparked interest in the possible therapeutic effects that Gdf6a could have for skeletal injuries. In a sheep model system, induced annular injury leads to the degeneration of vertebral discs, characterized by the loss of osteoblast cells, reduced collagen production, and loss of the extracellular matrix (Wei et al., 2009). Injection of Gdf6 protein into the site of injury significantly reduced the degree of vertebral bone degeneration while preventing the loss of collagens and extracellular matrix proteins. Thus Gdf6 may serve as a viable therapy for individuals with degenerative bone disorders in the future. It is not yet clear, however, how the supplementation of a protein, which inhibits bone formation, results in decreased degeneration of injured bone.

Pbx and Meis function as transcriptional regulators in multiple embryonic tissues, including the eye.

Proteins of the pre-B cell leukemia homeobox (Pbx) family, and the Myeloid ecotropic insertion site (Meis) family of transcription factors were first identified because of their ability to induce leukemic transformation of previously normal blood cells (Kamps et al., 1991; Moskow et al., 1995; Nourse et al., 1990). Additional studies revealed that Pbx and Meis proteins form trimeric complexes with Hox proteins in myleod cells (Shen et al., 1999). *hox* gene clusters, the vertebrate orthologs of the invertebrate *hom* genes, are also required globally to

pattern the anterior-posterior embryonic axis (Reviewed by Wellik, 2009), thus leading to the hypothesis that Pbx and Meis proteins may also be required as Hox co-factors during early embryonic patterning. Binding of Pbx proteins to that of Hox proteins was hypothesized to provide specificity to Hox-DNA binding (Chang et al., 1996; Shen et al., 1996), as there are multiple Hox proteins in vertebrates, and most contain similar DNA binding affinities (Pellerin et al., 1994). Pbx and Meis proteins have now been shown to function co-operatively in both Hox-dependent and Hox-independent function to pattern numerous embryonic tissues such as the hindbrain, muscle, eye, and tectum.

In the hindbrain, *pbx* and *meis* gene function are required to provide genetic specificity to spatially restricted segments called rhombomeres. Loss of two early expressed *pbx* genes, *pbx2* and *pbx4*, produces a homeotic shift of rhombomere identity, whereby rhombomeres 2 through 6 take on a default, rhombomere 1 identity (Waskiewicz et al., 2002). Pbx2 and Pbx4 thus act, in concert with Hox proteins, to modify this default state along the anterior-posterior axis of the hindbrain. Pbx dependent hindbrain patterning was also shown to involve Meis protein function, as expression of dominant negative *meis* constructs produced similar phenotypes to that of loss of Pbx2/4 function (Choe et al., 2002; Waskiewicz et al., 2001). In addition to Pbx and Meis protein binding to form transcriptional complexes in the nucleus, Meis was also shown to bind and stabilize Pbx proteins in the cytoplasm (Waskiewicz et al., 2001), thereby offering a second mechanism for Meis and Pbx protein cooperation in early tissue patterning. Outside of the hindbrain, Pbx has also been identified as a key

regulator of the anterior neural tube development, whereby Pbx cooperates with Engrailed proteins to maintain the midbrain-hindbrain and diencephalic-mesencephalic boundaries (Erickson et al., 2007).

The study of muscle differentiation in zebrafish has uncovered yet another role for Pbx proteins, and moreover, yields a mechanism for Pbx dependent transcriptional regulation. Skeletal and cardiac muscle cell differentiation is initiated by the transcription factor, Myogenic differentiation factor 1 (MyoD), which is required for the transcription of downstream muscle specific target genes, such as *myogenin*. Loss of Pbx results in reduced expression of MyoD specific target genes, such as *myogenin*, thereby implicating Pbx in MyoD dependent muscle cell differentiation (Maves et al., 2007). Gel shift analysis confirms that Pbx, Meis, and MyoD form a complex on the promoter region of *myogenin* in order to initiate its expression. Furthermore, Pbx and Meis proteins appear to bind prior to MyoD, indicating that binding of Pbx and Meis transcription factors may serve as a targeting mechanism to direct MyoD dependent gene transcription (Berkes et al., 2004). Meis and Pbx proteins have been shown to recruit histone deacetylases once bound to promoter regions (Choe et al., 2009), which can then remodel chromatin to provide accessibility for other transcriptional complexes. Although this mechanism has only been demonstrated on Hox promoters, it is likely that Pbx and Meis act in a similar manner to allow MyoD access to muscle specific enhancer regions during development.

In addition to neural patterning and muscle cell differentiation, Pbx and Meis have been shown to regulate the development of other embryonic tissues

such as the pancreas and blood cell populations. The transcription factor Pax6 is required for the differentiation of both islet and alpha cell differentiation (Sander et al., 1997); (St-Onge et al., 1997) and hormone production (Anderson et al., 1999; Ritz-Laser et al., 1999). The Pax6 enhancer region contains a conserved Pbx/Meis binding motif that is required for *pax6* expression (Delporte et al., 2008; Zhang et al., 2006). Pbx also binds and cooperates with the pancreatic specific transcription factor, pancreatic and duodenal homeobox 1 (Pdx1), and it has been shown that this interaction is required for the expansion of pancreatic cell lineages during embryonic development (Dutta et al., 2001). With respect to blood development, loss of Pbx and Meis proteins results in a complete lack of circulating blood in the early embryo, indicating that these transcription factors may play a role in early hematopoesis (Pillay et al., 2010). In addition, both Pbx and Meis are associated with abnormal blood cell development (Wong et al., 2007) and are detected on the promoters of leukemia-associated genes (Wang et al., 2006), indicating that gain of function Pbx and Meis mutations may result in leukemia. In support of this hypothesis, chromosomal translocations that fuse the activation domain of E2A protein with the DNA binding domain of Pbx lead to aberrant Pbx transcriptional properties and induction of leukemia (LeBrun and Cleary, 1994; Lu et al., 1994).

Lastly, Pbx and Meis proteins play a role in eye development in both invertebrate and vertebrate models, however there are far fewer data describing eye specific function when compared to other tissues. In Drosophila, the orthologs of *pbx* and *meis*, *entradenticle* (*Exd*) and *homothorax* (*Hth*), have been identified

as negative regulators of eye development. Both genes are expressed in the eye imaginal discs, and mutant phenotypes include ectopic eye formation, while targeted over-expression of *hth* is sufficient to abolish eye development (Pai et al., 1998). In vertebrates, mutations in a transcription factor that acts upstream of both Meis and Pbx result in a syndromic phenotype that includes smaller lens and apparent retinal duplication along the dorsal-ventral axis (Ferretti et al., 2006). The latter phenotype suggests a role for both Pbx and Meis proteins in early embryonic patterning in the retina, although no molecular analysis of patterning molecules was undertaken.

Purpose of the present study

The current work was done to further characterize the role of Pbx, Meis and Gdf6a proteins in zebrafish eye development, with specific emphasis on dorsal-ventral retinal patterning. In chapter three, I will analyze the function of both Pbx and Meis is regulating polarized gene expression in the retina and tectum. I demonstrate that Pbx and Meis are required for expression of marker genes of the dorsal retina, including *gdf6a*, in addition to previously characterized functions in other tissues. Chapter 4 will detail investigations into the specific role *gdf6a* plays in dorsal-ventral retinal patterning, resulting in aberrant topographic mapping in *gdf6a* mutant embryos. As *gdf6a* is expressed in numerous other tissues during embryonic development, Chapter 5 will include a whole embryo microarray analysis in *gdf6a* morphants, detailing gene regulation and possible function in tissues such as the lens, bone and cartilage, and pineal complex. In

chapter 6, I present a second, eye specific microarray, conduced at later stages of embryonic development which points toward a mechanism of Gdf6a induced microphthalmia. In chapter 7, I will summarize the main findings of my work, and how they have advanced research in eye development.

Bibliography

Andersen, F. G., et al., 1999. Pax6 and Pdx1 form a functional complex on the rat somatostatin gene upstream enhancer. FEBS Lett. 445**,** 315-20.

Asai-Coakwell, M., et al., 2009. Incomplete penetrance and phenotypic variability characterize Gdf6-attributable oculo-skeletal phenotypes. Hum Mol Genet. 18**,** 1110-21.

Bailey, T. J., et al., 2004. Regulation of vertebrate eye development by Rx genes. Int J Dev Biol. 48**,** 761-70.

Barbieri, A. M., et al., 2002. Vax2 inactivation in mouse determines alteration of the eye dorsal-ventral axis, misrouting of the optic fibres and eye coloboma. Development. 129**,** 805-13.

Barishak, Y. R., 1992. Embryology of the eye and its adnexae. Dev Ophthalmol. 24**,** 1-142.

Beaudoin, D. L., et al., 2008. Distinct expressions of contrast gain control in parallel synaptic pathways converging on a retinal ganglion cell. J Physiol. 586**,** 5487-502.

Behesti, H., et al., 2006. The level of BMP4 signaling is critical for the regulation of distinct T-box gene expression domains and growth along the dorso-ventral axis of the optic cup. BMC Dev Biol. 6**,** 62.

Belliveau, M. J., et al., 2000. Late retinal progenitor cells show intrinsic limitations in the production of cell types and the kinetics of opsin synthesis. J Neurosci. 20**,** 2247-54.

Berkes, C. A., et al., 2004. Pbx marks genes for activation by MyoD indicating a role for a homeodomain protein in establishing myogenic potential. Mol Cell. 14**,** 465-77.

Carl, M., et al., 2002. Six3 inactivation reveals its essential role for the formation and patterning of the vertebrate eye. Development. 129**,** 4057-63.

Cepko, C. L., et al., 1996. Cell fate determination in the vertebrate retina. Proc Natl Acad Sci U S A. 93**,** 589-95.

Chang, C. P., et al., 1996. Pbx modulation of Hox homeodomain amino-terminal arms establishes different DNA-binding specificities across the Hox locus. Mol Cell Biol. 16**,** 1734-45.

Cheyette, B. N., et al., 1994. The Drosophila sine oculis locus encodes a homeodomain-containing protein required for the development of the entire visual system. Neuron. 12**,** 977-96.

Chien, Y. H., et al., 2009. Eye anomalies and neurological manifestations in patients with PAX6 mutations. Mol Vis. 15**,** 2139-45.

Choe, S. K., et al., 2009. Meis cofactors control HDAC and CBP accessibility at Hox-regulated promoters during zebrafish embryogenesis. Dev Cell. 17**,** 561-7.

Choe, S. K., et al., 2002. Meis family proteins are required for hindbrain development in the zebrafish. Development. 129**,** 585-95.

Chow, R. L., et al., 1999. Pax6 induces ectopic eyes in a vertebrate. Development. 126**,** 4213-22.

Clement, J. H., et al., 1995. Bone morphogenetic protein 2 in the early development of Xenopus laevis. Mech Dev. 52**,** 357-70.

Connaughton, V. P., et al., 2004. Identification and morphological classification of horizontal, bipolar, and amacrine cells within the zebrafish retina. J Comp Neurol. 477**,** 371-85.

Dahm, R., et al., 2007. Development and adult morphology of the eye lens in the zebrafish. Exp Eye Res. 85**,** 74-89.

Dale, L., et al., 1992. Bone morphogenetic protein 4: a ventralizing factor in early Xenopus development. Development. 115**,** 573-85.

Delporte, F. M., et al., 2008. Expression of zebrafish pax6b in pancreas is regulated by two enhancers containing highly conserved cis-elements bound by PDX1, PBX and PREP factors. BMC Dev Biol. 8**,** 53.

Demb, J. B., 2008. Functional circuitry of visual adaptation in the retina. J Physiol. 586**,** 4377-84.

Dutta, S., et al., 2001. PDX:PBX complexes are required for normal proliferation of pancreatic cells during development. Proc Natl Acad Sci U S A. 98**,** 1065-70.

Ebisawa, T., et al., 2001. Smurf1 interacts with transforming growth factor-beta type I receptor through Smad7 and induces receptor degradation. J Biol Chem. 276**,** 12477-80.

Erickson, T., et al., 2007. Pbx proteins cooperate with Engrailed to pattern the midbrain-hindbrain and diencephalic-mesencephalic boundaries. Dev Biol. 301**,** 504-17.

Fadool, J. M., 2003. Development of a rod photoreceptor mosaic revealed in transgenic zebrafish. Dev Biol. 258**,** 277-90.

Ferretti, E., et al., 2006. Hypomorphic mutation of the TALE gene Prep1 (pKnox1) causes a major reduction of Pbx and Meis proteins and a pleiotropic embryonic phenotype. Mol Cell Biol. 26**,** 5650-62.

Glaser, T., et al., 1992. Genomic structure, evolutionary conservation and aniridia mutations in the human PAX6 gene. Nat Genet. 2**,** 232-9.

Golzio, C., et al., 2007. Matthew-Wood syndrome is caused by truncating mutations in the retinol-binding protein receptor gene STRA6. Am J Hum Genet. 80**,** 1179-87.

Goutel, C., et al., 2000. The ventralizing activity of Radar, a maternally expressed bone morphogenetic protein, reveals complex bone morphogenetic protein interactions controlling dorso-ventral patterning in zebrafish. Mech Dev. 99**,** 15-27.

Graw, J., et al., 2005. Three novel Pax6 alleles in the mouse leading to the same small-eye phenotype caused by different consequences at target promoters. Invest Ophthalmol Vis Sci. 46**,** 4671-83.

Hall, C. J., et al., 2002. Radar is required for the establishment of vascular integrity in the zebrafish. Dev Biol. 251**,** 105-17.

Hanel, M. L., Hensey, C., 2006. Eye and neural defects associated with loss of GDF6. BMC Dev Biol. 6**,** 43.

Hayashi, H., et al., 1997. The MAD-related protein Smad7 associates with the TGFbeta receptor and functions as an antagonist of TGFbeta signaling. Cell. 89**,** 1165-73.

Hindges, R., et al., 2002. EphB forward signaling controls directional branch extension and arborization required for dorsal-ventral retinotopic mapping. Neuron. 35**,** 475-87.

Hocking, J. C., McFarlane, S., 2007. Expression of Bmp ligands and receptors in the developing Xenopus retina. Int J Dev Biol. 51**,** 161-5.

Hornby, S. J., et al., 2003. Eye birth defects in humans may be caused by a recessively-inherited genetic predisposition to the effects of maternal vitamin A deficiency during pregnancy. Med Sci Monit. 9**,** HY23-6.

Hu, M., Easter, S. S., 1999. Retinal neurogenesis: the formation of the initial central patch of postmitotic cells. Dev Biol. 207**,** 309-21.

Huillard, E., et al., 2005. Defects in chicken neuroretina misexpressing the BMP antagonist Drm/Gremlin. Dev Biol. 283**,** 335-44.

Hyatt, G. A., et al., 1996. Retinoic acid establishes ventral retinal characteristics. Development. 122**,** 195-204.

Jarman, A. P., et al., 1993. atonal is a proneural gene that directs chordotonal organ formation in the Drosophila peripheral nervous system. Cell. 73**,** 1307-21.

Jordan, T., et al., 1992. The human PAX6 gene is mutated in two patients with aniridia. Nat Genet. 1**,** 328-32.

Kamps, M. P., et al., 1991. The human t(1;19) translocation in pre-B ALL produces multiple nuclear E2A-Pbx1 fusion proteins with differing transforming potentials. Genes Dev. 5**,** 358-68.

Kanekar, S., et al., 1997. Xath5 participates in a network of bHLH genes in the developing Xenopus retina. Neuron. 19**,** 981-94.

Kavsak, P., et al., 2000. Smad7 binds to Smurf2 to form an E3 ubiquitin ligase that targets the TGF beta receptor for degradation. Mol Cell. 6**,** 1365-75.

Kay, J. N., et al., 2001. Retinal ganglion cell genesis requires lakritz, a Zebrafish atonal Homolog. Neuron. 30**,** 725-36.

LeBrun, D. P., Cleary, M. L., 1994. Fusion with E2A alters the transcriptional properties of the homeodomain protein PBX1 in t(1;19) leukemias. Oncogene. 9**,** 1641-7.

Liu, J., et al., 2003. BMP receptor 1b is required for axon guidance and cell survival in the developing retina. Dev Biol. 256**,** 34-48.

Loosli, F., et al., 1998. Six3, a medaka homolog of the Drosophila homeobox gene sine oculis is expressed in the anterior embryonic shield and the developing eye. Mech Dev. 74**,** 159-64.

Loosli, F., et al., 2003. Loss of eyes in zebrafish caused by mutation of chokh/rx3. EMBO Rep. 4**,** 894-9.

Loosli, F., et al., 2001. Medaka eyeless is the key factor linking retinal determination and eye growth. Development. 128**,** 4035-44.

Loosli, F., et al., 1999. Six3 overexpression initiates the formation of ectopic retina. Genes Dev. 13**,** 649-54.

Lu, Q., et al., 1994. Fusion with E2A converts the Pbx1 homeodomain protein into a constitutive transcriptional activator in human leukemias carrying the t(1;19) translocation. Mol Cell Biol. 14**,** 3938-48.

Ma, W., et al., 2004. A role of ath5 in inducing neuroD and the photoreceptor pathway. J Neurosci. 24**,** 7150-8.

Mann, F., et al., 2002. Topographic mapping in dorsoventral axis of the Xenopus retinotectal system depends on signaling through ephrin-B ligands. Neuron. 35**,** 461-73.

Maves, L., et al., 2007. Pbx homeodomain proteins direct Myod activity to promote fast-muscle differentiation. Development. 134**,** 3371-82.

Morris, A. C., Fadool, J. M., 2005. Studying rod photoreceptor development in zebrafish. Physiol Behav. 86**,** 306-13.

Moskow, J. J., et al., 1995. Meis1, a PBX1-related homeobox gene involved in myeloid leukemia in BXH-2 mice. Mol Cell Biol. 15**,** 5434-43.

Murai, K. K., Pasquale, E. B., 2003. 'Eph'ective signaling: forward, reverse and crosstalk. J Cell Sci. 116**,** 2823-32.

Nelson, S. M., et al., 2009. Retinal homeobox 1 is required for retinal neurogenesis and photoreceptor differentiation in embryonic zebrafish. Dev Biol. 328**,** 24-39.

Neumann, C. J., Nuesslein-Volhard, C., 2000. Patterning of the zebrafish retina by a wave of sonic hedgehog activity. Science. 289**,** 2137-9.

Noren, N. K., Pasquale, E. B., 2004. Eph receptor-ephrin bidirectional signals that target Ras and Rho proteins. Cell Signal. 16**,** 655-66.

Nourse, J., et al., 1990. Chromosomal translocation t(1;19) results in synthesis of a homeobox fusion mRNA that codes for a potential chimeric transcription factor. Cell. 60**,** 535-45.

Oliver, G., et al., 1995. Six3, a murine homolog of the sine oculis gene, demarcates the most anterior border of the developing neural plate and is expressed during eye development. Development. 121**,** 4045-55.

Onichtchouk, D., et al., 1999. Silencing of TGF-beta signalling by the pseudoreceptor BAMBI. Nature. 401**,** 480-5.

Pai, C. Y., et al., 1998. The Homothorax homeoprotein activates the nuclear localization of another homeoprotein, extradenticle, and suppresses eye development in Drosophila. Genes Dev. 12**,** 435-46.

Palmer, A., Klein, R., 2003. Multiple roles of ephrins in morphogenesis, neuronal networking, and brain function. Genes Dev. 17**,** 1429-50.

Pan, Y., et al., Regulation of photoreceptor gene expression by the retinal homeobox (Rx) gene product. Dev Biol. 339**,** 494-506.

Pan, Y., et al., 2006. The Rx-like homeobox gene (Rx-L) is necessary for normal photoreceptor development. Invest Ophthalmol Vis Sci. 47**,** 4245-53.

Pellerin, I., et al., 1994. Hox proteins have different affinities for a consensus DNA site that correlate with the positions of their genes on the hox cluster. Mol Cell Biol. 14**,** 4532-45.

Picker, A., Brand, M., 2005. Fgf signals from a novel signaling center determine axial patterning of the prospective neural retina. Development. 132**,** 4951-62.

Picker, A., et al., 2009. Dynamic coupling of pattern formation and morphogenesis in the developing vertebrate retina. PLoS Biol. 7**,** e1000214.

Pillay, L. M., et al., 2010. The Hox cofactors Meis1 and Pbx act upstream of gata1 to regulate primitive hematopoiesis. Dev Biol. 340**,** 306-17.

Pugh, E. N., Jr., et al., 1999. Molecular mechanisms of vertebrate photoreceptor light adaptation. Curr Opin Neurobiol. 9**,** 410-8.

Quiring, R., et al., 1994. Homology of the eyeless gene of Drosophila to the Small eye gene in mice and Aniridia in humans. Science. 265**,** 785-9.

Rashid, T., et al., 2005. Opposing gradients of ephrin-As and EphA7 in the superior colliculus are essential for topographic mapping in the mammalian visual system. Neuron. 47**,** 57-69.

Raymond, P. A., et al., 1995. Developmental patterning of rod and cone photoreceptors in embryonic zebrafish. J Comp Neurol. 359**,** 537-50.

Ritz-Laser, B., et al., 1999. Pax-6 and Cdx-2/3 interact to activate glucagon gene expression on the G1 control element. J Biol Chem. 274**,** 4124-32.

Rivolta, C., et al., 2001. Novel frameshift mutations in CRX associated with Leber congenital amaurosis. Hum Mutat. 18**,** 550-1.

Roskies, A. L., O'Leary, D. D., 1994. Control of topographic retinal axon branching by inhibitory membrane-bound molecules. Science. 265**,** 799-803.

Sakuta, H., et al., 2001. Ventroptin: a BMP-4 antagonist expressed in a double-gradient pattern in the retina. Science. 293**,** 111-5.

Sakuta, H., et al., 2006. Role of bone morphogenic protein 2 in retinal patterning and retinotectal projection. J Neurosci. 26**,** 10868-78.

Sander, M., et al., 1997. Genetic analysis reveals that PAX6 is required for normal transcription of pancreatic hormone genes and islet development. Genes Dev. 11**,** 1662-73.

Schimmenti, L. A., et al., 2003. Novel mutation in sonic hedgehog in non-syndromic colobomatous microphthalmia. Am J Med Genet A. 116A**,** 215-21.

Schmid, B., et al., 2000. Equivalent genetic roles for bmp7/snailhouse and bmp2b/swirl in dorsoventral pattern formation. Development. 127**,** 957-67.

Schmidt, J. E., et al., 1995. Localized BMP-4 mediates dorsal/ventral patterning in the early Xenopus embryo. Dev Biol. 169**,** 37-50.

Schmitt, E. A., Dowling, J. E., 1994. Early eye morphogenesis in the zebrafish, Brachydanio rerio. J Comp Neurol. 344**,** 532-42.

Schmitt, E. A., Dowling, J. E., 1996. Comparison of topographical patterns of ganglion and photoreceptor cell differentiation in the retina of the zebrafish, Danio rerio. J Comp Neurol. 371**,** 222-34.

Schulte, D., et al., 1999. Misexpression of the Emx-related homeobox genes cVax and mVax2 ventralizes the retina and perturbs the retinotectal map. Neuron. 24**,** 541-53.

Scicolone, G., et al., 2009. Key roles of Ephs and ephrins in retinotectal topographic map formation. Brain Res Bull. 79**,** 227-47.

Seeliger, M. W., et al., 1999. Phenotype in retinol deficiency due to a hereditary defect in retinol binding protein synthesis. Invest Ophthalmol Vis Sci. 40**,** 3-11.

Seo, H. C., et al., 1998. Expression of two zebrafish homologs of the murine Six3 gene demarcates the initial eye primordia. Mech Dev. 73**,** 45-57.

Settle, S. H., Jr., et al., 2003. Multiple joint and skeletal patterning defects caused by single and double mutations in the mouse Gdf6 and Gdf5 genes. Dev Biol. 254**,** 116-30.

Shen, B., et al., 2009. BMP-13 emerges as a potential inhibitor of bone formation. Int J Biol Sci. 5**,** 192-200.

Shen, W. F., et al., 1996. Hox homeodomain proteins exhibit selective complex stabilities with Pbx and DNA. Nucleic Acids Res. 24**,** 898-906.

Shen, W. F., et al., 1999. HOXA9 forms triple complexes with PBX2 and MEIS1 in myeloid cells. Mol Cell Biol. 19**,** 3051-61.

Shkumatava, A., et al., 2004. Sonic hedgehog, secreted by amacrine cells, acts as a short-range signal to direct differentiation and lamination in the zebrafish retina. Development. 131**,** 3849-58.

Sidi, S., et al., 2003. Maternal induction of ventral fate by zebrafish radar. Proc Natl Acad Sci U S A. 100**,** 3315-20.

Sieber, C., et al., 2009. Recent advances in BMP receptor signaling. Cytokine Growth Factor Rev. 20**,** 343-55.

Souchelnytskyi, S., et al., 1998. Physical and functional interaction of murine and Xenopus Smad7 with bone morphogenetic protein receptors and transforming growth factor-beta receptors. J Biol Chem. 273**,** 25364-70.

Sperry, R. W., 1963. Chemoaffinity in the Orderly Growth of Nerve Fiber Patterns and Connections. Proc Natl Acad Sci U S A. 50**,** 703-10.

St-Onge, L., et al., 1997. Pax6 is required for differentiation of glucagon-producing alpha-cells in mouse pancreas. Nature. 387**,** 406-9.

Stenkamp, D. L., Frey, R. A., 2003. Extraretinal and retinal hedgehog signaling sequentially regulate retinal differentiation in zebrafish. Dev Biol. 258**,** 349-63.

Stenkamp, D. L., et al., 2002. Embryonic retinal gene expression in sonic-you mutant zebrafish. Dev Dyn. 225**,** 344-50.

Stenkamp, D. L., et al., 2000. Function for Hedgehog genes in zebrafish retinal development. Dev Biol. 220**,** 238-52.

Stiemke, M. M., Hollyfield, J. G., 1995. Cell birthdays in Xenopus laevis retina. Differentiation. 58**,** 189-93.

Stubbs, J., et al., 2000. Graded expression of EphA3 in the retina and ephrin-A2 in the superior colliculus during initial development of coarse topography in the wallaby retinocollicular projection. Eur J Neurosci. 12**,** 3626-36.

Stull, D. L., Wikler, K. C., 2000. Retinoid-dependent gene expression regulates early morphological events in the development of the murine retina. J Comp Neurol. 417**,** 289-98.

Swain, P. K., et al., 1997. Mutations in the cone-rod homeobox gene are associated with the cone-rod dystrophy photoreceptor degeneration. Neuron. 19**,** 1329-36.

Swaroop, A., et al., 1999. Leber congenital amaurosis caused by a homozygous mutation (R90W) in the homeodomain of the retinal transcription factor CRX: direct evidence for the involvement of CRX in the development of photoreceptor function. Hum Mol Genet. 8**,** 299-305.

Takahashi, H., et al., 2009. Functional mode of FoxD1/CBF2 for the establishment of temporal retinal specificity in the developing chick retina. Dev Biol. 331**,** 300-10.

Takahashi, H., et al., 2003. CBF1 controls the retinotectal topographical map along the anteroposterior axis through multiple mechanisms. Development. 130**,** 5203-15.

Take-uchi, M., et al., 2003. Hedgehog signalling maintains the optic stalk-retinal interface through the regulation of Vax gene activity. Development. 130**,** 955-68.

Taylor, D., 2007. Developmental abnormalities of the optic nerve and chiasm. Eye (Lond). 21**,** 1271-84.

Torres, M., et al., 1996. Pax2 contributes to inner ear patterning and optic nerve trajectory. Development. 122**,** 3381-91.

Trousse, F., et al., 2001. Bmp4 mediates apoptotic cell death in the developing chick eye. J Neurosci. 21**,** 1292-301.

Tsujikawa, M., Malicki, J., 2004. Genetics of photoreceptor development and function in zebrafish. Int J Dev Biol. 48**,** 925-34.

Veien, E. S., et al., 2008. Canonical Wnt signaling is required for the maintenance of dorsal retinal identity. Development. 135**,** 4101-11.

Vinothkumar, S., et al., 2008. Sequential and cooperative action of Fgfs and Shh in the zebrafish retina. Dev Biol. 314**,** 200-14.

Wagle, M., et al., 2004. EphrinB2a in the zebrafish retinotectal system. J Neurobiol. 59**,** 57-65.

Wang, G. G., et al., 2006. Persistent transactivation by meis1 replaces hox function in myeloid leukemogenesis models: evidence for co-occupancy of meis1-pbx and hox-pbx complexes on promoters of leukemia-associated genes. Mol Cell Biol. 26**,** 3902-16.

Wargelius, A., et al., 2003. Retinal expression of zebrafish six3.1 and its regulation by Pax6. Biochem Biophys Res Commun. 309**,** 475-81.

Waskiewicz, A. J., et al., 2001. Zebrafish Meis functions to stabilize Pbx proteins and regulate hindbrain patterning. Development. 128**,** 4139-51.

Waskiewicz, A. J., et al., 2002. Eliminating zebrafish pbx proteins reveals a hindbrain ground state. Dev Cell. 3**,** 723-33.

Wei, A., et al., 2009. BMP13 prevents the effects of annular injury in an ovine model. Int J Biol Sci. 5**,** 388-96.

Wellik, D. M., 2009. Hox genes and vertebrate axial pattern. Curr Top Dev Biol. 88**,** 257-78.

Wessely, O., et al., 2001. Neural induction in the absence of mesoderm: beta-catenin-dependent expression of secreted BMP antagonists at the blastula stage in Xenopus. Dev Biol. 234**,** 161-73.

Wong, P., et al., 2007. Meis1 is an essential and rate-limiting regulator of MLL leukemia stem cell potential. Genes Dev. 21**,** 2762-74.

Woo, S., et al., 2009. Retinotopic mapping requires focal adhesion kinase-mediated regulation of growth cone adhesion. J Neurosci. 29**,** 13981-91.

Ye, M., et al., 2010. Mutation of the bone morphogenetic protein GDF3 causes ocular and skeletal anomalies. Hum Mol Genet. 19**,** 287-98.

Young, R. W., 1985. Cell differentiation in the retina of the mouse. Anat Rec. 212**,** 199-205.

Zhang, X., et al., 2009. Mutational screening of 10 genes in Chinese patients with microphthalmia and/or coloboma. Mol Vis. 15**,** 2911-8.

Zhang, X., et al., 2006. Pax6 is regulated by Meis and Pbx homeoproteins during pancreatic development. Dev Biol. 300**,** 748-57.

Zhou, C. J., et al., 2008. Ocular coloboma and dorsoventral neuroretinal patterning defects in Lrp6 mutant eyes. Dev Dyn. 237**,** 3681-9.

Chapter 2

Materials and Methods

Selected figures from this chapter have been previously published.

*Asai-Coakwell M, **French CR** et al. Incomplete penetrance and phenotypic variability characterize Gdf6-attributable oculo-skeletal phenotypes. Hum Mol Genet. 2009 Mar 15;18(6):1110-21.*

*Asai-Coakwell M, **French CR** et al. GDF6, a novel locus for a spectrum of ocular developmental anomalies. Am J Hum Genet. 2007 Feb;80(2):306-15.*

Zebrafish strains, morpholinos, and in situ hybridization

All zebrafish (*Danio rerio*) were raised at temperatures ranging from 25.5^0C to 33^0C, and staged according to known developmental hallmarks (Kimmel et al., 1995). Zebrafish were raieThe mutant *pbx4* allele (b557), also known as *lazarus, (lzr),* was identified by altered expression patterns of *egr2b (krox20)* in the developing hindbrain, and has been described previous (Popperl et al., 2000). For the microarray experiments, *pbx2/4* null embryos were created by injecting *pbx2* (CCGTTGCCTGTGATGGGCTGCTGCG) translation blocking morpholinos into one-cell maternally and zygotically mutant *lzr* embryos (mz *lzr)*. Germ line transplantation was used to create mz *lzr* embryos and has been described previously (Waskiewicz et al., 2002). For all other experiments, *pbx2/4* null embryos were created by injecting *pbx2* and *pbx4* (AATACTTTTGAGCCGAATCTCTCCG) translation blocking morpholinos into one-cell stage zygotically mutant *lzr* embryos. These embryos are phenotypically indistinguishable from mz *lzr* embryos injected with *pbx2* morpholinos. Approximately 3 nl of *pbx2/4* morpholino was injected at a concentration of 1 mg/ml.

The *gdf6a* mutant allele (S327), also known as *dark half* was identified in a large-scale chemical mutagenesis screen for disruptions of visual behavior (Muto et al., 2005). The mutation introduces a C-to-A substitution in position 164 of the *gdf6a* ORF, resulting in a premature stop codon and truncated protein (Gosse and Baier, 2009). Homozygous *gdf6a* mutants have small eyes but

otherwise normal external morphology. Homozygous mutant embryos were identified via pair-wise crossing and analysis of Mendelian ratios.

Two splice blocking morpholinos were also used to knockdown Gdf6a function. This allows for normal maternal *gdf6a* function, as *gdf6a* is required for patterning the early embryo, but inhibits zygotic *gdf6a* function prior to eye development. The first morpholino binds to the splice donor site (MO1-GCAATACAAACCTTTTCCCTTGTCC) of the exon 1 – intron 1 boundary, while the second binds splice acceptor site of the intron 1 - exon 2 boundary (MO2-GAGATCGTCTGCAAGATAAAGAGAA) in the *gdf6a* pre-mRNA transcript. Both morpholinos result in the production of a *gdf6a* mRNA molecule with a frameshift mutation in the *gdf6a* open reading frame. To ensure specific effects, both *gdf6a* morpholinos were co-injected with a translation blocking morpholino directed against *p53* (GCGCCATTGCTTTGCAAGAATTG), which has been shown to reduce the severity of morpholino induced off-target effects (Robu et al., 2007). Injections consisted of 5-10 ng of *gdf6a* morpholino, and 2 ng of *p53* morpholino per embryo. All data shown are from embryos injected with *gdf6a* MO1 unless noted, however injections with MO2 produced the same phenotypes (Figure 2-1). In addition, we show that reducing the binding affinity of *gdf6a* MO1 by introducing 5 base pair mis-matches results in no ocular or skeletal defects when injected (at the same concentration as *gdf6a* MO1) into zebrafish embryos (Figure 2-2). Effectiveness of the morpholinos for reducing the level of properly spliced *gdf6a* mRNA was confirmed with RT-PCR (Figure 2-3). All wildtype embryos were injected with 2 ng of *p53* morpholino.

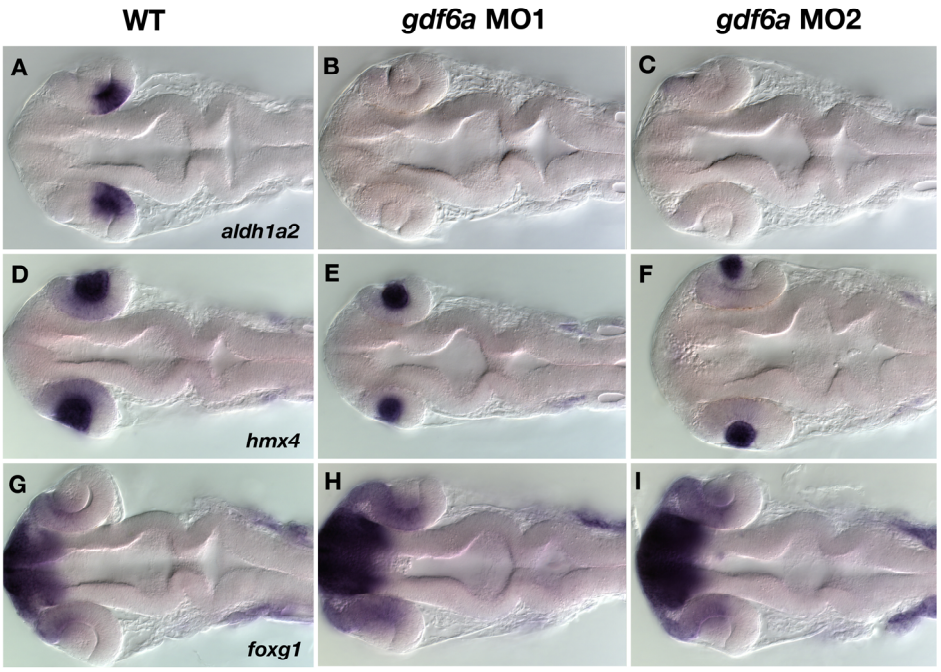

Figure 2-1: Inhibition of *gdf6a* mRNA splicing using two non-overlapping morpholinos produce the same gene expression phenotypes. The expression of *aldh1a2*, normally found in the dorsal retina (A) is absent in embryos injected with either MO1 (B) or MO2 (C). The expression of *hmx4* is found in the lens and retina in wildtype embryos (D), and is reduced in the retina but unaffected in the lens in embryos injected with either MO1 (E) or MO2 (F). The expression of *foxg1* is found in the retina (presumptive nasal domain) in wildtype embryos (G), and is expanded toward the presumptive temporal domain in embryos injected with either MO 1 (H) or MO2 (I).

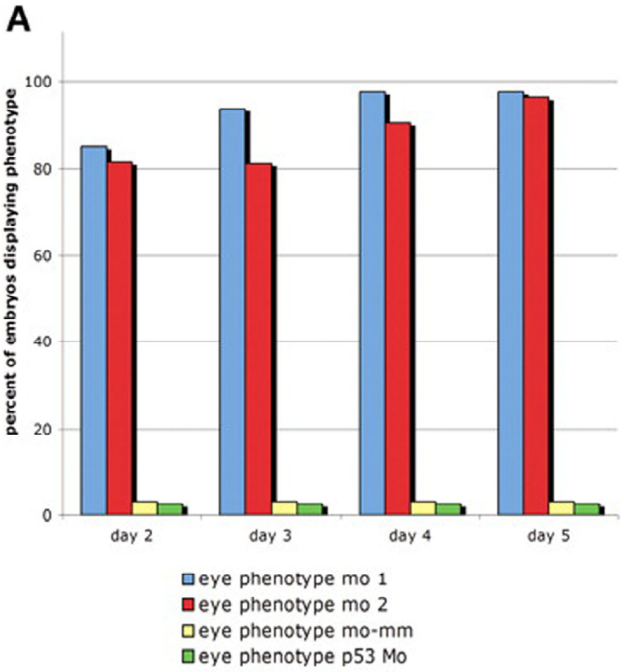
A
percent of embryos displaying phenotype
100
80
60
40
20
0
day 2
day 3
day 4
day 5
eye phenotype mo 1
eye phenotype mo 2
eye phenotype mo-mm
eye phenotype p53 Mo

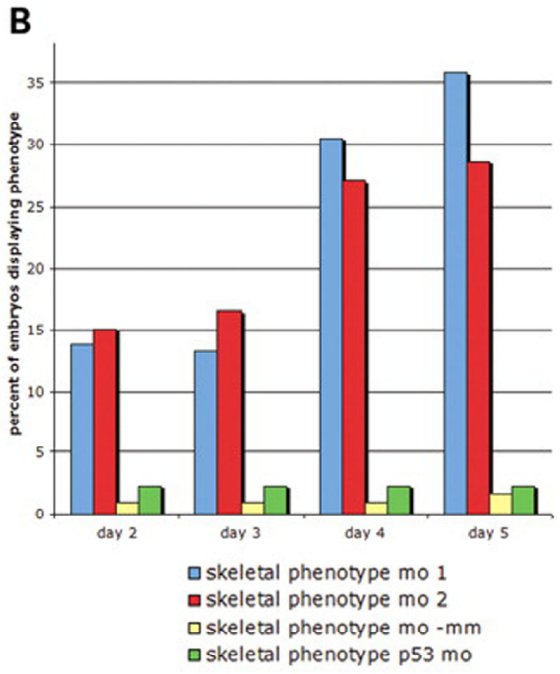
B
percent of embryos displaying phenotype
35
30
25
20
15
10
5
0
day 2
day 3
day 4
day 5
skeletal phenotype mo 1
skeletal phenotype mo 2
skeletal phenotype mo -mm
skeletal phenotype p53 mo

Figure 2-2: Injection of a 5 base-pair mis-matched morpholino demonstrates the specificity of *gdf6a* induced ocular and skeletal phenotypes. (A) Eye phenotypes, including microphthalmia and coloboma, are detected at high levels in embryos injected with either of the two non-overlapping (properly targeted) morpholinos. A similar trend is observed in (B), whereby injection of the properly targeted morpholinos produced kinked tails suggesting axial patterning defects. Injections of the mis-matched morpholino did not produce any discernable phenotype, nor did injection with *p53* morpholino on its own.

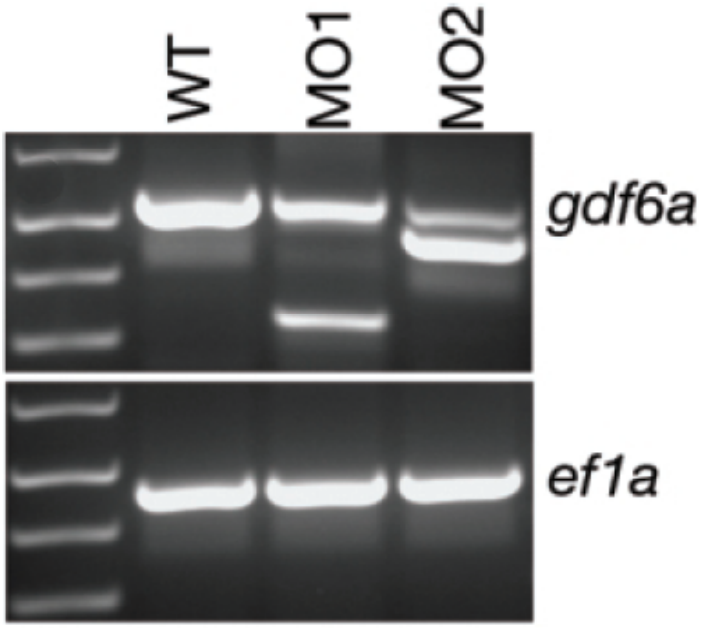

Figure 2-3: RT-PCR confirms that injection of two non-overlapping *gdf6a* morpholinos reduces the quantity of properly spliced *gdf6a* transcripts. The level of properly splice *gdf6a* transcript (upper band in lanes 3 and 4) is reduced compared to wildtype (lane 2). Blocking wildtype splicing with either morpholino causes the spliceosome machinery to utilize a cryptic splice site within the exonic sequence, creating a transcript lacking the lone intron and part of the coding sequence, thus creating a smaller transcript (lower band in lanes 3 and 4). Sequencing of the lower bands in lanes 3 and 4 confirmed the missing coding sequence.

For inhibition of Tbx5, a translation blocking morpholino was utilized (GAAAGGTGTCTTCACTGTCCGCCAT; (Ahn et al., 2002). To prevent off-target effects, co-injection with the *p53* morpholino was also performed. Each embryo was injected with 5 ng of *tbx5* morpholino and 2 ng of *p53* morpholino and compared to wild-type embryos injected with 2 ng of *p53* morpholino.

Inhibition of Bmp4 was accomplished using a *bmp4* splice blocking morpholino (GGTGTTTGATTGTCTGACCTTCATG; (Chocron et al., 2007). This morpholino phenocopies a *bmp4* null mutant (Stickney et al., 2007), causing mildly dorsalized embryos when injected at a dose of 6 ng per embryo. The *bmp4* morpholino was co-injected with 2ng of *p53* morpholino and compared to wild-type embryos injected with 2ng of *p53*morpholino.

For *in situ* analysis, anti-sense probes were designed to either the coding sequence or 5' UTR of the gene of interest. Probes were generated using two different methods: Some probes were generated by incorporating a T7 or T3 promoter onto the 5' end of the reverse primer used to clone the probe sequence, and has been described previously (Thisse and Thisse, 2008, Table 2-1). Alternatively, a number of sequences were subcloned into Topo4 (Invitrogen), or other suitable vectors for transcription of antisense sequences, using either the T7, T3, or Sp6 promoter depending on sequence orientation (Table 2-2). Antisense probes were then directly transcribed from purified PCR products. For *in situ* analysis, embryos were fixed overnight in 4% PFA in PBS, and subsequently rinsed 5 times in PBST. Embryos were permeabilized using Proteinase K treatment (10 ug/ml). Permeabilization was carried out for 30 seconds for young

Table 2-1: Primer sequences for anitsense PCR based RNA probes

Gene	Forward Primer (5'-3')	Reverse primer (5'-3')	Size (bp)	T(m)
*bmp4**	GCCGCTAAACGGAGACTCTTACC	GGGTCGCTTGGCTATGTGTTTC[1]	1278	52.0
*cad**	CGACCCCAACTCCTTTACTATGGC	TACGAGGTGGCAGAATGAACCG[1]	1076	52.0
*ccnf**	CTGCTGCCTGTTATCAAGCGAC	AAAGTGCTCGGTGTCTCTCTCG[1]	1032	52.0
foxg1	AAATGGCTTGAGTGTTGACAGACTCG	AAGAATGTGACCTGCATGGTGGTGAC[2]	1164	55.0
*foxi2**	AACCCCTCAGAGACGAGCACACTC	GCTGCGTAAAATCCCCCAAATG[1]	1012	54.0
*foxn4**	GAAGGTAGAGAATAAGATGAGCGGC	GCTTGGCAACACACCCATAGTC[1]	1238	52.0
*fpgs**	GCGGTATCTCGTCTTTAGGTATCG	GGCTCCTCCCACCAAGTGTAAG[1]	1025	52.0
myca	GTCTGACAGCAACTCAAATCGACTAAACG	GAACCTTTATGATTGAGTGAAAACATTGAAAACG[2]	658	53.0
mycn	AGACGCAACCACAACATCTTGG	GAACCCATTGACCCAGTTCTATGAACC[2]	1114	54.0
*uhfr1**	GGCAAACAGATGGAGGATGGTC	ACTGGCGTCATTACGACAATCG[1]	951	52.0
*tbx2b**	ATGGCTTACCACCCTTTCCACG	CGTCTTTCTTCTCCGCAATAGGC[1]	1144	53.0
*tbx4**	CCCTATCTTGACACGACATCATCTG	AGGTATGCTGTTTGTGCTTGGC[1]	830	52.0
*tbx5**	GAGGGAAGTTCGCTATCAACCG	TCCATTGTTTTCATCCGCCTTG[1]	713	52.0

1) 5' end of reverse primer modified with T7 promoter sequence TAATACGACTCACTATAGGG

2) 5' end of reverse primer modified with T3 promoter sequence CAATTAACCCTCACTAAAGG

* Probe construction by author

Table 2-2: Vector based antisense RNA probes used in this thesis

Gene	vector	antibiotic	cut	synthesis
aldh1a2	pSport	Carbacillin	EcoR1	Sp6
aldh1a3[1]	pCR4-Topo	Carbacillin	Not1	T3
atoh1a[1]	pCR4-Topo	Carbacillin	Pme1	T7
atoh7[1]	pCR4-Topo	Carbacillin	Pme1	T7
bambi	pCR4-Topo	Carbacillin	Not1	T3
crx[1]	pCR4-Topo	Carbacillin	Not1	T3
ccng1[1]	pCR4-Topo	Carbacillin	Not1	T3
cryba1b[1]	pCR4-Topo	Carbacillin	Pme1	T7
cryba2a[1]	pCR4-Topo	Carbacillin	Not1	T3
cx23[1]	pCR4-Topo	Carbacillin	Not1	T3
efna2	pSport	Carbacillin	EcoR1	Sp6
efna5a	pCR-Topo4	Carbacillin	Not1	T3
efnb2a	pCR-Topo4	Carbacillin	Not1	T3
ephb2[1] *(c11)*	pCR4-Topo	Carbacillin	Not1	T3
ephb3[1] *(c8)*	pCR4-Topo	Carbacillin	Pme1	T7
fabp7	pSport	Carbacillin	EcoR1	Sp6
gdf6a	pBSKII	Carbacillin	Not1	T7
hmx1	Pcr4-Topo	Carbacillin	Not1	T3
hmx4	pSport	Carbacillin	EcoR1	Sp6
lim2.3[1]	pCR4-Topo	Carbacillin	Not1	T3
mych	pBSK	Carbacillin	Xho1	Sp6
nat10	pSport	Carbacillin	EcoR1	Sp6
otx2	Unknown	Carbacillin	Not1	T7
rx1	pCR4-Topo	Carbacillin	Not1	T3
rx2	pCR4-Topo	Carbacillin	Not 1	T3
rx3	pCR-Topo4	Carbacillin	Pme1	T7
vax2	pCR4-Topo	Carbacillin	Not1	T3

[1] Sequence cloning and probe construction by author

embryos (3, 6, or 10 somites) 3 minutes for 18-24 hpf embryos, and 20 minutes for embryos between 24-48 hpf. Embryos were then refixed in 4% PFA for 2 minutes, and washed 5 x 5 minutes in PBST. Embryos were then incubated in prehybridization solution (50% formamide; 50 μg/ml heparin; 5X SSC 500 μg/ml yeast tRNA; 0.1% Tween-20) for 1 hour at 65^0C. Probes were diluted 1/200 in hybridization solution, and added to embryos for overnight incubation. Coloration reactions were performed using a combination of NBT and BCIP, or using BM Purple (Roche). Embryos were manually deyolked, and photographed using a Zeiss AxioImager Z1 compound microscope and an Axiocam HR digital camera or on an Olympus stereoscope with a Q-imaging micropublisher camera.

meis dominant negative RNA construction and injections

meis.1.1ΔC was constructed by creating a stop codon after residue 238 and has been described previously (Waskiewicz et al., 2001). This RNA molecule lacks the DNA binding homeodomain, but has a functional Pbx binding domain. *pbx4ΔC* contains only the N-terminus of the Pbx4 protein, and has been described previously (Choe et al., 2002). Expression of *pbx4ΔC* sequesters Meis in the cytoplasm, therefore reducing its ability to participate in nuclear complexes needed for downstream gene transcription. To produce a *meis* dominant negative phenotype, 5 nl of both *meis.1.1ΔC* and *pbx4ΔC* were injected into one cell embryos at a concentration of 1 mg/ml.

Microarray analyses

For each Pbx microarray hybridization (performed by Dr. Andrew Waskiewicz), target cDNA was synthesized from either mz *lzr,* or *lzr* embryos injected *pbx2* morpholino. cDNA was generated from RNA templates isolated at both 18 hpf and 28 hpf, using Trizol solution. cDNA was labeled with either Cy3 or Cy5, and hybridized to microarrays containing 8448 cDNA probes, including 768 controls spots (e.g. negative, positive, and normalization controls). An Axon scanner (Molecular Devices) and Genepix software (Molecular Devices) were to determine the intensities of each spot and normalize the data. All experiments were conducted in biological duplicate while simultaneously switching fluorescent labeling compounds.

Two separate sets of microarrays were conducted for identification of Gdf6a downstream genes. Firstly, total RNA was isolated from whole zebrafish *gdf6a* morphant embryos at 24 hpf. For the second set of microarray experiments, total RNA was isolated from homozygous *gdf6a* mutant eyes and wildtype sibling eyes at 2 dpf. For whole embryo RNA isolation, *gdf6a* morphant embryos were immediately disrupted and homogenized at 24 hpf. For identification of eye specific *gdf6a* targets at 2 dpf, embryos were place in a tricane solution (Sigma) for dissection, and eye tissue was immediately placed in RNAlater (Ambion) thereafter. RNA was isolated using an RNAaqueous kit (Ambion), and run on a bioanalyszer (Agilent) for quantification and assessment of mRNA integrity. Labeled (Cy3 or Cy5) cRNA was generated from 100 ng of total RNA using Agilent's QuickAmp kit. One Cy5 labeled sample was competitively hybridized

against one Cy3 using Agilent's 44K gene expression microarrays 65^0C for 17 hours. Arrays were hybridized in triplicate, with an additional array hybridized with reverse labeled cRNA from one biological replicate. Data was extracted using Agilent's Feature Extraction Software, and analyzed using ArrayStar (DNASTAR, Madison, WI).

Eye cross sections and Immunohistochemistry (*pbx 2/4 null embryos)*

Wild type and *pbx2/4* morpholino injected embryos were grown to 5 dpf, then fixed in 4% PFA. Embryos were embedded in Spurr's Resin for 1 μm ultramicrotome sectioning with a diamond blade, and stained with Richardson's blue for visualization of retinal layers. Sections were visualized using Zeiss Axioimager Z1 and photographed with Zeiss Axiocam HR. Retinal pigmented epithelium and total eye area were quantified using ImageJ software (National Institutes of Health, Maryland, USA).

The acetylated tubulin antibody (Sigma) stain protocol has been published previously (Kramer-Zucker et al., 2005). Briefly, zebrafish embryos (3 dpf) were fixed in Dent's fix (80% methanol/20%DMSO), and primary antibody incubation was completed overnight at 4ºC (1:500) after blocking in PBSDBT (1% DMSO/1% BSA/0.5% tween-20, 10% goat serum). After 5 washes in PBST, a secondary antibody (anti-mouse Alexaflour 546, Molecular Probes, 1:1000), was added and incubated overnight at 4ºC.

For zpr-1 (ZIRC, Eugene ON, 1:200) staining, embryos were fixed in 4% PFA overnight at 4ºC. Embryos were blocked in PBS 2% goat serum, 2 mg/ml

BSA, 0.1% triton X-100. After washing in PBSDTT, a secondary antibody (anti-mouse Alexaflour 588, Molecular Probes) was diluted 1:1000 and incubated overnight at 4ºC. Embryos were mounted in 70% glycerol for imaging on a SP2 confocal microscope (Leica) using both 20X and 40X (oil) objective.

***Eye cross sections and Immunohistochemistry* (*gdf6a morphant embryos*)**

Smad phosphorylation assays were carried out using a rabbit polyclonal antibody specific for phosphorylated Smads 1/5/8 (Cell Signaling, Danvers, MA). Embryos were fixed in 4% paraformaldehyde, and permeabilized with Proteinase K (10 ug/ml) for 1 minute (2 somite -10 somite embryos), or for 3 minutes (24-28 hpf embryos). Embryos were blocked in 10% goat serum, 1% BSA, 0.1% Triton X-100, and incubated overnight at 4^0 C in the primary antibody. Embryos were washed 5 times for 5 min in PBSDTT. Embryos were then incubated in anti-rabbit Alexa Fluor 488 or 586 (Invitrogen, Carlsbad, CA) for 2 hours at room temperature and washed 5 times for 15 minutes, in PBSDTT. Images were taken using either a Zeiss 510 or Leica TCS-SP2 confocal system.

For analysis of lens development in *gdf6a* morphant fish, 4 dpf wildtype and morphant larvae were fixed in 4% PFA, 5% sucrose, embedded and 10 μm cryosections were cut as previously described (Barthel and Raymond, 1990). Sections were stored at -20^0C, and were allowed to adhere for 1 hour at room temperature before rehydratation for 30 minutes in PBST prior to use. Sections were blocked in 5% BSA/1% goat serum in PBST for 1 hour at room temperature. The Zl-1 monoclonal antibody (ZIRC, Eugene OR) was added in blocking

solution (1/100) for overnight incubation at 4^0C. Embryos were then washed 5 times for 5 minutes in PBS and labeled with Phalloidin Alex Flour 568 (1/50) and Alexa Flour 488 (anti-mouse) for visualization of Zl-1. Hoechst nuclear stain was added at a concentration of 10 mg/ml. Slides were washed 5 times for 5 minutes in PBS, and mounted in 70% glycerol for imaging with a Zeiss Axioskop 2 and a RetigaEXi camera.

DiI and DiO RGC labeling

Two lipophylic dyes, DiI and DiO (Molecular Probes), were used to label retinal ganglion cell axons in *pbx* null embryos. DiI was dissolved in dimethylformamide (DMF), at a concentration of 12.5 mg/ml. DiO was dissolved in chloroform at a concentration of 12.5 mg/ml. Embryos were raised in 0.0015% phenylthiourea (PTU) to inhibit pigment formation and fixed in 4% paraformaldhyde at both 3.5 dpf and 5.5 dpf. Embryos were mounted dorsal side up in 1% in low melting point agrose for injections. DiI was injected into the dorsol-temporal domain of the right eye, while DiO was injected into the ventral-nasal domain of the right eye. Embryos were removed from the agrose and incubated in PBS 0.0001% tween-20 overnight at 28°C. Embryos were flat mounted in 70% glycerol, dorsal side up.

For labeling of all retinal ganglion cell axons in *gdf6a* mutant fish, DiI was injected into the entire RGC layer, or DiI and DiO were injected into the dorsal and ventral domains, respectively. Embryos were incubated overnight in 5 ug/ml Hoechst nuclear stain to outline the optic tectum, and washed 2 x 10 minutes in

PBS + 0.0001% Tween-20. All imaging was accomplished using an SP2 confocal microscope (Leica), using 20X objective.

Inhibitor studies

Dechorionated Embryos were incubated in Dorsomorphin (100 μM; BioMol, PA) beginning at tailbud stage until fixation at 28 hpf. Dorsomorphin was dissolved in DMSO and added to wildtype fish in fishwater for analysis. Wildtype embryos were incubated in an equal volume of DMSO/fishwater. For analysis of embryos at 4 dpf, dorsomorphin was added to embryo media containing 0.003% PTU at a concentration of (25 μM) starting at 2 dpf, and continuing until fixation.

Bone and cartilage staining

To visualize pharyngeal jaw cartilages and ossified bone, Alcian Blue and Alizarin Red staining were utilized. Embryos were fixed overnight at 4^0C, and washed 2 X 5 minutes in 80% ethanol/20% glacial acetic acid. Embryos were incubated overnight in 0.1% Alcian Blue, dissolved in 80% ethanol/20% glacial acetic acid. Embryos were then re-hydrated in PBST (5 minute washes in 20% PBST/80% ethanol, 40% PBST/60% ethanol, 60% PBST/40% ethanol, 80% PBST/20% ethanol, 100% PBST), and incubated in 3% H_20_2/1% KOH until all eye pigment was removed. Tissue was cleared in 0.05% trypsin dissolved in saturated Sodium tetraborate for 2 hours. Embryos were then washed 2 x 5

minutes in PBST, and incubated overnignt in 0.1% Alizarin Red dissolved in water.

qRTPCR analysis of rp9 expression in gdf6a morphants

RNA was isolated from from whole WT and *gdf6a* morphant embryos using Trizol reagent (Invitrogen). Three micrograms of RNA was used to synthesize cDNA using Suprscript III (Invitrogen) and 1 ul of oligodT primer. We performed standard curve analysis to validate primer efficiency using both *Rp9* and *odc1* (internal control), using a 1/10 dilution of cDNA. qRTPCR was performed using ΔΔCT analysis using a 1/40 dilution of cDNA and SybrGreen reagents (Applied Biosystems) on a ABIStepOne real time cycler (Applied Biosystems). Primer sequences for the *rp9* aplicon were as follows:

Forward, 5'-GAGGTCCAGAAACTCAAGCATGT-3',

reverse, TGGTTTCTCGGTGTCTTCCTTTAT-3'

Generation of transgenic fish

To drive Bmp-pathway genes specifically in the early eye fields, we used the Tol2kit multi-site Gateway cloning system (Kwan et al., 2007). A 3.6 Kbp fragment of the medaka *rx3* promoter (Kwan et al., 2007) was amplified by PCR and cloned into the pDONRP4-P1R 5' entry vector to generate p5E-*rx3*. Alterantively, a 2kb fragment of the *hsp70* promoter was amplified by PCR and cloned into pDONRP4-P1R 5' entry vector to create p5E-hsp70. Full length ORFs for zebrafish *gdf6a*, *smad7*, and a constitutively active version of human *BMPR1a* (a kind gift from the Niswander lab; Zou et al., 1997) were cloned into the

pDONR221 middle entry vector to generate pME-*gdf6a*, pME-*smad7* and pME-*caBMPR1a*. Four-way recombination reactions using LR clonase II + (Invitrogen) between p5E-*rx3*, p3E-polyA, pDestTol2pA2, and one of pME-*gdf6a*, pME-*smad7* or pME-*caBMPR1a* were performed to generate pDestTol2pA2;*rx3*:*gdf6a*-polyA, pDestTol2pA2;*rx3*:*smad7*-polyA and pDestTol2pA2;*rx3*:*caBMPR1a*-polyA constructs. Similar reactions were also carried out using p3E-IRES-EGFPpA in place of the p3E-polyA plasmid to yield pDestTol2pA2;*rx3:gdf6a*-IRES-EGFPpA, pDestTol2pA2;*rx3:caBMPR1a*-IRES-EGFPpA, and pDestTol2pA2;*rx3:smad7*-IRES-EGFPpA constructs. To create constructs to express *gdf6a* under the control of the *hsp70* promoter, Four-way recombination reactions were carried out between p5E-*hsp70,* p3E--IRES-EGFPpA, pDestTol2pA2, and p5E-*hsp70* to yield pDestTol2pA2;*hsp70:gdf6a*-IRES-EGFPpA. Transient transgenic zebrafish embryos were created by injecting 50 pg of the Tol2 constructs along with 25 pg of Tol2 transposase mRNA synthesized from NotI linearized pCS2FA-transposase plasmid using the SP6 mMessage mMachine kit (Ambion, Austin TX). For heat shock analysis in embryos expressing pDestTol2pA2;*hsp70:gdf6a*-IRES-EGFPpA, embryos were heast shocked in a 37^0C water bath for 1 hour, beginning at 22 hpf.

Bibliography

Ahn, D. G., et al., 2002. T-box gene tbx5 is essential for formation of the pectoral limb bud. Nature. 417**,** 754-8.

Barthel, L. K., Raymond, P. A., 1990. Improved method for obtaining 3-microns cryosections for immunocytochemistry. J Histochem Cytochem. 38**,** 1383-8.

Chocron, S., et al., 2007. Zebrafish Bmp4 regulates left-right asymmetry at two distinct developmental time points. Dev Biol. 305**,** 577-88.

Choe, S. K., et al., 2002. Meis family proteins are required for hindbrain development in the zebrafish. Development. 129**,** 585-95.

Gosse, N. J., Baier, H., 2009. An essential role for Radar (Gdf6a) in inducing dorsal fate in the zebrafish retina. Proc Natl Acad Sci U S A. 106**,** 2236-41.

Kimmel, C. B., et al., 1995. Stages of embryonic development of the zebrafish. Dev Dyn. 203**,** 253-310.

Kramer-Zucker, A. G., et al., 2005. Cilia-driven fluid flow in the zebrafish pronephros, brain and Kupffer's vesicle is required for normal organogenesis. Development. 132**,** 1907-21.

Kwan, K. M., et al., 2007. The Tol2kit: a multisite gateway-based construction kit for Tol2 transposon transgenesis constructs. Dev Dyn. 236**,** 3088-99.

Muto, A., et al., 2005. Forward genetic analysis of visual behavior in zebrafish. PLoS Genet. 1**,** e66.

Popperl, H., et al., 2000. lazarus is a novel pbx gene that globally mediates hox gene function in zebrafish. Mol Cell. 6**,** 255-67.

Robu, M. E., et al., 2007. p53 activation by knockdown technologies. PLoS Genet. 3**,** e78.

Stickney, H. L., et al., 2007. Zebrafish bmp4 functions during late gastrulation to specify ventroposterior cell fates. Dev Biol. 310**,** 71-84.

Thisse, C., Thisse, B., 2008. High-resolution *in situ* hybridization to whole-mount zebrafish embryos. Nat Protoc. 3**,** 59-69.

Waskiewicz, A. J., et al., 2001. Zebrafish Meis functions to stabilize Pbx proteins and regulate hindbrain patterning. Development. 128**,** 4139-51.

Waskiewicz, A. J., et al., 2002. Eliminating zebrafish pbx proteins reveals a hindbrain ground state. Dev Cell. 3**,** 723-33.

Zou H., et al., 1997. Distinct roles of type I bone morphogenetic protein receptors in the formation and differentiation of cartilage. Genes Dev. 11, 2191-203.

Chapter 3

Pbx homeodomain proteins pattern the zebrafish retina and tectum

A version of this chapter has been previously published.

***French CR**, Erickson T, Callander D, Berry KM, Koss R, Hagey DW, Stout J, Wuennenberg-Stapleton K, Ngai J, Moens CB, Waskiewicz AJ.*
Pbx homeodomain proteins pattern both the zebrafish retina and tectum.
BMC Dev Biol. 2007 Jul 16;7:85.

Introduction

Vertebrate embryos use a combination of transcription factors to specify position along the anterior-posterior axis. Of particular importance is the Pbx (pre-B cell leukemia homeobox)-family of TALE (Three Amino acid Loop Extension)-class transcription factors, which are required globally to pattern the anterior-posterior axis of the developing vertebrate embryo. Using mouse knockout and zebrafish knockdown models, researchers have shown that Pbx proteins are required to specify cell fate in the midbrain, hindbrain, somites, pancreas, and blood (Dutta et al., 2001; Okada et al., 2003; Waskiewicz et al., 2001; Waskiewicz et al., 2002). In the hindbrain, trimeric DNA-binding complexes of Pbx, Hox and Meinox (Meis/Pknox) proteins specify rhombomere identity. In the midbrain, Pbx cooperates biochemically with Engrailed (Eng) proteins to maintain both midbrain-hindbrain and the diencephalic-mesencephalic boundaries (Erickson et al., 2007).

Pbx clearly also plays a role in patterning regions outside of the midbrain and hindbrain. For example, mouse knockouts have demonstrated a critical role for Pbx during pancreatic development, in which interactions between Pbx and Insulin promoter factor 1 (Ipf1) are required for transcriptional activity, and subsequent expansion of pancreatic cell lineages (Dutta et al., 2001). Pbx also plays a role in the development of blood, as Pbx – Prep1 (also known as Pknox1) complexes are required for the production of normal populations of CD4 and CD8 T-lymphocytes (Penkov et al., 2005). Furthermore, Pbx - Meis complexes have been implicated in megakaryocyte differentiation in rats, through the ability to

initiate transcription from the platelet factor 4 (PF4) promoter (Okada et al., 2003). Recently, it has been shown during the development of skeletal muscle that Pbx is constitutively bound to the *Myogenin* promoter, can bind directly to the bHLH transcription factor MyoD, and is thus required for the development of muscle cell fates (Berkes et al., 2004). A zebrafish mutant, *lazarus (lzr)*, that contains a null mutation in the *pbx4* gene (Popperl et al., 2000), displays global defects in embryonic patterning including hindbrain, muscle, blood, and midbrain tissues.

The Meinox (Meis/Pknox/Prep) family of TALE-class transcription factors are well characterized as DNA-binding cofactors for both Pbx and Hox proteins (Moens and Selleri, 2006). Zebrafish contain at least six *meis* genes that are expressed dynamically in the embryo (Biemar et al., 2001; Vlachakis et al., 2000; Waskiewicz et al., 2001; Zerucha and Prince, 2001). In addition, zebrafish possess at least two *pknox/prep* genes that are both widely expressed (Deflorian et al., 2004). *meis* genes are prominently expressed in the developing retina (Biemar et al., 2001; Vlachakis et al., 2000; Waskiewicz et al., 2001; Zerucha and Prince, 2001) suggesting a role for *meis* in regulating eye formation or patterning. In zebrafish, over-expression of *hoxb2* throughout the embryo causes ectopic expression of hindbrain markers exclusively within the retina, demonstrating the existence of retinal specific Hoxb2 competency factors (Yan et al., 1998). Pbx and Meinox proteins function as two of these retinal Hoxb2-competency factors, demonstrating that both Pbx and Meis can function in the retina (Cooper et al., 2003; Hisa et al., 2004; Popperl et al., 2000; Waskiewicz et al., 2001). The idea

that Pbx and Meinox proteins play a role in eye formation is supported by studies in Drosophila, where the *pbx* homolog *extradenticle* (*exd)* and the *meis* homolog *homothorax* (*hth)* inhibit eye formation (Pai et al., 1998), and in mice where the *Pknox1* hypomorphic and *Meis1* knockout phenotypes include defects in retinal development (Ferretti et al., 2006; Hisa et al., 2004).

Zebrafish make an excellent model for the study of retinal development. The optic primordium is distinct from surrounding tissues as early as 12 hours post fertilization hours post fertilization (hpf), and by 24 hpf, eyecups have developed to include lens tissue and the surrounding neural retina (Schmitt and Dowling, 1994). By 32 hpf, the first post-mitotic neurons have differentiated (Burrill and Easter) and by 50 hpf, lamination is evident across the retina. Two partially redundant *pbx* genes, *pbx2* and *pbx4,* are expressed during early development when the optic primordium and optic cup are forming. The other zebrafish *pbx* genes, *pbx1* and *pbx3.1*, are expressed more strongly starting at 24 hpf. Thus, inhibition of Pbx2 and Pbx4 in a homozygotic *lazarus* (*lzr)* (*pbx4* mutant) embryo allows for analyses of development in the absence of Pbx function, prior to 24 hpf (see methods). The retina of *lazarus (pbx4*$^{-/-}$*)* zebrafish embryos is noticeably smaller than wild type embryos, but no analysis of patterning has yet been undertaken.

This chapter provides an analysis of Pbx and Meis function in the developing zebrafish retina, as well as a role for Pbx in patterning the tectum, and includes a microarray screen for *pbx* dependent transcripts in zebrafish to identify gene regulatory networks downstream of this critical homeodomain protein

(performed by Dr. Andrew Waskiewicz). We propose a model in which Pbx functions to specify regional identity in the developing zebrafish retina via activation of the dorsal specific growth factor *gdf6a*.

Results

Retinal laminar structure is normal but retinal ganglion cell axon outgrowth is aberrant in pbx2/4 null embryos

Previous studies have demonstrated a clear role for the homeodomain transcription factor Pbx in regulating cell fates in the hindbrain and at the midbrain-hindbrain boundary. The eyes of *lazarus* (*lzr* or *pbx4*$^{-/-}$) embryos are distinctly smaller than their wild type counterparts, indicating that Pbx is required in this tissue as well (Popperl et al., 2000). As a first step towards dissecting the role of Pbx proteins in eye development, we compared eye morphology between wild type and *pbx2/4* null (*pbx4*$^{-/-}$; *pbx2/4*MO) fish at 5 days post-fertilization (dpf). The laminar structure of the retina appears relatively normal in *pbx2/4* null embryos (compare wild types in Figure 3-1 A, B to *pbx2/4* nulls in Figure 3-1 D, E) and the optic nerve exits the eye in the correct location. All nuclear layers are clearly visible in *pbx2/4* null eyes, including the inner most retinal ganglion cell layer, and the outermost nuclear layer containing the photoreceptor cells. The retinal pigmented epithelium (RPE) of *pbx2/4* null embryos is thickened (9.14 +/- 1.9 % of total eye area) (Figure 3-1F) in comparison to wild type controls (5.95 +/- 0.3 % of total eye area, $p<0.05$) (Figure 3-1 C), indicating that Pbx has a role in regulating RPE differentiation. There is also a distinct change in layer

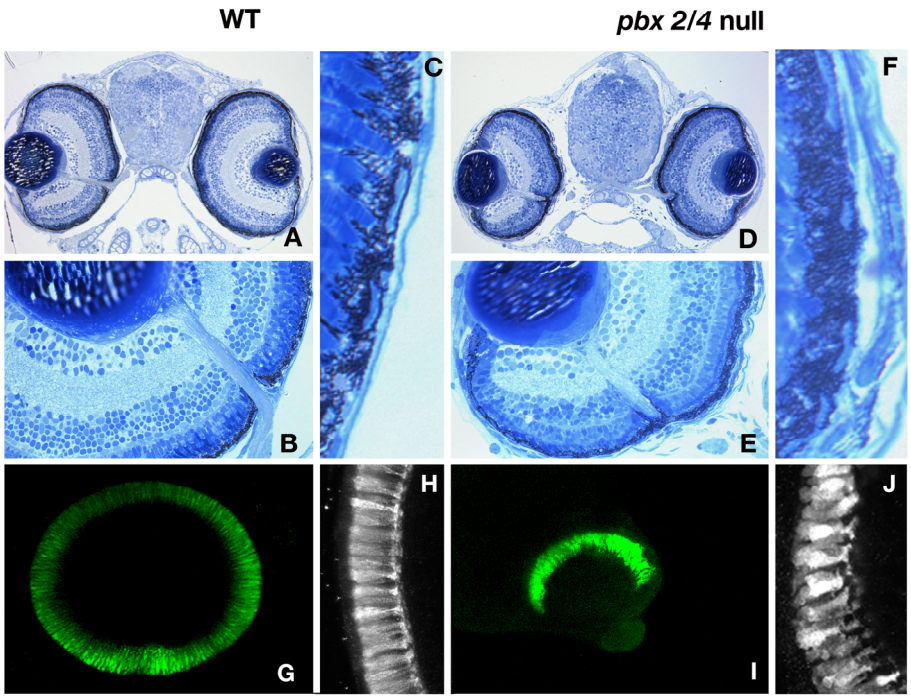

Figure 3-1: The laminar structure of *pbx2/4* null eyes is normal after 5 days of development. All laminar layers are present and in both wild type (A and B) and, and *lzr* mutants injected with *pbx2/4* morpholinos (D and E). We note a consistent decrease in eye size in *pbx2/4* null embryos, but the proportion of eye area occupied by the retinal pigmented epithelium in morphants is significantly increased (F verses C). The relative position of the optic nerve is similar in both wild type and morphant embryos. The retinal photoreceptor layer is absent in the ventral domain of the eye in *lzr* mutants injected with *pbx2/4* morpholinos (I) when compared to wildtype (G) and is disorganized (compare H, wildtype, with J, *lzr* mutants injected with *pbx2/4* morpholinos). Photoreceptor labeling was accomplished using the zpr-1 monoclonal antibody.

morphology, at the interface of the RPE and photoreceptor layer. In addition to thickened RPE, *pbx2/4* null embryos have a disorganized photoreceptor layer (compare Figure 3-1 H with 3-1 J), which likely contributes to the aberrant morphology seen at the interface. These data suggest that while *pbx2/4* null eyes are smaller than their wild type counterparts, Pbx proteins are not required for establishing the laminar structure of the eye.

In wild type embryos, retinal ganglion cells innervate the optic tectum to form an inverse topographic map of the eye. For example, axons that originate in the temporal retina innervate the anterior tectum (Figure 3-2 A, C), while axons that originate in the nasal retina innervate the posterior tectum (Figure 3-2 B, C). In embryos lacking both *pbx2* and *pbx4*, no topographic mapping of the RGC axons is observed at 3.5 or 5.5 dpf. In the majority of embryos (6/7 at 3.5 dpf, 11/14 5.5 dpf) the primary axon bundle projects toward the optic tectum, but axons appear stalled before entry to the tectum as no branching or outgrowth is observed (Figure 3-2 D-F, J-L). These results suggest that Pbx proteins regulate transcriptional pathways that control RGC axonal outgrowth.

Whole embryo microarray analysis of pbx mutants identifies known hindbrain patterning genes

In the presumptive hindbrain, Pbx2 and Pbx4 functions are critically required for initiation of *early growth regulator 2b* (*egr2b,* previously *krox20)*, *musculoaponeurotic fibrosarcoma oncogene family protein B (mafb,* previously

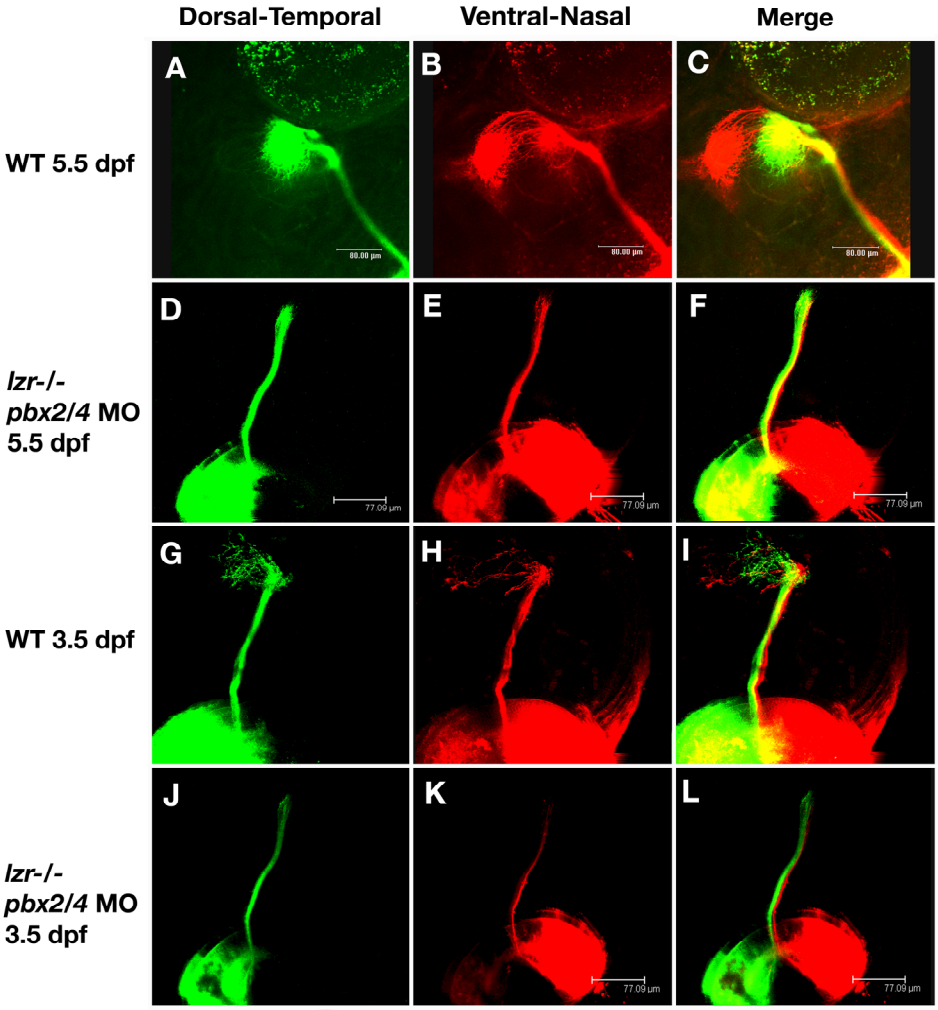
Dorsal-Temporal
Ventral-Nasal
Merge
WT 5.5 dpf
lzr-/-
pbx2/4 MO
5.5 dpf
WT 3.5 dpf
lzr-/-
pbx2/4 MO
3.5 dpf
A
B
C
D
E
F
G
H
I
J
K
L
80.00 µm
77.09 µm

Figure 3-2: *pbx2/4* null embryos exhibit RGC axonal outgrowth defects. In wild type embryos at 5.5 dpf, Retinal ganglion cells from the dorsal-temopral domain of the retina, and RGCs from the nasal-ventral domain of the retina map to separate locations on the optic tectum (A, B and C). This is also seen at 3.5 dpf (G-I) although the connections on the tectum are more diffuse. In *lzr-/-* mutants injected with *pbx2/4* morpholinos, all RGC axons fail to map onto the optic tectum at both 3.5 dpf (J-L) and 5.5 dpf (D-F).

valentino), *homeobox b1A (hoxb1a)*, *hoxa2b*, and *hoxb2*. To identify Pbx-dependent transcripts that might regulate retinal and tectal patterning, we conducted microarray comparisons between 18 hpf control embryos (*pbx2* MO injected) and *pbx2/4* null embryos (mz *lzr*; *pbx2* MO). Each array contained 8448 cDNA probes, including 768 controls spots (e.g., negative, positive, and normalization controls) derived from a normalized mixed stage zebrafish cDNA library (Clark et al., 2001). We identified 31 transcripts that were down-regulated by at least 2 fold and 284 transcripts that were down-regulated by at least 1.5 fold. We repeated these analyses using two independent biological replicates at 18 hpf, and two biological replicates at 28 hpf. Overall, we identified 366 ESTs that were down-regulated by 1.5 fold in at least two datasets. Student T-tests were conducted on genes of interest based on annotation and known expression patterns. Focusing on clones that were affected at 18 hours, we generated antisense probes and sequence information for 132 EST clones. We examined 70 of these clones by *in situ* hybridization, to which 33 showed Pbx dependence at 18 hpf. Among these clones, we identified *egr2b*, *hoxb3a*, *mafb*, and *engrailed 2b* (*eng2b,* previously *eng3)* (Table 3-1). Each of these clones is expressed in either the midbrain-hindbrain boundary or the hindbrain at 18 hpf and were previously shown to be down-regulated in *pbx2/4* null embryos (Waskiewicz et al., 2001; Waskiewicz et al., 2002). Given this validation, the microarray is clearly capable of identifying *bona fide* Pbx dependent transcripts.

Table 3-1: Expression of Pbx2/4 dependent transcripts at 18 hpf, identified by microarray analysis.

Gene	Expression pattern	Accession	Avg. fold change 18 hpf
egr2b	Rhombomere 3, 5	NM_130997	7.98
mafb	Rhombomere 5	AB006322	2.09
meis3	CNS, neural crest	NM_131778	1.88
eng2b	MHB	NM_131040	2.94
eng2a	MHB	NM_131044	1.78
aldh1a2	Dorsal retina, somites	NM_131850	1.80
tbx5	heart, fin, dorsal retina	NM_130915	1.88
hmx4	lens dorsal retina	NM_001045371	1.38
fabp7	eye, tectum, hindbrain	NM_021272	2.10
efna2	tectum, MHB	BC096783	1.37
nat10	eye, tectum, somites	BC057462	1.39

Fold change: WT/ *pbx2/4* null
MHB, Midbrain/hindbrain boundary
CNS, Central nervous system

Microarray and whole mount in situ analysis demonstrates that Pbx proteins regulate gene expression in the developing retina.

Microarray analysis also uncovered Pbx dependent transcripts expressed specifically in regions outside of the hindbrain, notably including genes expressed in the muscle (Maves et al., 2007) and in the retina and tectum (described in this chapter). Of the 132 ESTs studied, 13 are specifically expressed in the retina, tectum, or both. Three genes, *aldehyde dehydrogenase 1 family, member a2 (aldh1a2*, previously *raldh2*), *T-box 5* (*tbx5)*, and *H6 family homeobox 4* (*hmx4*, ortholog of chick *soho1*) are expressed in the dorsal retina. The transcripts for *aldh1a2,* and *tbx5* are expressed exclusively in the dorsal retina at both 18 and 24 hpf (Figure 3-3 A, C, E, G), while *hmx4* is specific to lens and dorsal retina (Figure 3-3 I, K). To examine retinal patterning in *pbx2/4* null embryos, we performed *in situ* hybridization with these three putative Pbx dependent genes as well as *orthodenticle homolog 2* (*otx2)*, a marker of retinal pigmented epithelium and the optic tectum at 24 hpf . Three of these genes, *aldh1a2*, *tbx5*, *hmx4*, are strongly down-regulated in *pbx2/4* null embryos at 18 hpf (Figure 3-3 B, F, J), thus supporting the microarray findings. At 24 hpf, the expression of *aldh1a2* and *tbx5* is down-regulated (Figure 3-3 D, H), but the expression of *hmx4* is unaffected (Figure 3-3 L). Although we do not observe any change in the expression of *otx2* in the tectum of *pbx2/4* null embryos at 24 hpf, there is a marked expansion of the domain of *otx2* expression to include the entire eye in these embryos (Figure 3-3 K, L). This demonstrates that Pbx proteins may function either directly or indirectly as key repressor of *otx2* expression. Taken

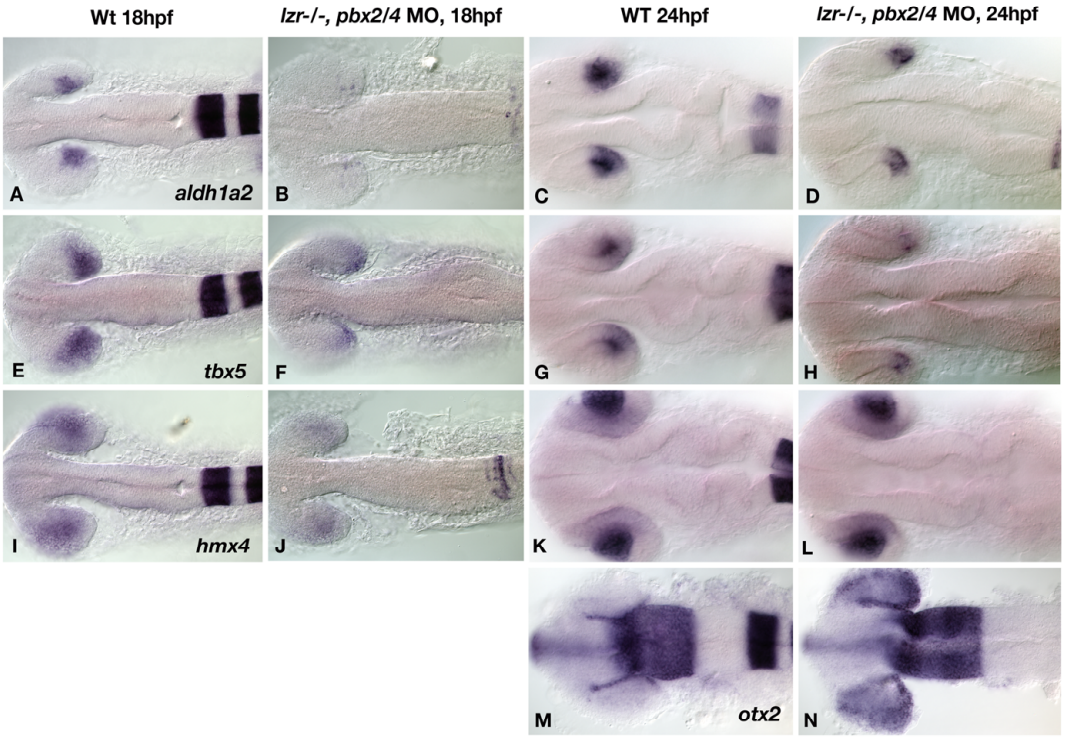

Figure 3-3: Gene expression analysis via *in situ* hybridization shows altered expression of Pbx dependent transcripts in *pbx2/4* null embryos. The expression of *aldh1a2* and *tbx5* is reduced in *pbx2/4* null embryos (B, F, and J), when compared to wild type (A, E, and I) at 18 hpf. At 24 hpf, *aldh1a2* and *tbx5* show reduced expression in *pbx2/4* null embryos (D and H) when compared to wildtype (C and G), while the expression of *hmx4* is unaffected (K and L). The expression of *otx2* is limited to the RPE at the periphery of the eye in wild type embryos at 24 hpf (M), and is expanded to the posterior retina in *pbx2/4* null embryos (N). All embryos were hybridized with the probe indicated, as well as *egr2b*, as an indicator of the level of Pbx function.

together, these data demonstrate a clear role for Pbx proteins in regulating gene expression within the vertebrate retina, especially within the dorsal region.

The role of Meis proteins in regulating retinal gene expression

Within the hindbrain, Pbx cooperates with Hox and Meis/Pknox proteins to drive expression of target genes. Although *hox* genes are not expressed in the retina, *meis/pknox* genes are expressed strongly in this tissue (Biemar et al., 2001; Vlachakis et al., 2000; Waskiewicz et al., 2001; Zerucha and Prince, 2001) and unpublished data. Furthermore, *pknox1* hypomorphs and *Meis1* knockout mice have morphological defects in retinal formation (Ferretti et al., 2006; Hisa et al., 2004). As there are multiple *meis/pknox* genes present in the retina during development (Waskiewicz et al., 2001; Wu et al., 2006), we utilized a dominant negative RNA approach to knockdown Meis function, which results in the reduction of *aldh1a2, tbx5* and *hmx4* in the retina (Figure 3-4 A-F). In addition, the expression of *otx2*, normally restricted to the periphery of the eye cup (in the presumptive retinal pigmented epithelium), is expanded throughout the retina at 18 hpf. These expression patterns are very similar to *pbx2/4* null embryos and are thus consistent with the idea that Meis and Pbx proteins cooperate to regulate transcription of these eye patterning genes.

Pbx is required for both early and late eye patterning genes

To determine when Pbx proteins are first required for eye patterning, we analyzed *retinal homeobox (rx)* gene expression in *pbx2/4* null embryos at early

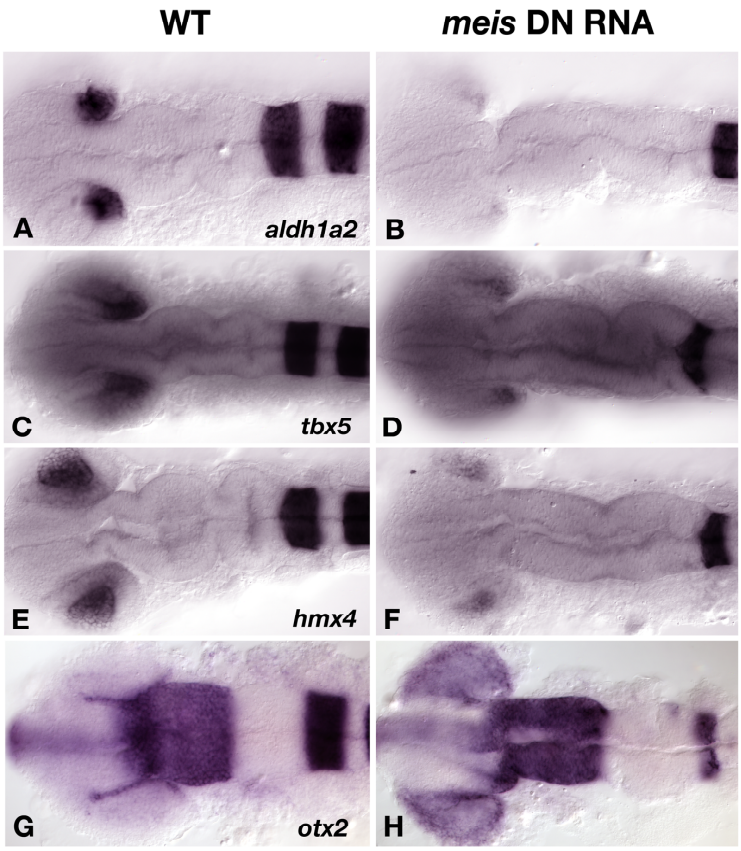

Figure 3-4: *meis* family proteins are required for expression of eye patterning genes. The expression of *aldh1a2* and *tbx5* are found in the dorsal retina (A and C) and are reduced in *meis* dominant negative embryos (B and D) when compared to wild type at 24 hpf. The expression of *hmx4,* found within the lens and retina (E), is reduced specifically in the retina, but unaffected in the lens (F). The expression of *otx2*, confined to the periphery of the eye at 24 hpf, (G) is expanded throughout the retina in *meis* dominant negative embryos (H).

stages of development. The expression of *rx* genes is limited to the eye fields during early development, and expression is required for proper eye development in zebrafish as over-expression leads to ectopic eye formation (Chuang et al. 1999). *rx3* is expressed in the optic primordium at the tailbud stage (Figure 3-5 A) , while both *rx2* and *rx3* are expressed after somitogenesis (Figure 3-5 C, G, E, I). In *pbx2/4* null embryos, the expression of *rx3* appears unaffected during early eye specification, but has failed to be downregulated by 10 somites (21/28 embryos). The expression of *rx2*, however, is reduced throughout somitogenesis in *pbx2/4* null embryos (n=17/20 embryos at 4 somites, n= 18/23 at 10 somites). Thus, *pbx* gene function plays a key role in the development of early eye tissue.

It is likely that *pbx2/4* function is also needed later in eye development as processes such as retinal ganglion cell outgrowth are also affected when Pbx function is inhibited. We therefore analyzed the expression of *atonal homolog 7 (atoh7)*, which is expressed in a wave-like fashion (Figure 3-5, K-M) in the inner retina prior to retinal ganglion cell differentiation (Kay et al., 2005). There is a marked reduction in the expression of *atoh7* in the dorsal retina at both 36 hpf (18/27 embryos) and 41 hpf (22/32 embryos) (Figure 3-5 O, P), while expression in the rest of the inner retinal tissue remains unaffected. This indicates that a lack of *atoh7* in the dorsal retina may affect retinal ganglion cell differentiation in this domain, which may contribute to the observed defects in retinal ganglion cell outgrowth.

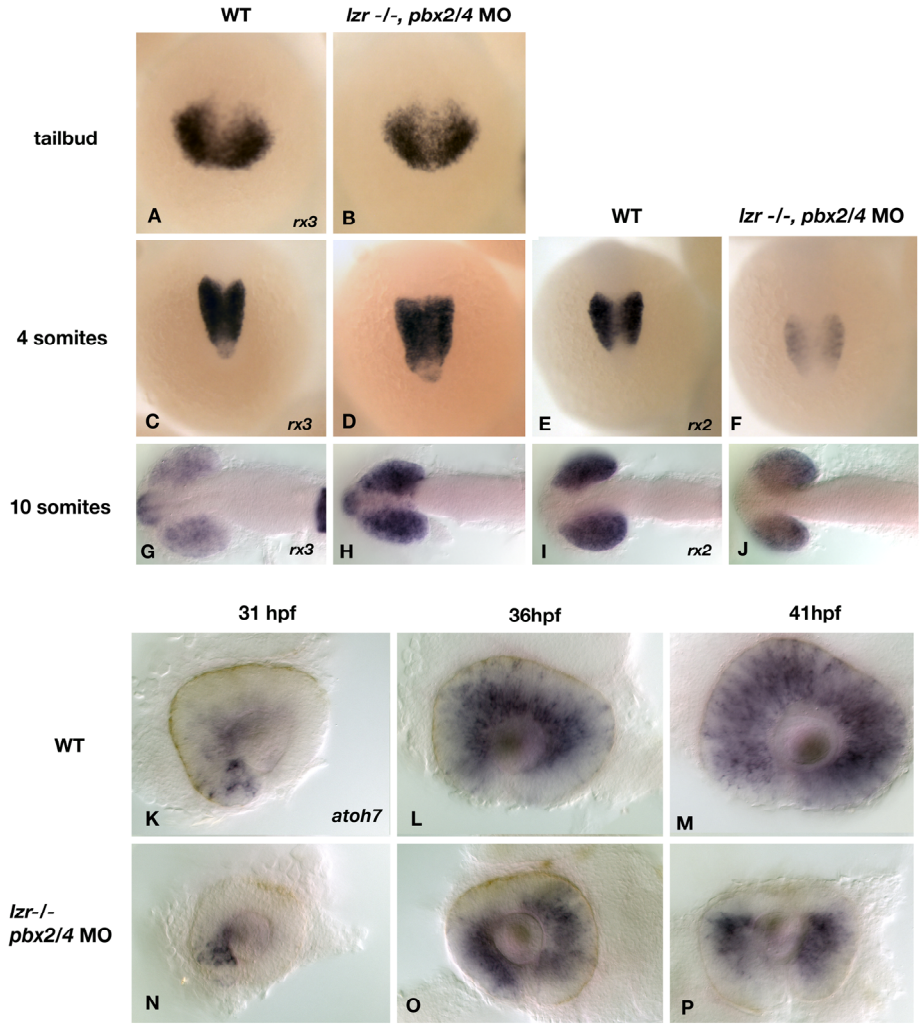
WT
lzr -/-, pbx2/4 MO
tailbud
A
rx3
B
WT
lzr -/-, pbx2/4 MO
4 somites
C
rx3
D
E
rx2
F
10 somites
G
rx3
H
I
rx2
J
31 hpf
36hpf
41hpf
WT
K
atoh7
L
M
lzr-/-
pbx2/4 MO
N
O
P

Figure 3-5: The expression of *rx2*, *rx3*, and *atoh7* is aberrant in *pbx2/4* null embryos. The expression of *rx3,* one of the earliest known eye field markers is unaffected at the tailbud and 4 somite stage (A-D) but is increased in expression at the 10 somite stage (H) when compared to wildtype (G). The expression of *rx2* is reduced at both the 4 and 10 somite stage in *pbx2/4* null embryos (F and J), when compared to wildtype (E and I). No expression of *rx2* is observed at the tailbud stage. The expression of *atoh7* was analyzed as a marker of differentiating retinal ganglion cells. In wild type embryos, expression begins in the ventral nasal domain of the retina at about 31 hpf (K). Expression proceeds in a wave-like fashion to include the dorsal retina by 36 hpf (L), and has filled the entire retina by 41 hpf (M). In *pbx2/4* null embryos, expression is initiated correctly at 31 hpf (N). Expression proceeds in a wave-like fashion but is excluded from the dorsal domain of the retina at both 36 hpf (O) and 41 hpf (P).

Pbx proteins regulate polarized gene expression in the optic tectum

Previous research has demonstrated a role for Pbx in patterning both the midbrain-hindbrain and diencephalic-mesencephalic boundaries. Consistent with this role, our microarray identified three putative Pbx dependent transcripts that are expressed within the tectum. These genes, *ephrin A2* (*efna2*), *fatty acid binding protein 7a* (*fabp7a*), *N-acetyltransferase 10* (*nat10*) were examined by whole mount *in situ* hybridization to confirm the results of the microarray experiment. *efna2* is expressed in the diencephalon and tectum (Figure 3-6 A). The other two genes, *fabp7a* and *nat10*, have significant expression in the retina as well as tectum (Figure 3-6 C and E). Each transcript is down-regulated in *pbx2/4* null embryos with residual expression of each gene found at the midbrain-hindbrain boundary (Figure 3- 6 B, D, F). This is consistent with previous findings showing that Pbx proteins are required for the maintenance of gene expression in the mesencephalon (Erickson et al., 2007).

As development proceeds, the tectum becomes highly organized and is characterized by the polarization of gene expression. At 48 hpf, the expression of *otx2* and *efnA5a* is strongest at the periphery of the tectum, with the highest expression observed distal to the eye (Figure 3-6 G) while decreasing proximally. These gradients are disrupted in *pbx2/4* null embryos, whereby expression of *otx2* is greatest proximal to the eye (Figure 3-6 H), and expression of *efnA5a* is confined to the posterior tectum (Figure 3-6 J). By 3 dpf, the optic tectum is smaller and disorganized in *lzr-/-*, *pbx2/4* morphant embryos (Figure 3-6 L), as

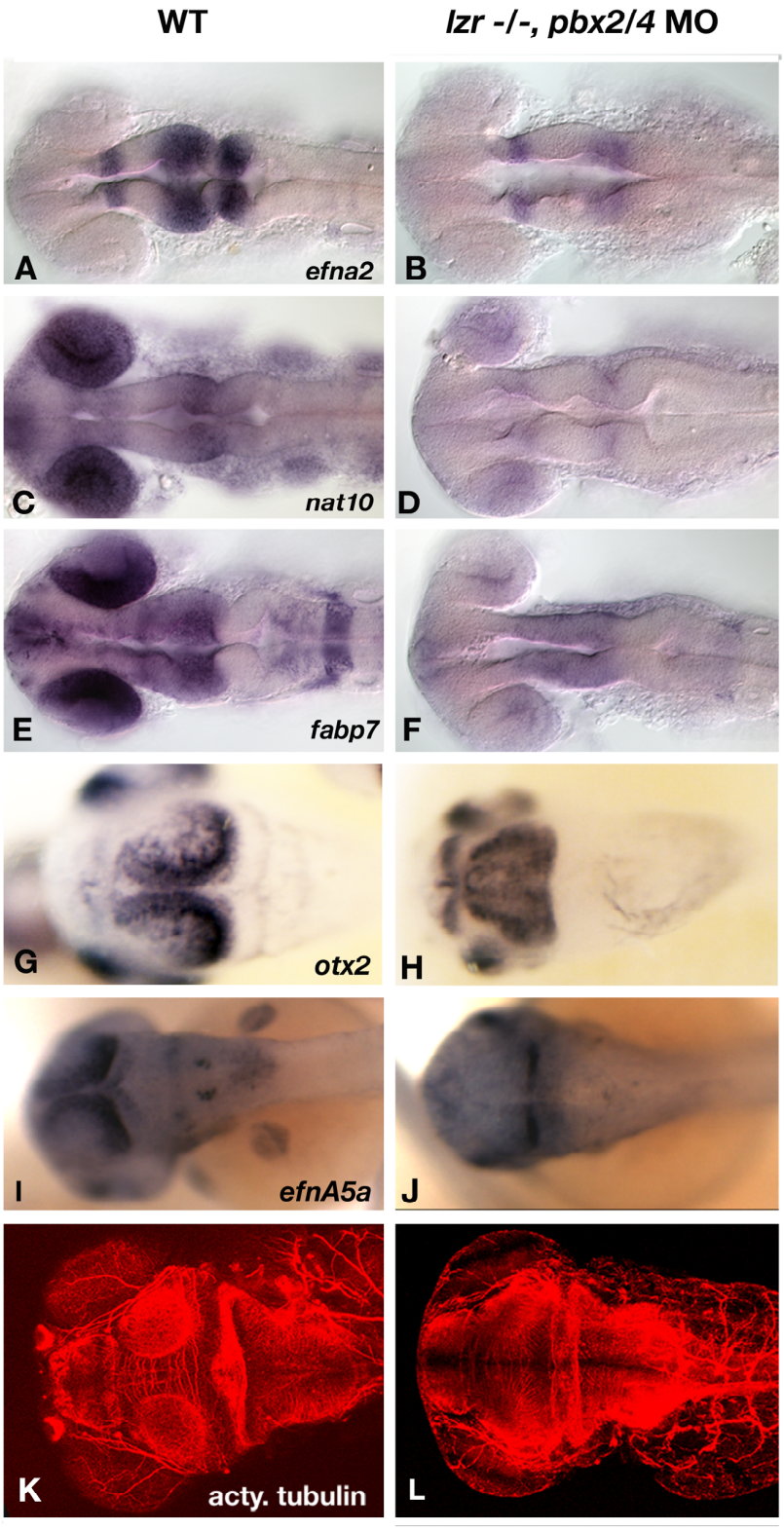
WT
lzr -/-, pbx2/4 MO
A
efna2
B
C
nat10
D
E
fabp7
F
G
otx2
H
I
efnA5a
J
K
acty. tubulin
L

Figure 3-6: Aberrant tectal patterning is observed in *pbx2/4* null embryos. *efna2* expression includes the posterior forebrain, the tectum, and the anterior hindbrain in wild type embryos (A), and is reduced in *pbx2/4* null embryos (B) at 24 hpf. The expression of both *nat10* and *fabp7a* includes both the eye and tectum in wild type embryos (C) and (E), and is almost completely absent in both regions in *pbx2/4* null embryos (D and F). *otx2* is expressed in the optic tectum at 48 hpf, specifically toward the periphery of the tectum with lower levels observed immediately adjacent to the eye (G). In *pbx2/4* null embryos, there is a distinct change in expression domain in which the highest levels of expression are observed immediately adjacent to the eye (H). The gradient of *efnA5a* expression, which decreases toward the anterior (I), is attenuated at 48 hpf in *pbx2/4* null embryos (J). The acetylated tubulin antibody marks the axons of the optic tectum at 3 dpf (K), which is smaller and disorganized in *pbx2/4* null embryos (L).

shown by visualization of acetylated tubulin-positive axons. These data clearly indicate a requirement for Pbx proteins in formation and patterning of the optic tectum.

Pbx and Meis proteins are required for expression of gdf6a, itself a regulator of dorsal retina patterning

Gdf6a is a growth factor of the BMP family, whose retinal expression is restricted to the dorsal domain. Knockdown of *gdf6a* results in smaller eyes, as well as reduced expression of eye markers in the dorsal retina (Asai-Coakwell et al., 2007). As such, we analyzed whether *pbx* and *gdf6a* function in the same pathway to regulate eye patterning, and further analyzed the expression of eye markers in *gdf6a* morphants. Knockdown of *gdf6a* results in the elimination of *aldh1a2* and *tbx5* expression (Figure 3-7 F, H), markers of the dorsal retina. As the expression of genes in the dorsal retina is similar in *gdf6a* morphant, *pbx2/4* null, and *meis* DN embryos, we tested whether *gdf6a* functions in the same genetic pathway as *pbx* and *meis.* When Pbx2/4 function is eliminated or *meis* gene function is reduced, the expression of *gdf6a* is strongly reduced in the dorsal (Figure 3-7 A, B, C, D), indicating that *gdf6a* functions genetically downstream of both *pbx2/4* and *meis* genes.

Discussion

In this paper, we present evidence that *pbx2/4* gene function is essential for proper retinal ganglion cell axon outgrowth. This phenotype likely results

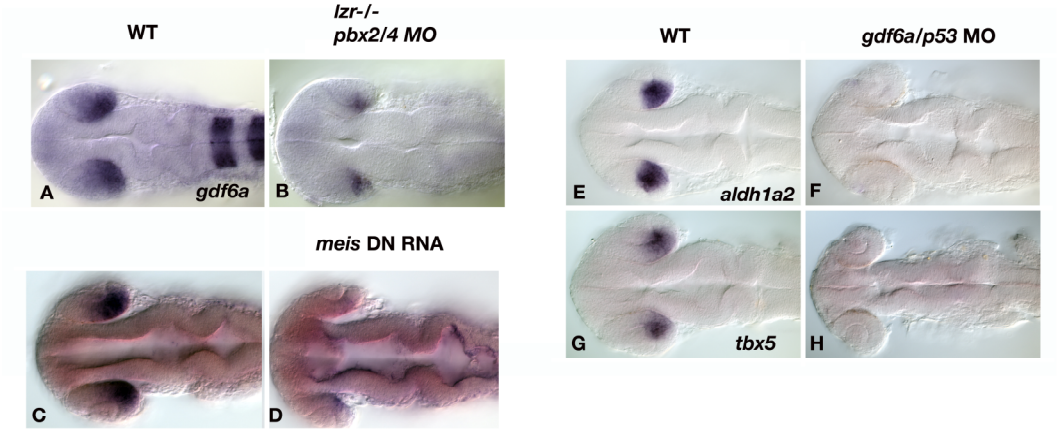

Figure 3-7: *gdf6a* is genetically downstream of *pbx2/4* and *meis,* and is necessary for expression of genes in the dorsal retina. Expression of *gdf6a* is strongly reduced in *pbx2/4* null embryos (B), when compared with wildtype (A) at 24 hpf. Expression of *meis* dominant negative RNA also strongly reduces *gdf6a* expression in the dorsal retina (D) when compared with wildtype (C). Knockdown of *gdf6a* results in a loss of *aldh1a2* and *tbx5* expression (D and F) when compared with wildtype (C and E). *pbx2/4* null were also hybridized with *egr2b* as a marker of *pbx* function.

from aberrant Pbx mediated gene transcription in both the eye and tectum of *pbx2/4* null embryos. Although the eye laminar structure is relatively normal after 5 days of development, connections between the RGC axons and the optic tectum are not made. Through microarray and *in situ* analysis, we have identified numerous candidate genes that may contribute to RGC axon guidance defects seen in embryos with reduced Pbx function. Abnormalities in eye patterning begin during early somitogenesis, and persist throughout development. Defects in the differentiation of retinal ganglion cells may also contribute to this phenotype, as the expression of *atoh7* is eliminated in the dorsal region of the neural retina in *pbx2/4* null embryos. The data presented here builds on current knowledge of Pbx proteins in embryonic patterning, and provides a novel role for Pbx in patterning the eye and tectum, and subsequently, the regulation of RGC axon outgrowth and pathfinding.

An absence of Pbx function results in reduced expression of genes involved in eye patterning. In *pbx2/4* null embryos, defects are seen in the expression of *rx2* during early somitogenesis, and at 10 somites, *rx3* expression has not been down-regulated as in wild type embryos (Chuang et al.). This could lead to defects in retinal ganglion cell and photoreceptor development, as *rx2* and *rx3* are also expressed in these subsets of cells later in development. We have identified *aldh1a2, hmx4,* and *tbx5* as Pbx-dependent transcripts at 18 hpf. Each of these genes has the potential to play a strong role in regulating retinal patterning. For example, *aldh1a2*, which is involved in the synthesis of retinoic acid, is likely to affect development of the visual system in zebrafish as retinoic

acid is required for development of photoreceptor cells and pigmented epithelium in the developing zebrafish eye (Prabhudesai et al., 2005). By 3 dpf, the photoreceptor layer is highly disorganized in fish with reduced *pbx2/4* gene function, indicating a possible effect of absent *aldh1a2* expression. Moreover, we also observed a down-regulation of *tbx5* via both microarray and *in situ* analysis, a downstream effector of retinoic acid signaling that is essential for establishment of the dorsoventral boundary of the eye (Golz et al., 2004; Leconte et al., 2004).

It has been documented that the homeodomain transcription factor *soho1* represses the expression of *epha3* in chicks, and is necessary for eye development. The zebrafish Pbx dependent gene *hmx4* is likely the functional ortholog of chick *soho1*, since it is expressed in the retina and shares extensive sequence similarity (Schulte and Cepko, 2000). Loss of *epha3* in chicks leads to premature arborization by RGC axons that originate in the nasal retina, while those that originate in the posterior retina appear unaffected (Feldheim et al., 2004). In *pbx2/4* null embryos, *hmx4* is down regulated during early eye patterning, and thus may also play a role in phenotypes observed in eyes with reduced *pbx* gene function, such as a lack of RGC axon outgrowth.

Given the profound changes in gene expression, it is surprising that laminar structure and positioning of the optic nerve is relatively normal without Pbx2/4 function. As such, there is no evidence for overt dorsal ventral patterning defects or improper cell differentiation. We believe a partial answer to this paradox lies in the expression of eye patterning molecules at 24 hpf, in which each of these Pbx-dependent transcripts has more normal levels of expression

Indeed, changes in *aldh1a2* and *tbx5* expression are more subtle, while the expression of *hmx4* is near wild-type levels at 24 hpf (when compared to 18 hpf), indicating that Pbx2/4 are essential for proper initiation of these transcripts, but that other factors are capable of regulating their transcription in the absence of Pbx2/4. At 24 hpf, other *pbx* genes, including *pbx1* and *pbx3.1*, are expressed in the zebrafish embryo. As such, these Pbx proteins or other transcription factors may regulate eye patterning genes at 24 hpf.

Although not identified in our microarray screen for Pbx dependent transcripts, we analyzed the expression of *otx2*, which in wild type embryos, is expressed throughout the optic vesicle early in development (Martinez-Morales et al., 2001), but is restricted to the RPE between 22-24 hpf. *otx2* is also strongly expressed in the optic tectum, and could therefore be responsible for axon guidance through either eye or tectal patterning. We noticed an expansion of expression to include the entire eye in *pbx2/4* null embryos at 24 hpf, indicating that these embryos are unable to restrict the expression of *otx2* as development proceeds. Loss of retinoid signaling in mice leads to reduced expression of *tbx5* and expanded expression of *otx2* throughout the retina, placing both genes downstream of *aldh1a2* (Halilagic et al., 2007). This provides a possible signaling mechanism for the expansion of *otx2* in *pbx2/4* null zebrafish whereby Pbx is required for expression of *aldh1a2*, which, in turn, is required for the restriction of *otx2* to the RPE. As restriction of *otx2* expression is required for specification of the RPE layer, it is logical that *pbx2/4* null embryos would have defects in the specification of RPE cells. In both *lzr* and *pbx2/4* null embryos, the RPE is

thickened in a subtle, but reproducible manner. Thus it is likely that the ectopic expression of *otx2* in *pbx2/4* null embryos leads to the thickening of the RPE, but aberrant expression of other retinal transcripts may also be involved.

Many Pbx functions, such as hindbrain patterning and blood development, are known to involve Meinox (Meis) binding partners. Meinox proteins can stabilize Pbx proteins, and are often essential for Pbx function through cooperative DNA binding. (Moens and Selleri, 2006; Waskiewicz et al., 2001). *Meis1* knockout mice and *Prep/Pknox* mutants have morphological defects in retinal formation including an inappropriately positioned optic nerve (Hisa et al., 2004). The position of the optic nerve implies that Meis proteins are required for proper dorsal-ventral patterning of the retina, although marker analysis has yet been performed. To create zebrafish with reduced Meis function, we injected embryos with *meis* DN RNA which blocks the function of all Meinox proteins (Choe et al., 2002; Waskiewicz et al., 2001). As with *pbx2/4* null embryos, loss of Meis function reduced or eliminated *aldh1a2* and *tbx5* expression. Thus, it is likely that Pbx2/4 and Meis proteins act cooperatively to regulate at least some aspects of eye patterning. This is in concert with previously published reports that indicate that both proteins are needed to pattern tissues such as the hindbrain (Feldheim et al., 2004, Waskiewicz et al., 2002).

Using our microarray approach, we have also identified reduced tectal expression of *fabp7a*, *nat10*, and *efna2* in *pbx2/4* null embryos. Interestingly, *fabp7a* and *nat10* also show decreased expression in the eye in *pbx2/4* null embryos, and thus may be important in patterning both structures in a Pbx

dependent fashion. *FABP7* has been identified as a downstream target of Pbx/Meinox signaling in humans, whereby increased expression of PKNOX1 (human *prep1* homolog) leads to over-expression of *FABP7* in fetal trisomy leading to Down's Syndrome (Sanchez-Font et al., 2003).

Further in development, the optic tectum becomes highly polarized in wild type embryos, which is required for proper retinal ganglion cell axon outgrowth and mapping. By 48 hpf, tectal gradients of *otx2* and *ephrinA5a* expression have been disrupted in embryos with reduced Pbx function, indicating its vital role for patterning this tissue. Given these results, it is possible that RGC axon outgrowth defects may result in part from *pbx* dependent patterning defects in the tectum in concert with *pbx* patterning defects in the retina.

It has recently been reported that a knockdown of *gdf6a*, a growth factor of the BMP family, results in smaller eyes in both zebrafish and frogs (Asai-Coakwell et al., 2007; Hanel and Hensey, 2006). Furthermore, the expression of marker genes in the dorsal domain of the retina is dependent on Gdf6a function. We have expanded on the marker analysis in *gdf6a* morphants to include *aldh1a2* and *tbx5,* which are both eliminated in *gdf6a* morphants. Moreover, *gdf6a* expression is strongly reduced in *pbx2/4* null and *meis* DN embryos, indicating that *gdf6a* acts genetically downstream of both *pbx, meis* genes for patterning the dorsal retina.

Conclusions

The results presented support a model where aberrant eye and tectal patterning in *pbx2/4* null embryos leads to RGC axon outgrowth errors. Eye

patterning in the dorsal domain of the retina also involves the function of Meis protein family members, and a downstream growth factor, *gdf6a*.

Bibliography

Asai-Coakwell, M., et al., 2007. GDF6, a novel locus for a spectrum of ocular developmental anomalies. Am J Hum Genet. 80**,** 306-15.

Berkes, C. A., et al., 2004. Pbx marks genes for activation by MyoD indicating a role for a homeodomain protein in establishing myogenic potential. Mol Cell. 14**,** 465-77.

Biemar, F., et al., 2001. Cloning and expression of the TALE superclass homeobox Meis2 gene during zebrafish embryonic development. Mech Dev. 109**,** 427-31.

Burrill, J. D., Easter, S. S., Jr., 1995. The first retinal axons and their microenvironment in zebrafish: cryptic pioneers and the pretract. J Neurosci. 15**,** 2935-47.

Choe, S. K., et al., 2002. Meis family proteins are required for hindbrain development in the zebrafish. Development. 129**,** 585-95.

Chuang, J. C., et al., 1999. Expression of three Rx homeobox genes in embryonic and adult zebrafish. Mech Dev. 84**,** 195-8.

Clark, M. D., et al., 2001. An oligonucleotide fingerprint normalized and expressed sequence tag characterized zebrafish cDNA library. Genome Res. 11**,** 1594-602.

Cooper, K. L., et al., 2003. Autonomous and nonautonomous functions for Hox/Pbx in branchiomotor neuron development. Dev Biol. 253**,** 200-13.

Deflorian, G., et al., 2004. Prep1.1 has essential genetic functions in hindbrain development and cranial neural crest cell differentiation. Development. 131**,** 613-27.

Dutta, S., et al., 2001. PDX:PBX complexes are required for normal proliferation of pancreatic cells during development. Proc Natl Acad Sci U S A. 98**,** 1065-70.

Erickson, T., et al., 2006. Pbx proteins cooperate with Engrailed to pattern the midbrain-hindbrain and diencephalic-mesencephalic boundaries. Developmetal Biology.

Erickson, T., et al., 2007. Pbx proteins cooperate with Engrailed to pattern the midbrain-hindbrain and diencephalic-mesencephalic boundaries. Dev Biol. 301**,** 504-17.

Feldheim, D. A., et al., 2004. Loss-of-function analysis of EphA receptors in retinotectal mapping. J Neurosci. 24**,** 2542-50.

Ferretti, E., et al., 2006. Hypomorphic mutation of the TALE gene Prep1 (pKnox1) causes a major reduction of Pbx and Meis proteins and a pleiotropic embryonic phenotype. Mol Cell Biol. 26**,** 5650-62.

Golz, S., et al., 2004. Retinoic acid-dependent regulation of BMP4 and Tbx5 in the embryonic chick retina. Neuroreport. 15**,** 2751-5.

Halilagic, A., et al., 2007. Retinoids control anterior and dorsal properties in the developing forebrain. Dev Biol. 303**,** 362-75.

Hanel, M. L., Hensey, C., 2006. Eye and neural defects associated with loss of GDF6. BMC Dev Biol. 6**,** 43.

Hever, A. M., et al., 2006. Developmental malformations of the eye: the role of PAX6, SOX2 and OTX2. Clin Genet. 69**,** 459-70.

Hisa, T., et al., 2004. Hematopoietic, angiogenic and eye defects in Meis1 mutant animals. Embo J. 23**,** 450-9.

Kay, J. N., et al., 2005. Staggered cell-intrinsic timing of ath5 expression underlies the wave of ganglion cell neurogenesis in the zebrafish retina. Development. 132**,** 2573-85.

Leconte, L., et al., 2004. Pax6 interacts with cVax and Tbx5 to establish the dorsoventral boundary of the developing eye. J Biol Chem. 279**,** 47272-7.

Martinez-Morales, J. R., et al., 2001. Otx genes are required for tissue specification in the developing eye. Development. 128**,** 2019-30.

Maves, L., et al., 2007. Pbx homeodomain proteins direct Myod activity to promote fast-muscle differentiation. Development. 134**,** 3371-82.

Moens, C. B., Selleri, L., 2006. Hox cofactors in vertebrate development. Dev Biol. 291**,** 193-206.

Okada, Y., et al., 2003. Homeodomain proteins MEIS1 and PBXs regulate the lineage-specific transcription of the platelet factor 4 gene. Blood. 101**,** 4748-56.

Pai, C. Y., et al., 1998. The Homothorax homeoprotein activates the nuclear localization of another homeoprotein, extradenticle, and suppresses eye development in Drosophila. Genes Dev. 12**,** 435-46.

Penkov, D., et al., 2005. Involvement of Prep1 in the alphabeta T-cell receptor T-lymphocytic potential of hematopoietic precursors. Mol Cell Biol. 25**,** 10768-81.

Popperl, H., et al., 2000. lazarus is a novel pbx gene that globally mediates hox gene function in zebrafish. Mol Cell. 6**,** 255-67.

Prabhudesai, S. N., et al., 2005. Targeted effects of retinoic acid signaling upon photoreceptor development in zebrafish. Dev Biol. 287**,** 157-67.

Sanchez-Font, M. F., et al., 2003. Overexpression of FABP7 in Down syndrome fetal brains is associated with PKNOX1 gene-dosage imbalance. Nucleic Acids Res. 31**,** 2769-77.

Schmitt, E. A., Dowling, J. E., 1994. Early eye morphogenesis in the zebrafish, Brachydanio rerio. J Comp Neurol. 344**,** 532-42.

Schulte, D., Cepko, C. L., 2000. Two homeobox genes define the domain of EphA3 expression in the developing chick retina. Development. 127**,** 5033-45.

Vlachakis, N., et al., 2000. A novel pbx family member expressed during early zebrafish embryogenesis forms trimeric complexes with Meis3 and Hoxb1b. Dev Dyn. 217**,** 109-19.

Waskiewicz, A. J., et al., 2001. Zebrafish Meis functions to stabilize Pbx proteins and regulate hindbrain patterning. Development. 128**,** 4139-51.

Waskiewicz, A. J., et al., 2002. Eliminating zebrafish pbx proteins reveals a hindbrain ground state. Dev Cell. 3**,** 723-33.

Wu, S., et al., 2006. A role for GnRH in early brain regionalization and eye development in zebrafish. Mol Cell Endocrinol. 257-258**,** 47-64.

Yan, Y. L., et al., 1998. Ectopic expression of hoxb2 after retinoic acid treatment or mRNA injection: disruption of hindbrain and craniofacial morphogenesis in zebrafish embryos. Dev Dyn. 213**,** 370-85.

Zerucha, T., Prince, V. E., 2001. Cloning and developmental expression of a zebrafish meis2 homeobox gene. Mech Dev. 102**,** 247-50.

Chapter 4

Gdf6a is required for the initiation of dorsal-ventral retinal patterning

A version of this chapter has been published previously

***French CR**, Erickson T, French DV, Pilgrim DB, Waskiewicz AJ.Gdf6a is required for the initiation of dorsal-ventral retinal patterning and lens development. Dev Biol. 2009 Sep 1;333(1):37-47*

Introduction

In the developing vertebrate retina, early proliferating cells are imparted positional information through the expression of spatially restricted genes. This positional information is required for accurate topographic mapping of retinal ganglion cell (RGC) axons to the optic tectum, the primary visual processing center in zebrafish. In addition, aberrant retinal patterning can lead to coloboma (Barbieri et al., 2002; Sehgal et al., 2008), where the ventral choroid fissure fails to fuse during development.

The eye is patterned along the dorsal-ventral and nasal-temporal axes immediately after formation of the optic vesicle. Along the dorsal-ventral axis, studies in model organisms have implicated Bmp and Wnt signaling pathways in the determination of dorsal cell fate (Behesti et al., 2006; Gosse and Baier, 2009; Plas et al., 2008; Sakuta et al., 2001; Sakuta et al., 2006; Veien et al., 2008; Zhou et al., 2008), while retinoic acid and Sonic Hedgehog signaling are required for specifying ventral cell identity (Halilagic et al., 2007; Lupo et al., 2005). However, these models have not yet resolved what factors are required for the initiation of dorsal cell fate.

Current models of dorsal-ventral retinal patterning involve a dorsal-high to ventral-low gradient of Bmp signaling, resulting from *bmp2* and *bmp4* expression in the dorsal retina and surrounding tissues (Plas et al., 2008; Sakuta et al., 2001; Sakuta et al., 2006) and the expression of Bmp inhibitors in the ventral retina (Sakuta et al., 2001). In zebrafish, the Bmp ligand Gdf6a is necessary for late stages of dorsal-ventral retinal patterning (Gosse and Baier, 2009, and this work),

possibly requiring interactions with Bmp4 (Gosse and Baier, 2009). This Bmp signaling gradient drives the expression of dorsally restricted transcription factors, with the *t-box* (*tbx)* family of homeodomain proteins being of particular importance in retinal patterning. Over-expression studies have supported an antagonistic relationship between dorsal *tbx5* and the *ventral anterior homeobox* (*vax2*) gene, thereby maintaining distinct dorsal and ventral domains within the retina (Koshiba-Takeuchi et al., 2000; Schulte et al., 1999). Additionally, these transcription factors regulate the polarized expression of axon guidance molecules, mainly of the *ephrin (efn)* family of ligands in the dorsal retina, and their receptors, the *eph* receptor tyrosine kinases in the ventral retina (Erskine and Herrera, 2007) leading to correct topographic mapping of RGCs on the optic tectum.

Retinal patterning begins immediately after evagination of retinal precursors, as evidenced by initiation of *tbx5* expression in the presumptive dorsal retina (Veien et al., 2008). Abrogation of the canonical Wnt pathway results in reduced dorsal marker gene expression, but Wnt signaling has no effect on initiation of these genes. Given these data, we can conclude that there are two phases of dorsal retinal patterning, the initiation of dorsal markers, such as *tbx5*, and subsequently the maintenance phase, where discrete signaling pathways cause dorsal identity to persist. Although Bmp molecules are necessary for dorsal identity, it is not known if they function in either initiation or maintenance phases.

Loss of dorsal-ventral retinal patterning can have profound effects on the development of the visual system. In wildtype embryos, RGC axons extend from

the eye via the optic nerve beginning between 2-3 dpf (Zolessi et al., 2006), extend past the optic chiasm, and map onto the optic tectum in a position dependent manner. Retinal ganglion cells from the dorsal retina map onto the lateral tectum, while axons from the ventral retina map onto the medial tectum. Loss of positional identity in the retina can cause mapping defects in visual processing centers, with the expression of Bmp family members and downstream signaling molecules being important for these processes in other model systems (Plas et al., 2008; Sakuta et al., 2006).

In this chapter I describe a role for Gdf6a in dorsal-ventral retinal patterning. Gdf6a is a growth factor expressed in the early embryo with a defined role in patterning the dorsal-ventral body axis (Sidi et al., 2003). It acts upstream of other Bmp molecules (Sidi et al., 2003) and can affect eye development in humans and model organisms (Asai-Coakwell et al., 2007; French et al., 2007; Gosse and Baier, 2009) leading to coloboma and microphthalmia when mutated (Asai-Coakwell et al., 2009). Here, we present evidence using both knockdown and transgenic ectopic expression experiments, that Gdf6a is required for the initiation of dorsal retinal identity in zebrafish independent of Bmp4 function. Loss of dorsal retinal identity in these animals leads to aberrant mapping of retinal ganglion cells on the optic tectum (Gosse and Baier, 2009, and this work), coloboma, as well as ectopic fissure formation in the retina.

Results

Knockdown of gdf6a causes microphthalmia and ectopic fissures

During early development, the vertebrate eye contains a transient ventral fissure that is essential for the entry of mechesenchyme cells into the retina, where they will give rise to blood vessels that nourish the eye throughout the life of the organism (Barishak, 1992). Failure to close the optic fissure results in a loss of ventral tissue known as coloboma. Knockdown of *gdf6a* results in coloboma (Figure 4-1 B and C, black arrow) as well ectopic fissure formation in the dorsal retina (Figure 4-1 A and B, red arrow). In addition, knockdown of *gdf6a* results in microphthalmia (Figure 4-1 E, F), which will be discussed in detail in chapter 6 of this work. Laminar structure is relatively normal in *gdf6a* morphant embryos, as evidenced by phalloidin staining in *gdf6a* morphant eyes (Figure 4-1 G ad H). It should be noted that coloboma, microphthalmia, and the development of an ectopic dorsal fissure are not fully penetrant in *gdf6a* morphant embryos (Figure 4-1 I-K, Figure 2-2).

Loss of gdf6a results in aberrant retinal-tectal topographic mapping

In wildtype embryos, retinal ganglion cell axons innervate the optic tectum in a position dependent manner. As evidenced by labeling of dorsal and ventral retinal ganglion cell populations, retinal ganglion cell axons from the dorsal retina innervate the lateral tectum while axons emanating from cell bodies in the ventral retina innervate the medial tectum (Figure 4-2 A). Wildtype embryos thus display innervations throughout the medial-lateral axis of the optic

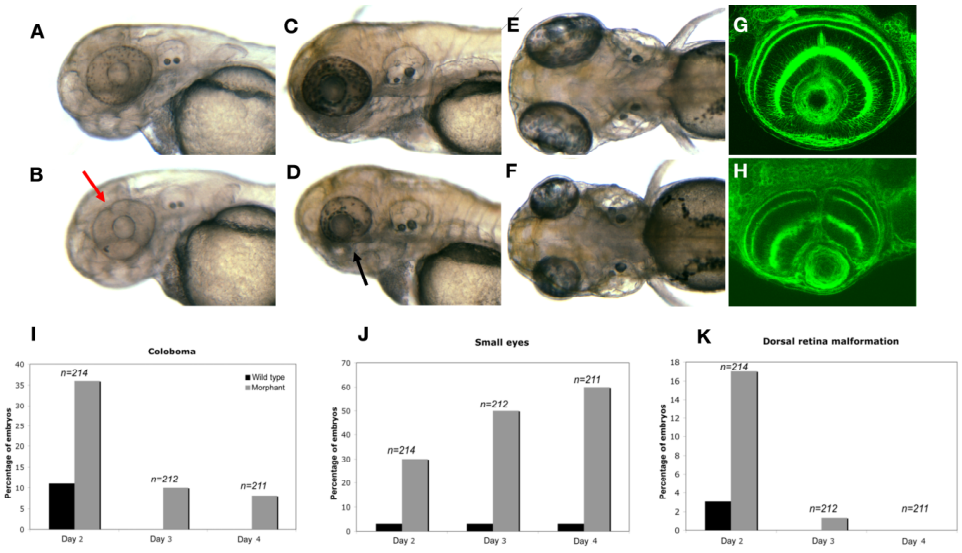

Figure 4-1: Morphological analysis of *gdf6a* morphant eyes. At 48 hpf, an ectopic fissure is observed in dorsal retina (B, red arrow), when compared with wildtype siblings (A). At 72 hpf, the ventral retina has not fused, resulting in coloboma (D, black arrow), when compared with wildtype (C). At both 48 hpf, and 72 hpf (E, F), the eye of *gdf6a* morphants is smaller (microphthmalia) than wildtype siblings. Phalloidin staining at 72 hpf indicates that laminar structure of the retina is relatively normal in *gdf6a* morphants (G and H). All ocular phenotypes were quantified from 2 -4 dpf; (I) coloboma, (J) microphthmalia, and (K) ectopic fissure formation.

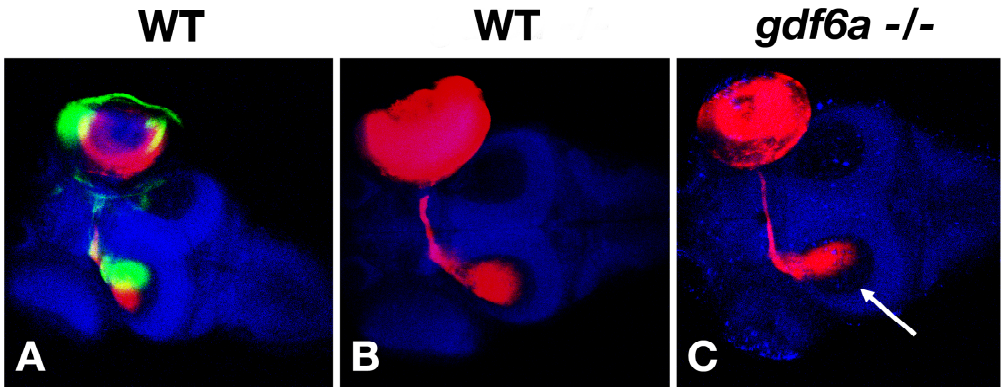

Figure 4-2: Loss of *gdf6a* results in retinal-tectal mapping defects. In wild type embryos, RGC axons from the dorsal retina (red) map onto the lateral optic tectum, while axons from the ventral retina (green) map onto the medial tectum (A). Labeling all retinal ganglion cells with one (red) dye allows for observation of all innervations along the medial lateral axis, as seen on wildtype embryos (B). The lateral tectum does not display innervation when *gdf6a* is lost (C, white arrow). All embryos stages to 4.5 dpf.

tectum (Figure 4-2 A and B). Loss of *gdf6a* results in a complete lack of terminalization fields in the lateral tectum, the area normally innervated by retinal ganglion cell axons from the dorsal retina (Figure 4-2 C, n=6/6).

Knockdown of Gdf6a results in loss of dorsal retinal identity and expansion of ventral retinal identity

As the presence of coloboma, ectopic dorsal retinal fissures, and lack of lateral optic tectum innervation indicates aberrant patterning along the dorsal-ventral retinal axis, we investigated the expression of patterning molecules that show polarized axial expression, as well as Smad 1/5/8 phosphorylation, which is required for canonical Bmp signaling. In wild-type embryos, phosphorylation of Smads 1/5/8 is observed in the dorsal retina (Figure 4-3 A). Knockdown of Gdf6a using a splice blocking morpholino abolishes Smad phosphorylation in the dorsal retina at 28 hours post fertilization (Figure 4-3 B) and all dorsal retinal markers tested. The expression of *tbx5*, a transcription factor required for dorsal cell identity, is lost in *gdf6a* morphants (Figure 4-3 C, D). Similarly, the expression of both *aldehyde dehydrogenase 1a2* (*aldh1a2*), which encodes a protein necessary for the synthesis of retinoic acid (RA), and *bambi*, a Bmp pseudoreceptor under the transcriptional control of Tgf-β signaling (Sekiya et al., 2004), are also absent in *gdf6a* morphants (Figure 4-3 E-H).

In contrast to the normal restricted expression of *vax2* to the ventral region of the retina and optic stalk (Figure 4-3 I), this expression is expanded throughout the entire retina in *gdf6a* morphant embryos (Figure 4-3 J) indicating

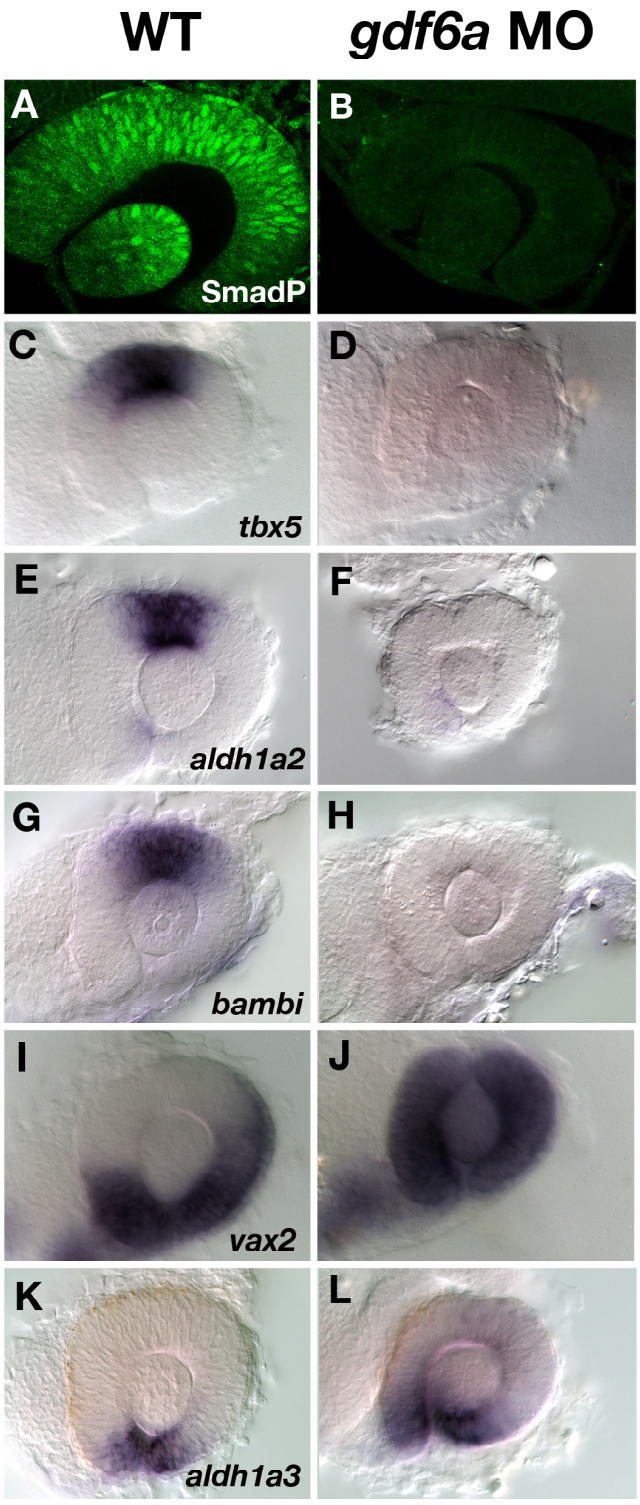
WT
gdf6a MO
A
SmadP
B
C
tbx5
D
E
aldh1a2
F
G
bambi
H
I
vax2
J
K
aldh1a3
L

Figure 4-3: Loss of dorsal signaling and expansion of ventral gene expression in *gdf6a* morphants. The phosphorylation of Smad 1/5/8 proteins is found in the dorsal retina and lens (A) and is lost in *gdf6a* morphants (B). The expression of dorsal markers *tbx5*, *aldh1a2*, *bambi*, (C, E, G) are lost in *gdf6a* morphants (D, F, H). The expression of the ventral specific *vax2* (I) and is expanded throughout the retina in *gdf6a* morphants (J). The expression of the ventral specific *aldh1a3* is found also in the ventral retina (M), and is expanded in *gdf6a* morphants (N). All embryos were staged to 28 hpf.

ventralization of the retina. Expression of *aldehyede dehydrogenase 1a3* (*aldh1a3*), normally found in only a few cells surrounding the choroid fissure (Figure 4-3 K), is expanded in *gdf6a* morphants, albeit to a lesser extent than that of *vax2* (Figure 4-3 L). Taken together, these experiments demonstrate that Gdf6a is required for the specification of dorsal identity in the retina, and in the absence of Gdf6a, the retinal cells adopt a ventral fate.

Expression of axon guidance molecules of the ephB/ephrinB family is altered in gdf6a morphants

The expression of *ephrin* ligands, found in the dorsal retina, and *eph* receptors, found in the ventral retina, are known to influence axon pathfinding and topographic mapping of retinal ganglion cells. In wildtype embryos, *ephrinb2a* (*efnb2a*) is expressed in the dorsal retina and lens at 28 hpf (Figure 4-4 A). Morpholino inhibition of *gdf6a* results in loss of the dorsal retinal specific expression, while lenticular expression is unaffected (Figure 4-4 B). Expression of the *eph receptor B2* (*ephb2)* is found specifically in the ventral domain of the retina in wildtype embryos at 28 hpf (Figure 4-4 C), and is expanded throughout the entire retina in *gdf6a* morphants (Figure 4- 4 D), in a manner similar to that of *vax2* (compare to 4-3 J). In contrast, the expression of *ephb3*, which is observed in a more restricted ventral domain in wildtype embryos at 28hpf (Figure 4 E), is expanded dorsally, but is not found throughout the retina (Figure 4-4 F). Overall, we conclude that Gdf6a signaling is responsible for the restricted expression of a subset of axon guidance molecules within the retina.

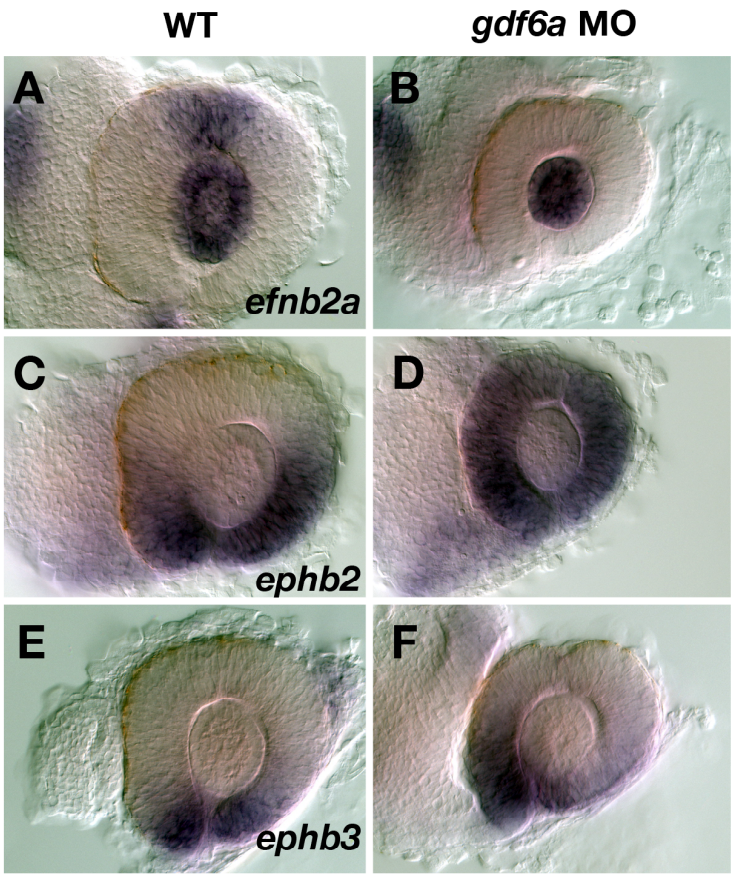

Figure 4-4: Morpholino inhibition of *gdf6a* results in aberrant expression of axon guidance molecules. The expression of *efnb2a* is found in the dorsal retina and lens (A) and is lost in the retina in *gdf6a* morphants. Expression in the lens is not affected (B). The expression of *ephb2* and *ephb3* is found in the ventral retina in wildtype animals (C, E), although the domain of *epbb3* is more restricted compared to *ephb2*. The expression of *ephb2* is expanded throughout the retina in *gdf6a* morphants (D), as is the expression of *ephb3* (F), albeit to a lesser extent that *ephb2*. All embryos were staged to 28 hpf.

Both gdf6a and bmp4 are expressed within or adjacent to the eye field during early development

Chick Bmp4 has previously been implicated in regulating dorsal retinal identity, implying that its zebrafish ortholog may play a similar role in the retina. Previous research has analyzed Bmp expression patterns during eye formation (Veien et al., 2008). We extended the range of embryonic stages of this analysis by performing *in situ* hybridization with probes against zebrafish *bmp4* and *gdf6a* during all stages of optic vesicle formation. The expression of *gdf6a* is first detected adjacent to the eye fields at the 3 somite stage (Figure 4-5 A), while *bmp4* expression is limited to the extraembryonic polster (Figure 4-5 B). By the 6 somite stage, *gdf6a* continues to be expressed adjacent to the eye fields, however the domain does not extend as far posteriorly as seen at 3 somites (Figure 4-5 C). *bmp4* expression continues to be restricted to the polster at this time (Figure 4-5 D). By the 10 somite stage, expression of both *gdf6a* and *bmp4* is found in the developing eye vesicle (Figure 4-5 E, F), and is highly reduced via morpholino knockdown of *gdf6a* (Figure 4-5 I, J). This finding indicates not only that Gdf6a is required to regulate *bmp4* expression in the retina, but also that the initial extraocular source of Gdf6a is required to initiate its own retinal expression. The same trends are observed at 28 hpf, when both *gdf6a* and *bmp4* are expressed specifically within the dorsal retina (Figure 4-5 G, H), and are lost in *gdf6a* morphants (Figure 4-5 K, L).

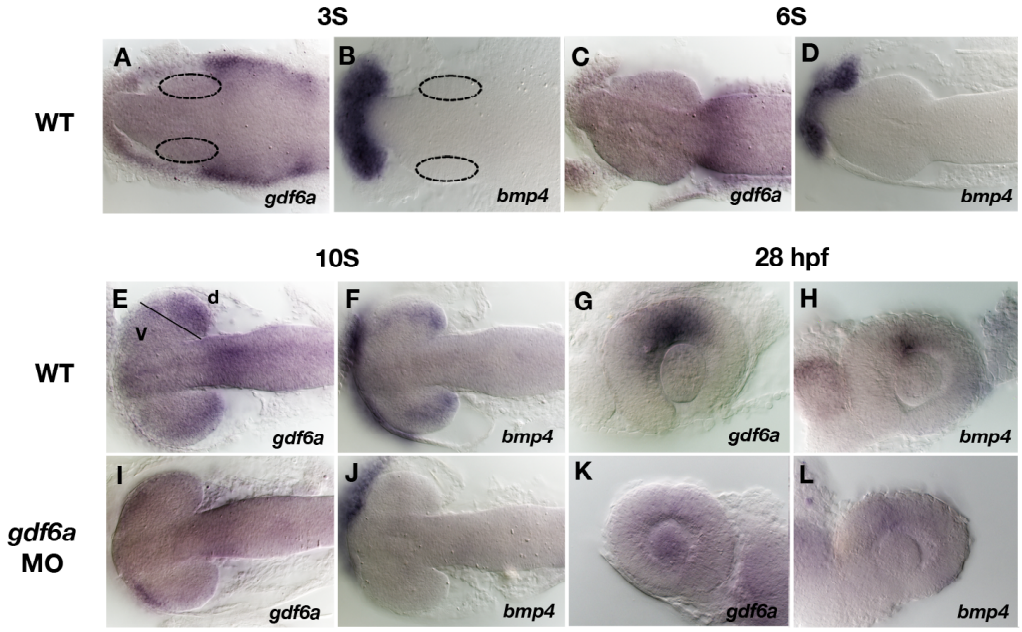

Figure 4-5: Analysis of *bmp* expression in the retina. *gdf6a* expression is first detected at the 3 somite stage adjacent to the developing eye field (A), while *bmp4* expression is limited to the polster (B). The expression domain of *gdf6a* is reduced by 6 somites, but still located adjacent to the eyecups (C). *bmp4* expression is still confined to the polster at 6 somites (D). By 10 somites, both *gdf6a* and *bmp4* expression is found within the presumptive dorsal retina (E, F). Morpholino inhibition of Gdf6a reduces the expression of *gdf6a* and *bmp4* (I, J,). By 28 hpf, both *gdf6a* and *bmp4* are confined to the dorsal retina (G, H), and are down-regulated in *gdf6a* morphants at 28 hpf (K, L).

Gdf6a is required for initiation of dorsal retinal patterning

The expression of the dorsal specific transcription factor, *tbx5,* is not detected at the 3 somite stage in either wildtype or *gdf6a* morphant embryos (Figure 4-6 G, J) and is first detected in wildtype embryos at 12 hpf (6 somite stage; Veien et al., 2008 and Figure 4 H), when *gdf6a* is expressed just posterior to the eye (Rissi et al., 1995; Veien et al., 2008; and Figure 4-6 C). The phosphorylation of Smad 1/5/8 proteins is first detected in the developing eye at this time (Figure 4-6 B) indicating that Bmp signaling is active. Phosphorylation becomes more robust by the 10 somite stage (Figure 4-6 C), as does the expression of *tbx5* (Figure 4-6 I). Morpholino inhibition of Gdf6a abolishes Smad phosphorylation at all tested developmental time points (Figure 4-6 E, F), indicative of a complete lack of canonical Bmp signaling in the retina. Similarly, the expression of *tbx5* is not initiated at the 6 somite stage in *gdf6a* morphants (Figure 4-6 K), and remains absent at the 10 somite stage (Figure 4-6 L). Thus, Gdf6a function is required for the phosphorylation of Smads 1/5/8 proteins and the expression of *tbx5* from the earliest stage of retinal patterning, indicating that dorsal retinal patterning is never initiated in a *gdf6a* morphant background. The expression of *bambi* is initiated in the polster at the 2 somite stage (Figure 4-6 M), and is found in the developing eye vesicle by the 6 somite stage (Figure 4-6 N). Like *tbx5,* retinal *bambi* expression becomes more robust by the 10 somite stage (Figure 4-6 O). Expression of *bambi* is strongly down-regulated in the eye vesicle at both the 6 somite and 10 somite stage, (Figure 4-6 Q, R) in *gdf6a* morphants, but some residual expression persists. In contrast to our observations in the retina,

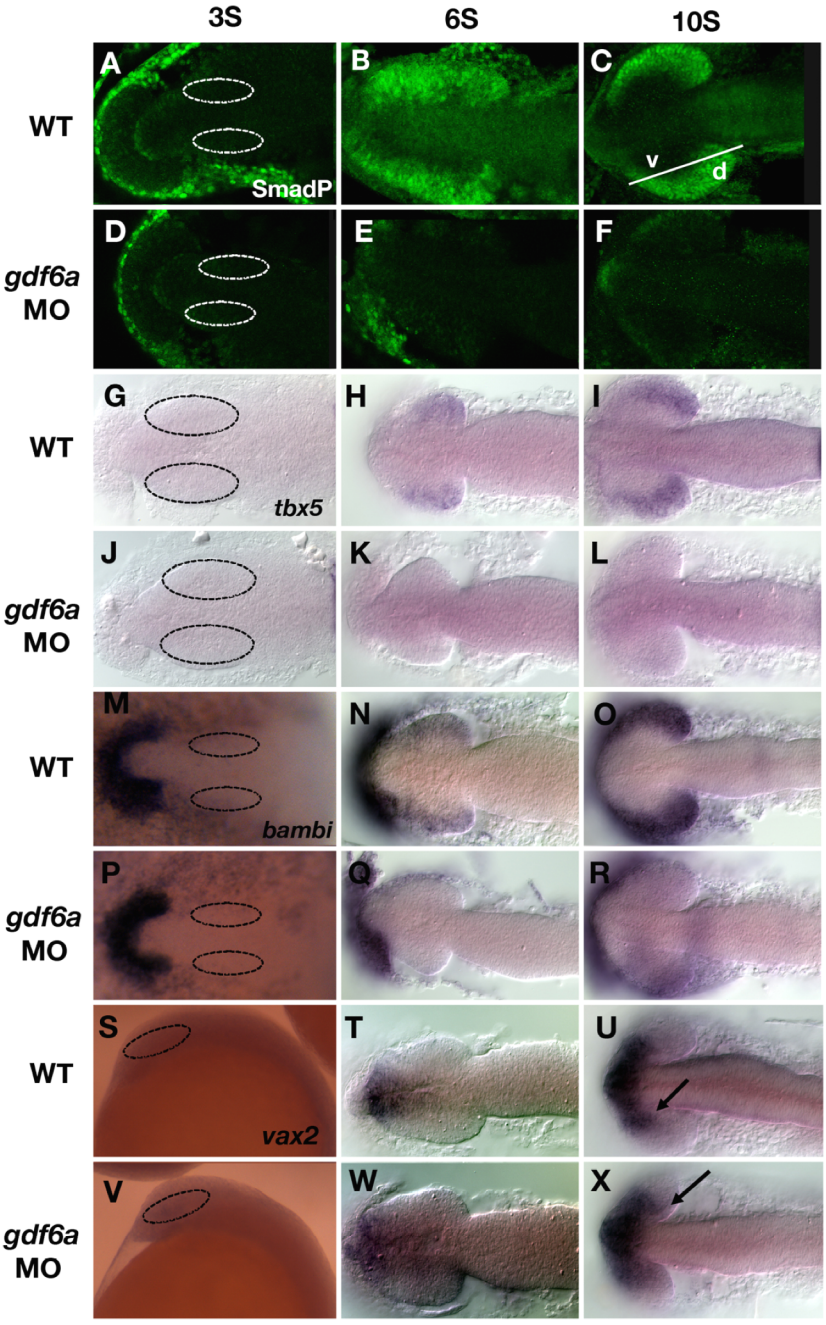
3S
6S
10S
WT
gdf6a MO
WT
gdf6a MO
WT
gdf6a MO
WT
gdf6a MO
A
B
C
SmadP
v
d
D
E
F
G
H
I
tbx5
J
K
L
M
N
O
bambi
P
Q
R
S
T
U
vax2
V
W
X

Figure 4-6: Gdf6a is required for initiation of dorsal-ventral retinal patterning. The phosphorylation of Smad 1/5/8 proteins is not observed in wildtype or morphant embryos at 3 somites (A, D), nor is the expression of the dorsal markers *tbx5* and *bambi* (G, J, M, P). Phosphorylation of Smad proteins is observed by the 6 somite stage (B), and is not detected in *gdf6a* morphants (E). Phosphorylation becomes more robust by 10 somites in wildtype embryos (C) and is still not detected in *gdf6a* morphants (F). The expression of *tbx5* and *bambi* is initiated in the retinal tissue at 6 somites (H, N), and are not detected in *gdf6a* morphants (K, Q). Expression becomes more robust at 10 somites (I, O), and is still not detected in *gdf6a* morphants (L, R). The expression of *vax2* is not detected in either wildtype or morphant animals at 3 somites (S, V). Expression is confined to the forebrain at 6 somites (T) and is not altered in *gdf6a* morphants (W). Expression of *vax2* is detected in the forebrain and presumptive ventral retina in wildtype animals at 10 somites (U), and is mildly expanded in *gdf6a* morphants (X). Dotted circles delineate the optic cup. Black arrows point to expanded expression of *vax2* in *gdf6a* morphants.

expression in the polster at 3 somites is not affected by morpholino inhibition of Gdf6a (Figure 4-6 P). As no Smad phosphorylation is observed in the polster at this time (Figure 4-6 D), this expression is likely due to Gdf6a-independent signaling mechanisms.

The expression of *vax2* is not detected at the 3 somite stage in both wildtype or *gdf6a* morphant embryos (Figure 4-6 S, V) and is first detected at the 6 somite stage (Figure 4-6 T), at the same time as *tbx5*. Expression is confined to the forebrain and proximal optic vesicle at this time. Retinal expression becomes more robust by the 10 somite stage (Figure 4-6 U). In *gdf6a* morphants, *vax2* expression at the 6 somite stage is not altered (Figure 4-6 W). The expression domain of *vax2* is expanded at the 10 somite stage (Figure 4-6 X), however expression is not found throughout the entire retina as seen in *gdf6a* morphants at 28 hpf. This implies that *vax2* expression is under multiple regulatory inputs, including antagonistic signals from the dorsal retina and activating signals from the ventral retina, which differ between the 6 somite stage and 28 hpf.

bmp4 is not required for dorsal-ventral retinal patterning

As other Bmp ligands are expressed at early stages of eye development, we tested whether Bmp4 is required for either initiation or maintenance of dorsal retinal patterning. Mopholino inhibition of Bmp4 does not affect the phosphorylation of Smad 1/5/8 proteins at any stage tested (Figure 4-7 A-G), nor is the expression of *tbx5* altered in these embryos (Figure 4-7, H-M), indicating that Bmp4 is not required for these processes. Knockdown of Bmp4 does,

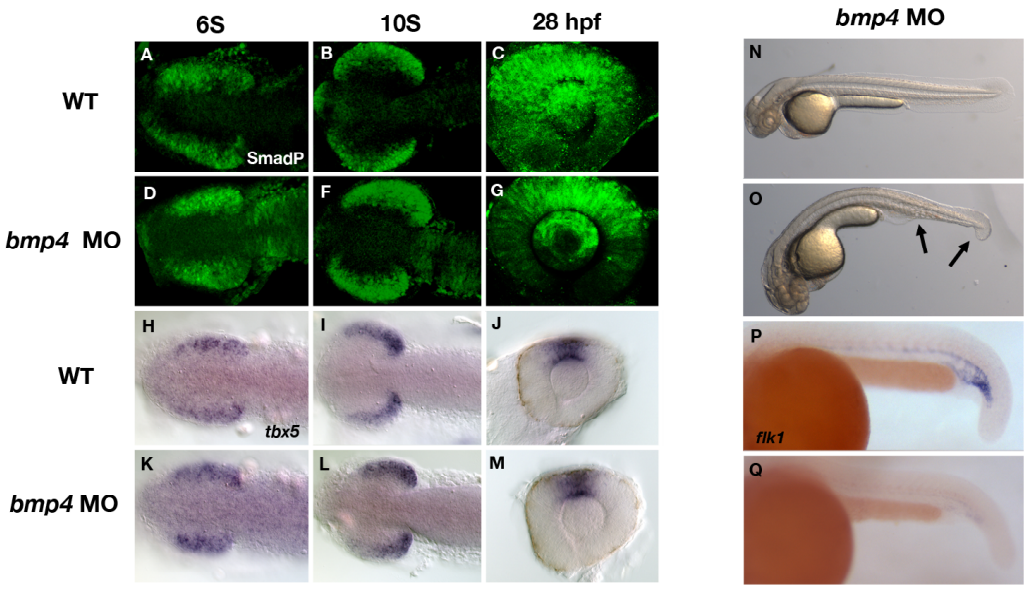

Figure 4-7: Morpholino inhibition of *bmp4* has no effect on eye patterning. Phosphorylation of Smad 1/5/8 proteins in not affected at any stage tested, including 6 somites (A, D), 10 somites (B, F), or 28 hpf (C, G). Similarly, the expression of *tbx5* is normal at 6 somites (H, K) 10 somites (I, L) and 28 hpf (J, M). Morphological phenotypes of *bmp4* morphants at 2 dpf (compare O with N) showing a C2 dorsalized phentoype (Mullins et al., 1996) involving loss of the ventral tail fin and ventral vein. Expression of a Bmp4 target gene, *flk1* 24 hpf, is down regulated in *bmp4* morphants (compare Q with P). Both phenotypes are observed in a previously published *bmp4* null mutant (Stickney et al., 2007). Arrows denote the extent of ventral tissue loss.

however, cause a loss of the ventral tail fin (Figure 4-7 N, O), as well as reduction of *flk1* expression, phenotypes that are identical to the previously published *bmp4* null mutant (Figure 4-7 P, Q) (Stickney et al., 2007).

Over-expression of Gdf6a signaling components in the early eye field induces dorsal gene expression and represses ventral gene expression.

Embryo-wide over-expression of *gdf6a* profoundly ventralizes the embryo, and suppresses eye formation (Goutel et al., 2000). To circumvent this difficulty and to test whether Gdf6a signaling is sufficient to drive expression of dorsal retinal markers, we over-expressed *gdf6a*, and a constitutively active form of the human *Bmp type 1 receptor* (*caBMPR1a*) under the control of the *retinal homeobox 3* (*rx3*) promoter from Medaka (*Oryzias latipes*). The *rx3* promoter can drive gene expression in all retinal progenitor cells from the onset of their specification (Loosli et al., 2001; Rembold et al., 2006). The effectiveness of this system is demonstrated by the observation that we can restore Smad phosphorylation in *gdf6a* morphants expressing *rx3:gdf6a* (Figure 4-8 A-C). Similarly, we can restore *tbx5* and *bambi* expression in *gdf6a* morphants by expressing either *rx3:gdf6a* or *rx3:BMPR1a* (Figure 4-8 D-K).

Expression of *gdf6a* throughout the eye vesicle increases phosphorylation of Smad 1/5/8 proteins in all embryos tested, and expands the domain where phosphorylation is detected to the presumptive ventral region (n =18/18, compare Figure 4-9 A and 5B). This effect is non-cell autonomous, as cells expressing *rx3:gdf6a* induce the phosphorylation of Smad 1/5/8 proteins in surrounding cells

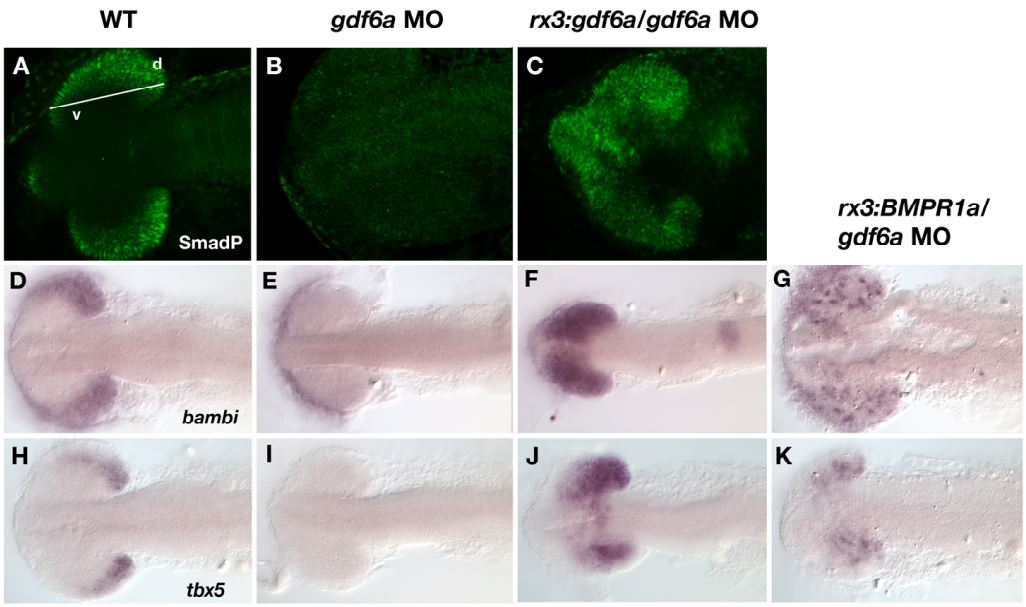

Figure 4-8: Over-expression Bmp signaling components can rescue *gdf6a* morpholino phenotypes. Over-expression of *gdf6a* rescues Smad 1/5/8 phosphorylation in the presumptive retina (A-C). Similarly, the expression of *tbx5* and *bambi*, which are lost in the presumptive dorsal retina in *gdf6a* morphants (compare D and H with E and I) is restored via over-expression of *gdf6a*. Over-expression of *caBMPR1*, can also rescue these phenotypes, but in a cell autonomous fashion (G and K).

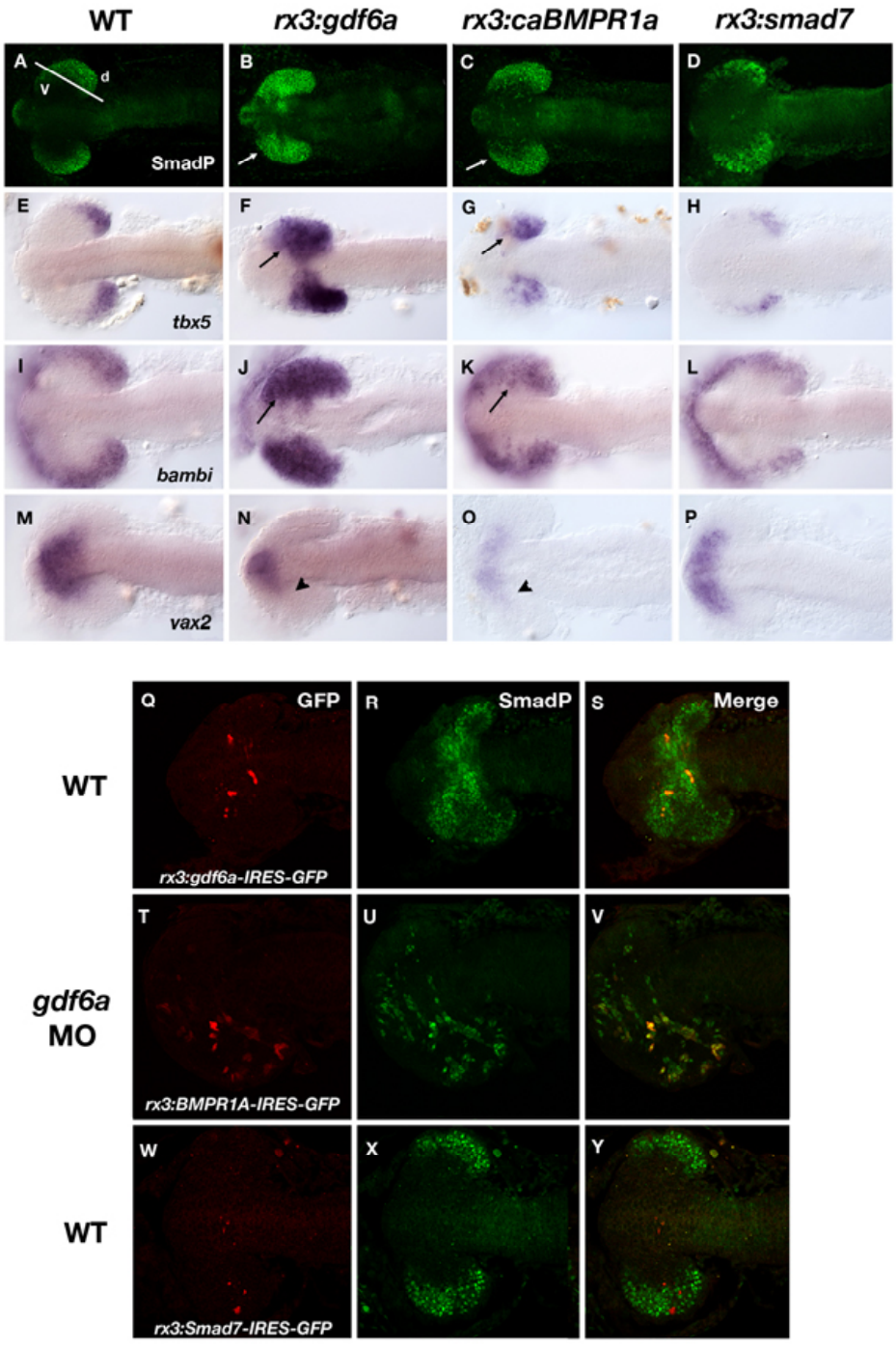
WT
rx3:gdf6a
rx3:caBMPR1a
rx3:smad7
A
d
v
SmadP
B
C
D
E
tbx5
F
G
H
I
bambi
J
K
L
M
vax2
N
O
P
Q
GFP
R
SmadP
S
Merge
WT
rx3:gdf6a-IRES-GFP
T
gdf6a
MO
rx3:BMPR1A-IRES-GFP
U
V
W
WT
rx3:Smad7-IRES-GFP
X
Y

Figure 4-9: Over-expression of Gdf6a signaling components induces dorsal identity and represses ventral identity. The phosphorylation of Smad 1/5/8 proteins is induced in the presumptive ventral retina when either *gdf6a* or *BMPR1a* is expressed using the Medaka *rx3* promoter (B, C). This effect is cell non-autonomous with respect to *gdf6a,* and phsophosylation is induced in cells surrounding those that express *rx3:gdf6a-IRES-GFP* (Q-S). Expression of *caBMPR1a* exerts its effects in a cell autonomous fashion as phosphorylation is detected specifically in cells that express *rx3:caBMPR1a-IRES-GFP* (T-V). The expression of *tbx5* (E, F) and *bambi* (I, J) are also induced ectopically in the retina under both conditions. The expression of *vax2* is found in the retina just proximal to the forebrain in wildtype embryos (M), and this expression is lost in embryos expressing either *gdf6a* (N) or *BMPR1a* (O). Expression of the inhibitory *smad7* via the *rx3* promoter inhibits phosphorylation of Smad 1/5/8 proteins (D), as well as the expression of *tbx5* (H) and *bambi* (L). Smad7 works in a cell autonomous fashion as Smad phosphorylation is specifically inhibited in cells expressing *rx3:smad7-IRES-GFP* (W-Y). Expression of *smad7* has no effect on the retinal expression of *vax2* (P). All embryos were staged to 10 somites. White arrows indicate etopic Smad 1/5/8 phosphorylation in the presumptive ventral retina, while black arrows indicate ectopic expression of dorsal genes in the presumptive ventral retina. Arrowheads point to the reduction of *vax2* expression in the presumptive ventral retina in embryos over-expressing *gdf6a* or *caBMPR1a.*

(Figure 4-9 Q-S). We observe the same phenotype in embryos expressing *caBMPR1a* (n=13/13, Figure 4-7 C), though the effects are more mosaic, representing the cell autonomous nature of the constitutively active receptor (Figure 4-9 T-V). To determine whether these changes in Smad phosphorylation result in altered retinal dorsal-ventral axis specification, we examined *tbx5*, *bambi*, and *vax2* expression. We observe that the expression of both *tbx5* and *bambi* is induced in the presumptive ventral retinal when *gdf6a* (n=11/15 embryo for *tbx5*; 16/16 embryos for *bambi*; Figure 4-7 E, F, I, J) or *caBMPR1a* are ectopically expressed (n=1/14 embryos for *tbx5*; 3/16 embryos for *bambi*; Figure 4-9 E, G, I, K). Moreover, the expression of the ventral specific *vax2* is repressed in the presumptive ventral retina when either *gdf6a* (n=18/19) or *caBMPR1* (n=9/15) are ectopically expressed (Compare figure 4-9 N and O with 4-9 M). Taken together, Gdf6a signaling is sufficient to drive the expression of dorsal retinal markers, and to inhibit the expression of ventral markers within the presumptive retina.

To corroborate our morpholino knockdown experiments, we also expressed inhibitory *smad7* under the transcriptional control of the *rx3* promoter to block Bmp signaling in the early developing eye. The effectiveness of this assay is demonstrated by the fact that Smad 1/5/8 phosphorylation is not detected in cells expressing the *smad7* transgene (Figure 4-9 W-Y) and thus inhibits Smad 1/5/8 phosphorylation in a mosaic and cell autonomous fashion (Figure 4-9 D). Additionally, the expression of *tbx5* (n=11/15) and *bambi* (n=8/16) is inhibited via over-expression of *smad7* (Figure 4-9 H, L). In contrast to the Gdf6a

knockdown results, the expression of *vax2* is not expanded or found in the presumptive dorsal retina at early stages of eye development through over-expression of *smad7* (Figure 4-9 P). Overall, the results of *smad7* over-expression in the developing retina suggest that Gdf6a exerts its influence on dorsal patterning through Smads 1/5/8-mediated transcriptional regulation of Bmp target genes.

Morpholino knockdown of Tbx5 inhibits dorsal gene expression, but has no affect on ventral gene expression

Tbx5 has known roles in fin and heart development, in addition to retinal patterning. Mutations in *tbx5*, or inhibition of Tbx5 using a translation blocking morpholino, results in aberrant pectoral fin development (Ahn et al., 2002; Garrity et al., 2002) and cardiac phenotypes that include stretched and un-looped hearts (Garrity et al., 2002). To ensure our *tbx5* morpholino specifically knocked down Tbx5 function, we quantified pectoral fin and heart defects in *tbx5* morphants, in addition to retinal phenotypes. *tbx5* morphants displayed a complete loss of pectoral fins by 72 hpf (30/30 embryos, 100%), while 18/30 (60%) had un-looped or stretched hearts. In addition, 23/30 (23/30, 77%) displayed microphthalmia, and (6/30, 20%) displayed severe coloboma. Both of these phenotypes have been previously associated with a knockdown of Gdf6a function (Asai-Coakwell et al., 2007).

With respect to eye patterning, morpholino inhibition of Tbx5 results in a severe reduction in the expression of *efnb2a* and *bambi* in the dorsal retina

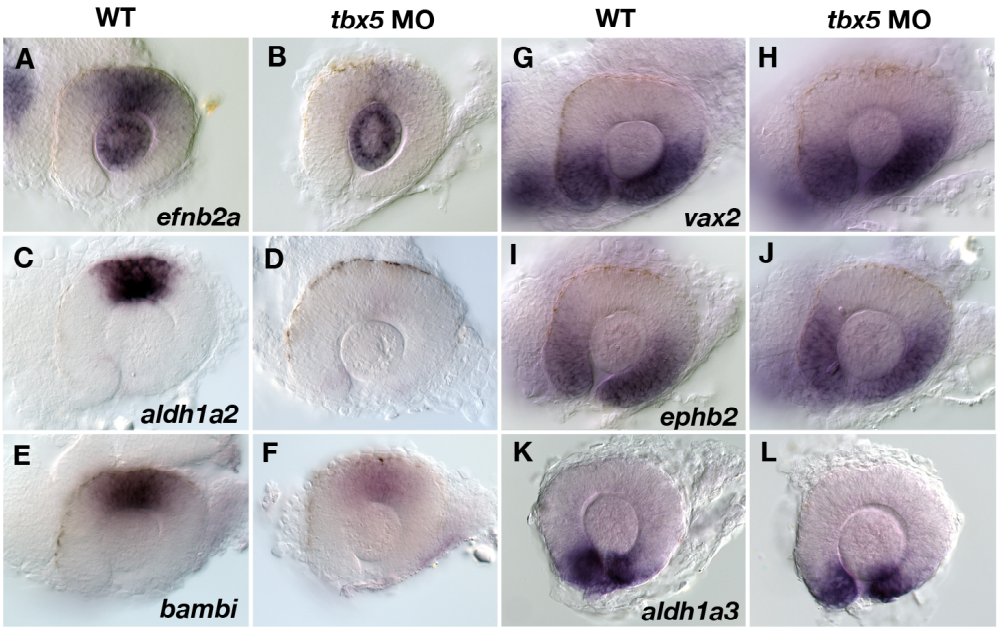

Figure 4-10: Morpholino inhibition of Tbx5 affects dorsal, but not ventral gene expression. The retinal expression of *efnb2a* is lost in *tbx5* morphants, while the lens specific expression remains unchanged (A, B). The expression *aldh1a2* is lost (C, D), while the expression of *bambi* is highly down-regulated (E, F). In the ventral retina, *vax2* (G and H), *ephb2* (I and J), and *aldh1a3* (K, L) are not altered in *tbx5* morphants. All embryos were staged to 28hpf.

(Figure 4-10 A, B, E, F), though some residual expression does remain. Similar to that of *gdf6a* morphants, the expression of *aldh1a2* is absent in the dorsal retina upon inhibition of Tbx5 (Figure 4-10 C, D). The expression of ventral markers is unaffected in *tbx5* morphants. Neither *vax2* (Figure 4-10 G, H), *ephb2* (Figure 4-10 I, J) or *aldh1a3* (Figure 4-10 K, L) are expanded in *tbx5* morphants, indicating that *tbx5* is not sufficient for inhibition of the ventral patterning pathway as shown by over-expression models.

Discussion

As the eye forms, cellular identity is specified along both nasal-temporal and dorsal-ventral axes, promoting differential fates of cells within these distinct regions. Bmp growth factors are critically important for eye development, as mutations in Bmp signaling components have been mapped in human patients with ocular disorders (Asai-Coakwell et al., 2007; Asai-Coakwell et al., 2009; Bakrania et al., 2008). Studies in model organisms have revealed a specific role for Bmps in dorsal-ventral patterning of the retina (Behesti et al., 2006; Gosse and Baier, 2009; Plas et al., 2008; Sakuta et al., 2001; Sakuta et al., 2006). This research shows a clear role for Bmp signaling in retinal patterning, but the signal that initiates dorsal identity has remained unclear. Here, we show that in a zebrafish model system, Gdf6a is both necessary and sufficient to initiate dorsal retinal identity.

Loss of Gdf6a results in profound alterations to patterning of the nascent optic vesicle with loss of dorsal markers such as *tbx5* and expansion of ventral

markers such as *vax2*. An analysis of dorsal-ventral identity demonstrates that this early alteration of patterning results in later effects on *eph* and *ephrin* gene expression and therefore affects regional cell identity in the retina. As a result of altered dorsal-ventral patterning in the early retina, retinal ganglion cell axons exhibit aberrant mapping onto the optic tectum. In *gdf6a* mutant embryos, the lateral tectum lacks innervation by RGC axons, an area normally occupied by RGC axons that originate in the dorsal retina. These data support the hypothesis that the lack of dorsal retinal patterning in the early embryo results in the inability to construct the proper neural connections between the retina and visual processing centers later in development.

In other model systems, dorsal-ventral retinal patterning requires the actions of Bmp4 (Sakuta et al., 2001; Sakuta et al., 2006). Although Gdf6a is able to transcriptionally regulate *bmp4* expression at later stages of eye patterning, our data indicates that Bmp4 is not expressed near the presumptive dorsal retina during initiation of retinal identity. Furthermore, we conclude that Bmp4 is not necessary for the initiation or maintenance of retinal patterning, as knockdown of Bmp4 produces no discernable retinal phenotype. In these *bmp4* morphant embryos, the expression of dorsal retinal markers is initiated normally at the 6 somite stage, and is maintained until at least 28 hpf. Although our data argue against a role for Bmp4, there are other Bmp ligands expressed in the eye at early stages, such as Bmp2b (Veien et al., 2008). As Bmp ligands are known to function as heterodimers (Little and Mullins, 2009), it is plausible that Bmp2b and Gdf6a cooperatively pattern the dorsal retina. However, the absence of eye-

specific Smad phosphorylation observed in *gdf6a* morphant embryos indicates that any other retinal Bmp signaling must be dependent on Gdf6a.

Corroboration for these morpholino-based experiments is provided by a novel gain-of-function approach, where components of the Gdf6a signaling pathway are expressed under regulatory control of the Medaka *rx3* promoter. By expressing *gdf6a* and a constitutively active form of the human *BMPR1a* receptor in retinal progenitor cells, it is possible to induce markers of dorsal cell fate in the presumptive ventral retina, indicating that *gdf6a* is sufficient to induce dorsal cell fate in retinal tissues.

It has been shown that other signaling mechanisms such as the Wnt signaling pathway (Veien et al., 2008; Zhou et al., 2008) can act during the maintenance phase of retinal patterning, and regulate the expression of *bmp* genes including *gdf6a* (Veien et al., 2008). Through careful time course analysis, our data clearly shows that *gdf6a* acts at the initiation stage of dorsal patterning. Expression of *gdf6a* is first detected in the optic vesicle at 6 somites, the same time that Smad phosphorylation and the expression of dorsal markers are initiated. In *gdf6a* morphants, no Smad phosphorylation is observed at 6 somites, and the expression of *tbx5* is never initiated. We also show that Gdf6a can regulate the expression of the Bmp pseudoreceptor *bambi*, which can positively regulate the Wnt signaling pathway (Lin et al., 2008). Therefore, in addition to initiating dorsal retinal patterning, Gdf6a signaling may also ensure positive regulation of maintenance phase signaling components.

The restricted expression of ventral markers in the retina appears to be independent of Tbx5 function, as morpholino inhibition of *tbx5* reduces dorsal marker expression, but has little effect on ventral gene expression. At a developmental stage of 10 somites, the expression of *tbx5* is completely lost in *gdf6a* morphants, while *vax2* is not expanded throughout the retina, further supporting this hypothesis. This contradicts models from over-expression experiments where ectopic *tbx5* inhibits the expression of ventral *vax2* expression gene expression (Koshiba-Takeuchi et al., 2000). Taken together with the results of over-expression models, *tbx5* is sufficient to drive expression of dorsal retinal markers, but inhibition is not sufficient to allow for expansion of ventral retinal markers. Overlapping functions of other *tbx* paralogs in the zebrafish genome may be able to compensate for a loss of Tbx5 function, thereby maintaining the dorsal limit of *vax2* expression when Tbx5 function is lost. At early stages of eye development *tbx2b* is expressed in the developing eye field (Gross and Dowling, 2005), and is thus a likely candidate for this proposed partial redundancy.

Conclusions

In summary, we have shown that Gdf6a is both necessary and sufficient to initiate dorsal gene expression in the developing zebrafish eye through both knockdown and over-expression analysis. In the absence of Gdf6a signaling, the retina is competent to adopt a ventral cell fate, as evidenced by expanded ventral gene expression and aberrant mapping of RGC axons on the optic tectum.

Bibliography

Ahn, D. G., et al., 2002. T-box gene tbx5 is essential for formation of the pectoral limb bud. Nature. 417**,** 754-8.

Asai-Coakwell, M., et al., 2007. GDF6, a novel locus for a spectrum of ocular developmental anomalies. Am J Hum Genet. 80**,** 306-15.

Asai-Coakwell, M., et al., 2009. Incomplete penetrance and phenotypic variability characterize Gdf6-attributable oculo-skeletal phenotypes. Hum Mol Genet. 18**,** 1110-21.

Bakrania, P., et al., 2008. Mutations in BMP4 cause eye, brain, and digit developmental anomalies: overlap between the BMP4 and hedgehog signaling pathways. Am J Hum Genet. 82**,** 304-19.

Barbieri, A. M., et al., 2002. Vax2 inactivation in mouse determines alteration of the eye dorsal-ventral axis, misrouting of the optic fibres and eye coloboma. Development. 129**,** 805-13.

Barishak, Y. R., 1992. Embryology of the eye and its adnexae. Dev Ophthalmol. 24**,** 1-142.

Behesti, H., et al., 2006. The level of BMP4 signaling is critical for the regulation of distinct T-box gene expression domains and growth along the dorso-ventral axis of the optic cup. BMC Dev Biol. 6**,** 62.

Erskine, L., Herrera, E., 2007. The retinal ganglion cell axon's journey: insights into molecular mechanisms of axon guidance. Dev Biol. 308**,** 1-14.

French, C. R., et al., 2007. Pbx homeodomain proteins pattern both the zebrafish retina and tectum. BMC Dev Biol. 7**,** 85.

Garrity, D. M., et al., 2002. The heartstrings mutation in zebrafish causes heart/fin Tbx5 deficiency syndrome. Development. 129**,** 4635-45.

Gosse, N. J., Baier, H., 2009. An essential role for Radar (Gdf6a) in inducing dorsal fate in the zebrafish retina. Proc Natl Acad Sci U S A. 106**,** 2236-41.

Goutel, C., et al., 2000. The ventralizing activity of Radar, a maternally expressed bone morphogenetic protein, reveals complex bone morphogenetic protein interactions controlling dorso-ventral patterning in zebrafish. Mech Dev. 99**,** 15-27.

Gross, J. M., Dowling, J. E., 2005. Tbx2b is essential for neuronal differentiation along the dorsal/ventral axis of the zebrafish retina. Proc Natl Acad Sci U S A. 102**,** 4371-6.

Halilagic, A., et al., 2007. Retinoids control anterior and dorsal properties in the developing forebrain. Dev Biol. 303**,** 362-75.

Koshiba-Takeuchi, K., et al., 2000. Tbx5 and the retinotectum projection. Science. 287**,** 134-7.

Lin, Z., et al., 2008. The pseudoreceptor BMP and activin membrane-bound inhibitor positively modulates Wnt/beta-catenin signaling. J Biol Chem. 283**,** 33053-8.

Little, S. C., Mullins, M. C., 2009. Bone morphogenetic protein heterodimers assemble heteromeric type I receptor complexes to pattern the dorsoventral axis. Nat Cell Biol. 11**,** 637-43.

Loosli, F., et al., 2001. Medaka eyeless is the key factor linking retinal determination and eye growth. Development. 128**,** 4035-44.

Lupo, G., et al., 2005. Dorsoventral patterning of the Xenopus eye: a collaboration of Retinoid, Hedgehog and FGF receptor signaling. Development. 132**,** 1737-48.

Mullins, M. C., et al., 1996. Genes establishing dorsoventral pattern formation in the zebrafish embryo: the ventral specifying genes. Development. 123**,** 81-93.

Plas, D. T., et al., 2008. Bone morphogenetic proteins, eye patterning, and retinocollicular map formation in the mouse. J Neurosci. 28**,** 7057-67.

Rembold, M., et al., 2006. Individual cell migration serves as the driving force for optic vesicle evagination. Science. 313**,** 1130-4.

Sakuta, H., et al., 2001. Ventroptin: a BMP-4 antagonist expressed in a double-gradient pattern in the retina. Science. 293**,** 111-5.

Sakuta, H., et al., 2006. Role of bone morphogenic protein 2 in retinal patterning and retinotectal projection. J Neurosci. 26**,** 10868-78.

Schulte, D., et al., 1999. Misexpression of the Emx-related homeobox genes cVax and mVax2 ventralizes the retina and perturbs the retinotectal map. Neuron. 24**,** 541-53.

Sehgal, R., et al., 2008. Ectopic Pax2 expression in chick ventral optic cup phenocopies loss of Pax2 expression. Dev Biol. 319**,** 23-33.

Sekiya, T., et al., 2004. Transcriptional regulation of the TGF-beta pseudoreceptor BAMBI by TGF-beta signaling. Biochem Biophys Res Commun. 320**,** 680-4.

Sidi, S., et al., 2003. Maternal induction of ventral fate by zebrafish radar. Proc Natl Acad Sci U S A. 100**,** 3315-20.

Stickney, H. L., et al., 2007. Zebrafish bmp4 functions during late gastrulation to specify ventroposterior cell fates. Dev Biol. 310**,** 71-84.

Veien, E. S., et al., 2008. Canonical Wnt signaling is required for the maintenance of dorsal retinal identity. Development. 135**,** 4101-11.

Zhou, C. J., et al., 2008. Ocular coloboma and dorsoventral neuroretinal patterning defects in Lrp6 mutant eyes. Dev Dyn. 237**,** 3681-9.

Zolessi, F. R., et al., 2006. Polarization and orientation of retinal ganglion cells in vivo. Neural Dev. 1**,** 2.

Chapter 5

Microarray analysis and associated phenotypes of *gdf6a* morphant embryos

Selected figures from this chapter have been previously published

***French CR**, Erickson T, French DV, Pilgrim DB, Waskiewicz AJ.*
Gdf6a is required for the initiation of dorsal-ventral retinal patterning and lens development. Dev Biol. 2009 Sep 1;333(1):37-47.

Introduction

Although *gdf6a* is maternally contributed and expressed ubiquitously in the early embryo (Goutel et al., 2000), expression is refined to specific structures later in development. In addition to the neural retina, expression is also detected in the roof plate of the neural tube (Bonner et al., 2008), neural crest cells, jaw cartilage, hypochord, and the primitive gut endoderm (Hall et al., 2002; Qian et al., 2005; Reed and Mortlock, 2010). *gdf6a* morphants show defects in vascular integrity, resulting in hemorrhages in the trunk of the embryo during development (Hall et al., 2002). The trunk axial blood vessels develop in a position flanked by the hypochord and primitive gut endoderm, which is a known source of signals required for vascular development. Thus it is likely that *gdf6a* expression in these tissues is required for maintenance of vascular integrity. Within the roof plate, *gdf6a* expression has been used as a marker for dorsal neural tube specification (Bonner et al., 2008), and loss of function analysis suggests a role in the survival of cells within the dorsal neural tube (Delot et al., 1999).

Bmp signaling has also been implicated in the development of non-neural ocular tissues, mainly the induction of lens tissue and subsequent differentiation of lens fiber cells. The vertebrate lens is induced by contact of the surface ectoderm with the optic vesicle, resulting in the invagination of the lens placode (Dahm et al., 2007). Upon formation of the lens vesicle, epithelial cells in the anterior half continue to proliferate, while cells in the posterior half differentiate into primary and secondary fiber cells characterized by increased length and *crystallin* gene expression. Mice lacking both *Bmp4* and *Bmp7* have severe

defects in lens placode induction, indicating that Bmps control the earliest stages of lens development (Furuta and Hogan, 1998; Wawersik et al., 1999). Inhibition of Bmp receptors, either in mice or cell culture systems, also blocks differentiation of primary lens fibers (Faber et al., 2002). Moreover, in a cell culture system that allows normal lens cell development at early stages, but perturbs Bmp signaling at later stages of development, secondary fiber cell differentiation was aberrant (Boswell et al., 2008), indicating that Bmps can potentially affect all stages of lens development in vertebrates.

Although Bmp signaling has been implicated is numerous processes in lens development, no study has indicated whether *gdf6a* in particular is required for lens formation or function. *gdf6a* expression is not detected in the lens, however phosphorylation of Smad proteins 1, 5, and 8 is evident in the lens (Chapter 4, figure 3), indicating that Bmp signaling is active in this tissue. In the zebrafish lens, Smad phosphorylation is detected at 24 hpf when *gdf6a*, *bmp4* and *bmp2b* are expressed in the dorsal retina, and moreover, Smad phosphorylation remains at normal levels when *bmp4* expression is inhibited (Chapter 4, figure 7). Thus, other Bmp ligands, including *gdf6a* may be sufficient for lens development in the absence of Bmp4 function.

Within the forebrain, Bmp signaling has been implicated in the development of the pineal complex, which includes the pineal gland and the parapineal body, that function to regulate circadian rhythm in some vertebrate model systems including zebrafish (Chaurasia et al., 2005; Quay, 1963; Quay, 1965; Quay, 1966; Ziv et al., 2005). *bmp2* expression is detected in the *Xenopus*

pineal gland (Clement et al., 1995; Knochel et al., 2001), while *GDF6* is expressed in the human pineal gland (Katoh and Katoh, 2006). The function of Gdf6a signaling in the pineal complex, however, remains uncharacterized as no loss or gain of function studies have been reported.

Bone morphogenetic proteins were first identified and named due to their ability to induce bone and cartilage formation in cultured cells or when injected into mice (Urist et al., 1979; Urist et al., 1976). Gdf6, and a closely related Gdf family member, Gdf5, have both been implicated in skeletal development. Gdf6 is expressed in and around pharyngeal jaw cartilage elements 3 through 7, and contains a jaw specific evolutionary conserved enhancer element indicating that the use of Gdf6 for specifying jaw elements evolved in animals long ago (Reed and Mortlock, 2010). In addition, *GDF6* sequence variants have been associated with vertebral fusions manifesting in Klippel-Feil syndrome (Asai-Coakwell et al., 2009; Tassabehji et al., 2008). The closely related Gdf5, the protein product encoded by the *brachypodism* locus in mouse, (Storm et al., 1994) is expressed in transverse stripes across developing skeletal elements and is one of the earliest known markers of joint formation during vertebrate skeletal development (Merino et al., 1999; Storm et al., 1994). Although mutations in both *Gdf5* and *Gdf6* cause multiple defects in skeletal development, double knockout mice have additional defects not seen in either single mutant (Settle et al., 2003), implying at least partially independent functions for Gdf5 and Gdf6 during skeletal development.

To gain insight into the role Gdf6a may play in the zebrafish embryo (in addition to dorsal-ventral retinal patterning), we performed microarray analysis on

gdf6a whole morphant embryos. In addition to identifying retinal patterning genes already known to be downstream of Gdf6a, we uncovered Gdf6a dependent transcripts mainly in the roof plate, lens, and scleratome (which eventually give rise to vertebrae). Reported here are the results of the microarray analysis and further characterization of lens and skeletal phenotypes in *gdf6a* morphant embryos.

Results

Validation of microarray analysis

Microarray analysis on whole *gdf6a* morphant embryos at 24 hpf uncovered 109 features (corresponding to approximately 54 transcripts) that were down-regulated by 2 fold, while 538 features (corresponding to approximately 269 transcripts) were down-regulated by 1.5 fold. 72 features (corresponding to approximately 36 transcripts) were up-regulated in *gdf6a* morphants by 2 fold, while 163 features (corresponding to approximately 81 transcripts) were up-regulated by 1.5 fold. Genes involved in the development of numerous embryonic tissues were discovered to be regulated by Gdf6a, including those involved in fast muscle-cell differentiation, lens, pineal blood, skeletal, and eye development. Selected genes from this list are displayed in Table 5-1. A list of all genes down-regulated by at least 2 fold is displayed in Appendix A. All genes up-regulated by at least 2-fold are displayed in Appendix B.

In agreement with the microarray data, *in situ* hybridization demonstrated that genes such as *fabp7a* and *rx2* were found to be down-regulated in the eye

Table 5-1: Selected genes differentially regulated in *gdf6a* morphant embryos at 24 hpf.

Gene		Gene ontology	Fold change	Validation
vtn	*vitronectin*	liver, hypothalamus development	7.3	None
cryba1b	*crystallin beta A1b*	lens development	5.4	ISH
cryba2a	*crystallin beta A2a*	lens development	4.9	ISH
atoh1a	*atonal homolog 1a*	neurogenesis	3.5	ISH
crybb1	*crystallin beta B1*	lens development	3.4	None
rp9	*retinitis pigmentosa homolog 9*	spliceosome function	2.7	qPCR
hmx4	*H6 homeobox 4*	axial patterning	2.4	ISH
lim2.3	*lens intrinsic membrane protein 1*	lens development	2.1	ISH
cx23	*connexin 23*	lens development	2.0	ISH
mcm4	*mini-chromosome maintenance protien 4*	proliferation, DNA replication	1.9	None
tbx2b	*t-box transcription factor 2b*	patterning, differentiation (PRL)	1.9	ISH
fabp7a	*fatty acid binding protein 7a*	brain, eye development	1.8	ISH
crx	*cone rod homeobox*	differentiation , PRL, pineal gland	1.8	ISH

Fold change: WT/*gdf6a* morphant

Table 5-1: Selected genes differentially regulated in *gdf6a* morphant embryos at 24 hpf (continued from previous page).

Gene		Gene ontology	Fold change	Validation
ascl1a	*achaete-scute complex-like 1a*	Pineal, nervous system dev.	1.6	None
nog3	*noggin 3*	Bmp inhibition, bone repair	1.6	None
nog1	*noggin 1*	Bmp inhibition, bone repair	1.5	ISH
bambi a	*BMP/activin membrane-bound inhibitor a*	eye, cancer development	1.3	ISH
flh	*floating head transcription factor*	pineal development	1.3	None
ccng1	*cyclin G1*	cell cycle, apoptosis	0.20	ISH
rdh1	*retinol dehydrogenase 1*	retinoic acid metabolism	0.46	None
fst1l	*follistatin -like 1*	Bmp inhibition	0.50	None

Fold change: WT/*gdf6a* morphant

(Figure 5-1 A-D), while expression of *fabp7a* remains at wild type levels within the tectum (Figure 5-1A, B). The expression of the Bmp pseudoreceptor *bambi*, which inhibits Bmp signaling, was identified on the microarray as down-regulated by 30%, and *in situ* hybridization indicates a complete loss of expression in the retina, but is unaffected in other areas of the embryo (Figure 5-1, E-F). The expression of *tbx2b*, known for its role in eye, ear, and pineal development (Alvarez-Delfin et al., 2009; Gross and Dowling, 2005; Snelson et al., 2008a; Snelson et al., 2008b), is down-regulated in the retina of *gdf6a* morphant embryos (Figure 5-1 G, H). Within the roof plate of the neural tube, the expression of the pro-neural gene *atonal homolog 1a* (*atoh1a*) was identified as significantly down-regulated by both microarray and *in situ* analysis (Table 5-1 and figure 5-1 K and L), indicating that Gdf6a may be involved in neurogenesis within the neural tube at 24 hpf. The cell cycle regulator *ccng*, normally expressed in the eye and at the midbrain-hindbrain boundary at 24 hpf, is up regulated throughout the embryo in *gdf6a* morphant embryos (Figure 5-1 I and J).

Analysis of photoreceptor development in gdf6a morphant embryos

Our microarray analysis identified five genes are required for development of the pineal and parapineal gland in zebrafish, many of which are implicated specifically in the development of pineal photoreceptors. *crx* is required for photoreceptor cell development and thus functionality of the pineal/parapineal complex (Gamse et al., 2002). The expression of *crx* is near wildtype levels in the pineal gland of *gdf6a* morphant embryos, however the expression domain is

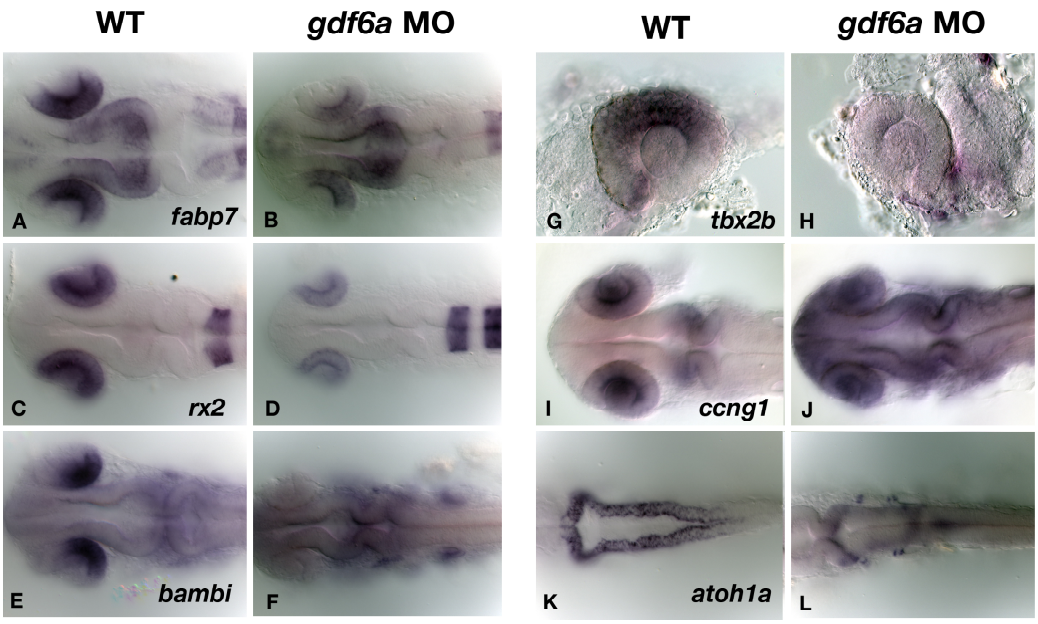

Figure 5-1: Validation of selected microarray Gdf6a dependent transcripts by *in situ* hybridization. The expression of *fabp7a*, found in the retina and tectum in wildtype animals (A) is highly reduced in the retina of *gdf6a* morphants but unaffected in the tectum (B) The expression of *rx2*, found throughout the retina at 24 hpf (C) is also reduced in *gdf6a* morphants (D). The expression of the Bmp pseudoreceptor *bambi*, and the t-box transcription factor *tbx2b* is localized to the dorsal retina at 24 hpf (E and G) and is eliminated in *gdf6a* morphants (F and H). The expression of *cyclin G1*, found in the eye and midbrain-hindbrain boundary (I) is up-regulated in *gdf6a* morphants (J), while the expression of the pro-neural *atoh1a* is reduced in the roofplate of *gdf6a* morphant embryos (K and L).

reduced in size, indicating that Gdf6a may affect organ size, as opposed to specification of cell types (Figure 5-2 A and B). Similar results are seen using the zpr-1 antibody, which stains the pineal gland and parapineal complex. Signal intensity of the staining is normal, but highlights a smaller area within the forebrain, supporting the idea that the size of the pineal gland is reduced in *gdf6a* morphants (Figure 5-2 C and D). Additionally, four genes specifically implicated in neurogenesis within the pineal gland, mainly *achaete/scute like complex 1a (ascl1a*), *neurogenin1* (*ngn1*), the *floating head transcription factor* (*flh*), and *tbx2b* were found to be down-regulated in *gdf6a* morphants (Table 5-1).

In addition to photoreceptor development in the pineal complex, our microarray analysis revealed decreased expression of *retinitis pigmentosa homolog 9* (also known as *PAP-1*) a gene that encodes a ubiquitously expressed spliceosome factor and results in Retinitis Pigmentosa when mutated in humans (Keen et al., 2002; Maita et al., 2004). Retinitis Pigmentosa is a severe form of macular degeneration that begins with the loss of photoreceptors, indicating that Rp9 is required for photoreceptor survival. Microarray analysis revealed a 2.7 fold decrease of *rp9* expression in *gdf6a* morphants when compared with wildtype animals (Table 5-1), which was confirmed with quantitative PCR (qPCR) (Figure 5-3 A). Further analysis of photoreceptor development was undertaken using the zpr-1 monoclonal antibody that specifically recognizes red-green cone pairs in the zebrafish retina. These cones are lost in the ventral most region of the retina upon *gdf6a* morpholino inhibition (Figure 5-3 B and C), but appear normal elsewhere

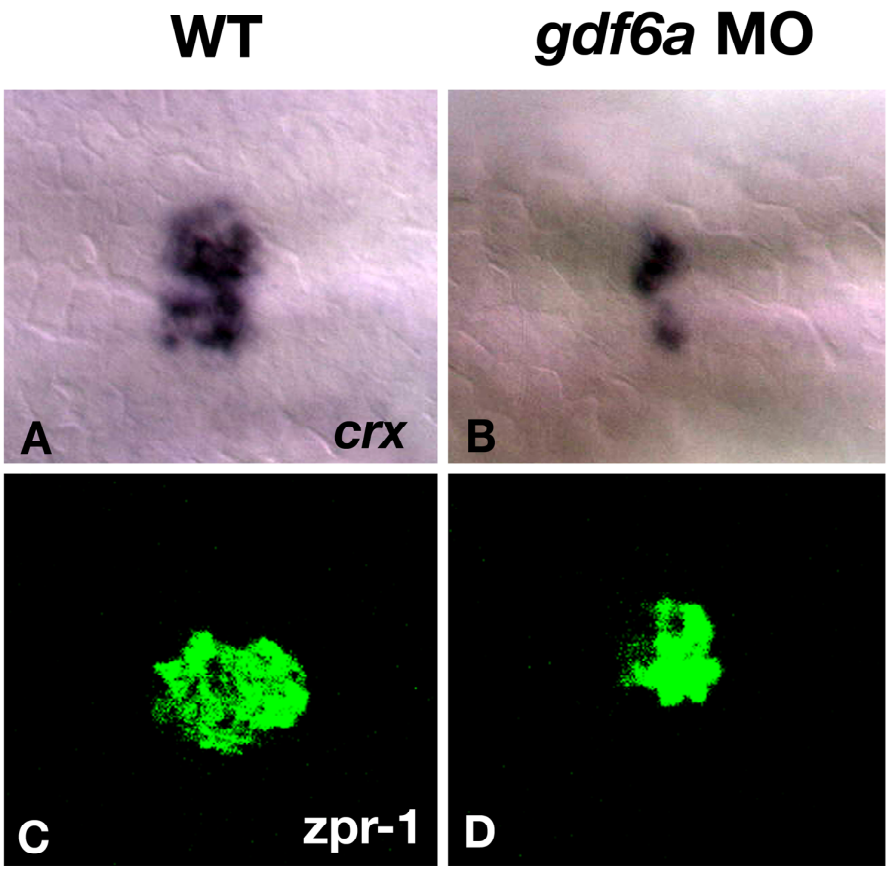

Figure 5-2: Reduced pineal/parapineal gland size in *gdf6a* morphants at 24 hpf. The expression domain of *cone-rod homeobox* (*crx*) is reduced in size in *gdf6a* morphants (compare B with A). Similarly, the area of the forebrain highlighted by zpr-1, which identifies pineal photoreceptors, is reduced in a similar fashion (Compare C with D).

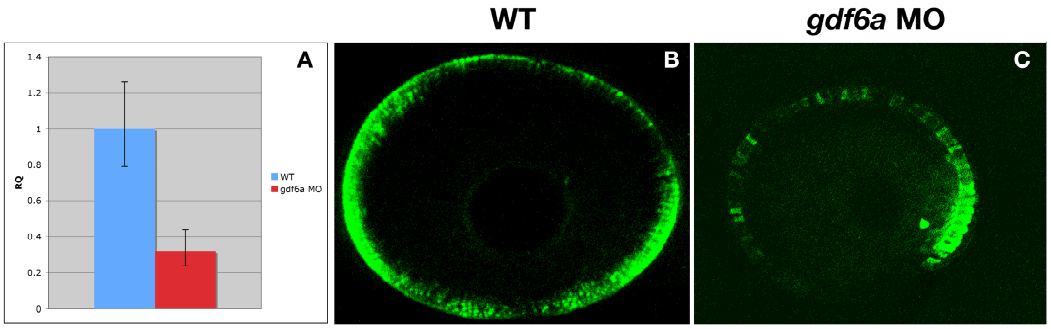

Figure 5-3: Quantitative PCR for validation of *rp9* expression in *gdf6a* morphant embryos. (A) Reaction quotient (0.34) indicating 2.9 fold down-regulation of *gdf6a* morphants. Immunohistochemistry for zpr-1, which detects red/green photoreceptor pairs in the zebrafish retina. Staining intensity is decreased throughout the retina in *gdf6a* morphants, and is absent in the ventral most regions where coloboma is evident.

in the retina. Thus loss of *gdf6a* may influence cone photoreceptor development and/or survival in the ventral retina.

Analysis of lens development in gdf6a morphant embryos

Inhibition of Gdf6a can cause defects in lens development, including size reduction, degeneration, or extrusion from the developing eyecup (Asai-Coakwell et al., 2007). Genes involved in lens fiber differentiation were identified as down-regulated according to microarray analysis (Table 5-1). Bmp signaling is active in the dorsal half of the lens, as indicated by the phosphorylation of Smad 1/5/8 proteins (Figure 4-3 A), and is eliminated in *gdf6a* morphants (Figure 4-3B). We therefore examined the expression of genes involved in lens fiber cell differentiation and function. The expression of *lens intrinsic membrane protein 2.3* (*lim2.3,* an ortholog of mammalian *LIM2*) is robustly expressed in the lens at 28 hpf (Figure 5-4 A), and is severely down-regulated in *gdf6a* morphants (Figure 5-4B). Moreover, expression of *cx23*, a *connexin* required for hemichannel formation specifically in the lens (Iovine et al., 2008), is down-regulated upon inhibition of Gdf6a (Figure 5-4 C and D). The expression of *crystallin* genes are associated with the differentiation of lens fiber cells (Boswell et al., 2008; Morozov and Wawrousek, 2006), and are found at high levels in the lens at 28 hpf. The expression of *crystallin beta a2a* (*cryba2a*), is highly down-regulated in *gdf6a* morphants (Figure 5-4 E, F), while the expression of the closely related *crystallin beta a1b (cryba1b)* is down-regulated (Figure 5-4 G, H), although more subtly than *cryba2a.*

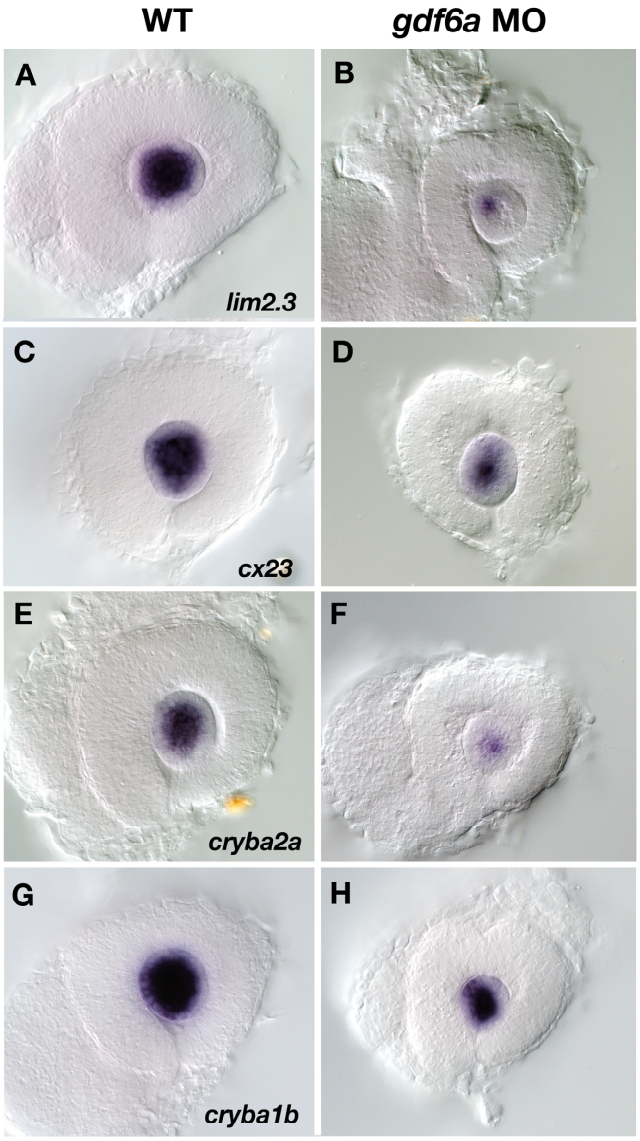

Figure 5-4: *in situ* hybridization for lens specific probes identified as down-regulated in *gdf6a* morphants by microarray analysis. The expression of *lim2.3* is down-regulated at 28 hpf in *gdf6a* morphant embryos (A and B), as is the expression of *cx23* (C, D) and *cryba2a* (E, D). The expression of the related *cryba1b* is also down-regulated (G, H).

To further characterize the role Gdf6a plays in lens development, we examined zebrafish morphant embryo lens nuclei and differentiating lens fibers (Figure 5-5 E-H, I-L). We also stained lens sections with phalloidin, which binds to filamentous actin and thus marks cell boundaries (Figure 5-5 A-D). Subtle defects are observed at 4 dpf with respect to phalloidin staining in *gdf6a* morphants (Figure 5-5 B). The staining of differentiating lens fibers by the Zl-1 monoclonal antibody was increased in morphant lenses (5/8 62.3%) (Figure 5-5 F), however the lens is clear and devoid of nuclei (Figure 5-5 J). To further inhibit Bmp signaling at later stages of lens development, wildtype and *gdf6a* morphant embryos were incubated in Dorsomorphin. This compound inhibits Bmp signaling (Hao et al., 2008), as evidenced by reduced Smad/5/8 phosphorylation and decreased *tbx5* expression (Figure 5-6 A-D). Dorsomorphin on its own has no effect on lens development (Figure 5-5 C, G, K, O), however when added to *gdf6a* morphants, immunoreactivity is increased for Zl-1 (Figure 5-5 H, n=6/6), and nuclei are visible within the lens (Figure 5-5 L, n=4/6), indicating aberrant lens fiber cell differentiation in these embryos. Ectopic phalloidin can is also observed in the lens of these embryos (Figure 5-5 D). The relative positions of ectopic nuclei, phalloidin and ZL-1 imunoreactiviry can be seen in merged images (Figure 5-5 M-P).

Analysis of skeletal development in gdf6a morphant embryos

Gdf6, as well as the closely related Gdf5, have known roles in skeletal development. In addition, our microarray analysis identified *noggin1* (*nog1*), a

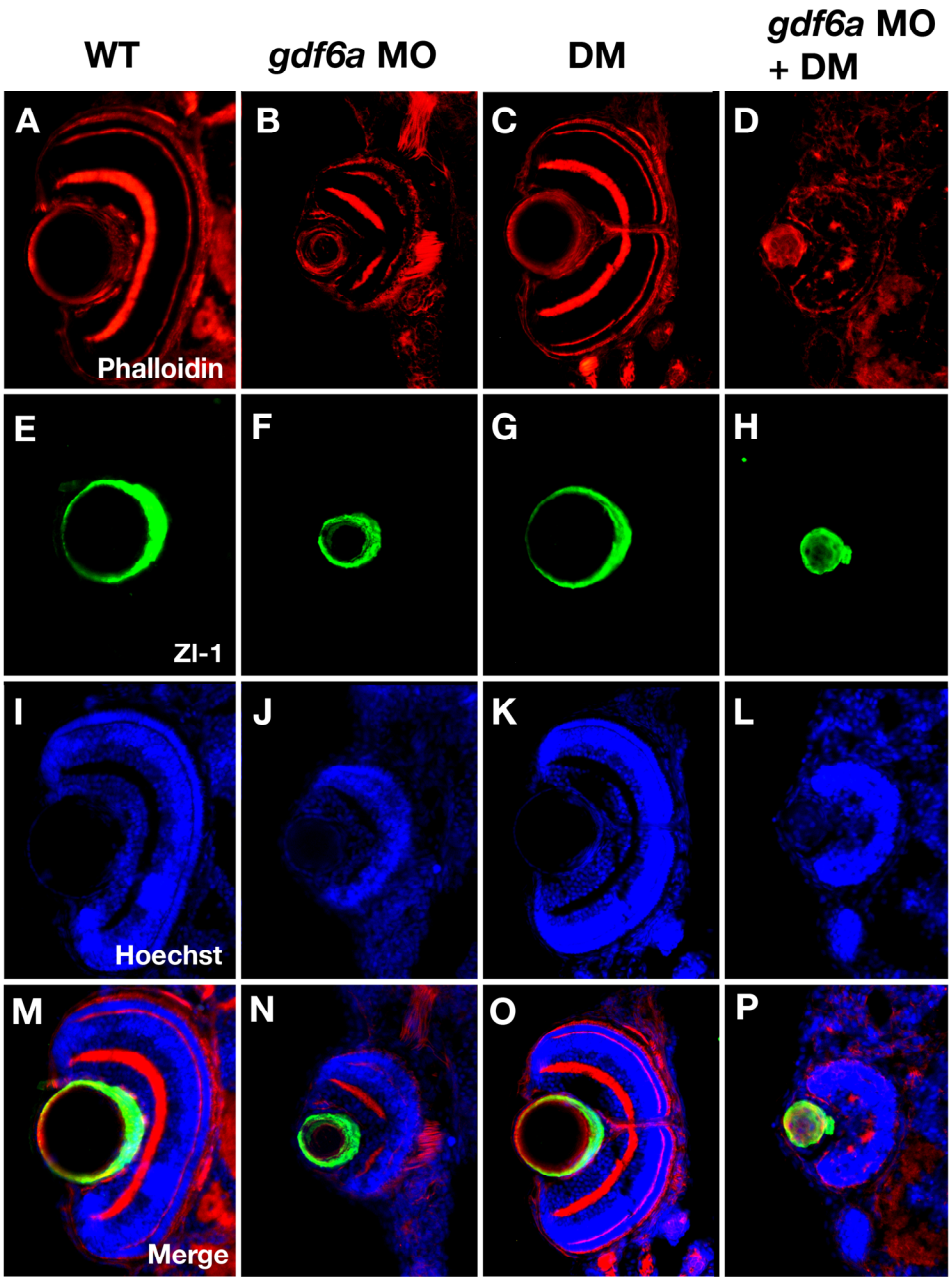
WT
gdf6a MO
DM
gdf6a MO + DM
A
B
C
D
Phalloidin
E
F
G
H
Zl-1
I
J
K
L
Hoechst
M
N
O
P
Merge

Figure 5-5: Analysis of lens fiber differentiation in *gdf6a* morphants. At 4 dpf, there is little difference in the organization of F-actin in *gdf6a* morphants, as phalloidin staining is relatively normal (A, B). There is also no change in Dapi staining, indicating no residual nuclear retention in *gdf6a* morphants (I, J). There is, however, a slightly higher level of Zl-1 staining in the morphant lens, which identifies differentiating lens fibers (E, F). Incubation in Dorsomorphin has no effect on lens development (C, G, K, O), but when combined with *gdf6a* morpholino inhibition, ectopic phalloidin and Zl-1 is observed in the lens (D, H), and there is evidence of nuclear retention (L). A merged image of all staining is shown in panels (M-P).

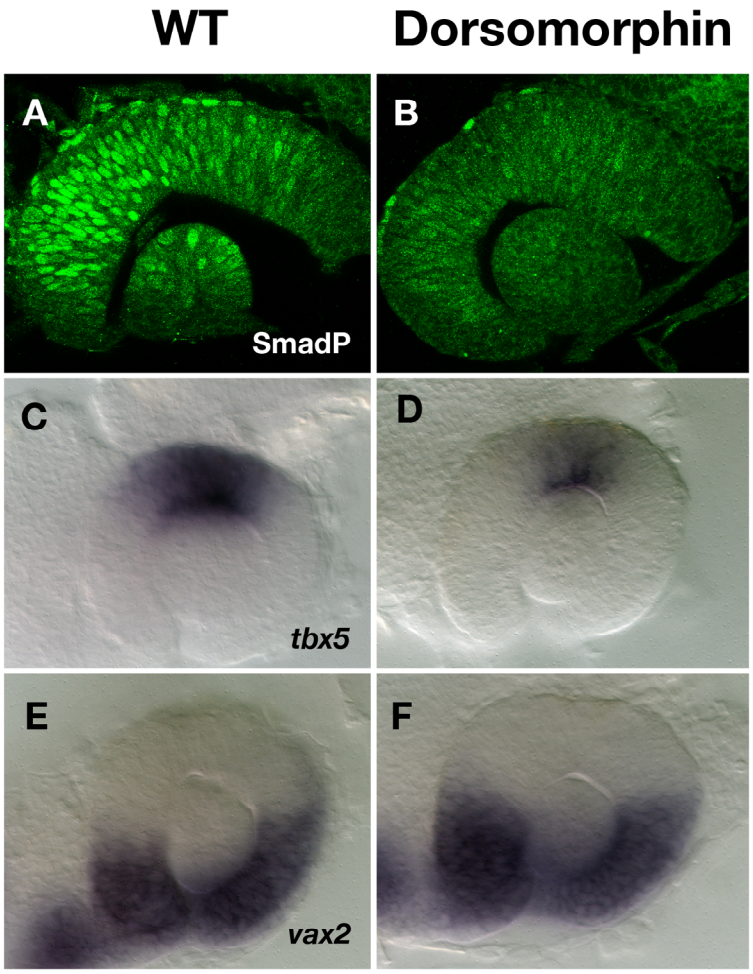

Figure 5-6: Dorsal patterning phenotypes in embryos incubated in Dorsomorphin. Incubation of embryos in Dorsomorphin results in a marked reduction in nuclear Smad 1/5/8 phosphorylation (n=9/13) (Figure A, B). As expected, the expression of *tbx5* was also reduced (n=14/15, C, D). Unlike morpholino inhibition of *gdf6a*, incubation in Dorsomorphin has only a subtle effect on the expression of *vax2*, as the dorsal boundary of expression is only slightly expanded compared with that of *gdf6a* morphants (n=8/16 E, F). Thus, Dorsomorphin is only able to partially phenocopy *gdf6a* morphants with respect to dorsal-ventral retinal patterning.

Bmp signaling inhibitor implicated in bone fracture healing and cartilage development (Brunet et al., 1998; Dean et al., 2010) as down-regulated in *gdf6a* morphant embryos. Inhibition of *gdf6a* induces a range of axial phenotypes in developing zebrafish embryos, mainly consisting of kinked or curly tails (Figure 5-7, A-C). Co-injection with p53 morpholino does not alter these phenotypes, and thus non-specific cell death, often induced via morpholino injection (Robu et al., 2007), is likely not responsible for this phenotype. The expression of *noggin1* and *noggin2* is detected in the scleratome (region of the somite that give rise to bones including vertebrae) by *in situ* hybridization, (Figure 5-7 D, F), and is down-regulated in *gdf6a* morphant embryos (Figure 5-7, G) and thus may play a role in *gdf6a* induced axial phenotypes.

At later stages of development, *gdf6a* is expressed in pharyngeal jaw arches (Reed and Mortlock, 2010), suggesting Gdf6a may also be required for the proper development of these structures. We analyzed the expression of *gdf5*, a known marker of pharyngeal jaw structure, which is expressed at the first pharyngeal arch joint and the midline of the second pharyngeal arch (Miller et al., 2003). Expression of *gdf5* at the first arch joint is normal in *gdf6a* morphant embryos, however expression at the midline of the second arch is lost (Figure 5-8 A, B), suggesting that Gdf6a acts upstream of Gdf5 to pattern the second pharyngeal arch. We further analyzed jaw cartilage development and ossification using Alcian blue (cartilage) and Alizarin red (calcified bone) staining. No differences are seen in the structure of jaw cartilage in *gdf6a* morphants despite the loss of *gdf5* expression in the second pharyngeal arch (Figure 5-8 C-F).

Figure 5-7: Morphological and molecular phenotypes in the tail of *gdf6a* morphants. Kinked and curly tails are evident by 2 dpf (B and C), while the expression of the Bmp inhibitors *noggin1* and *noggin2* are down regulated in the sceleratome at 22 hpf.

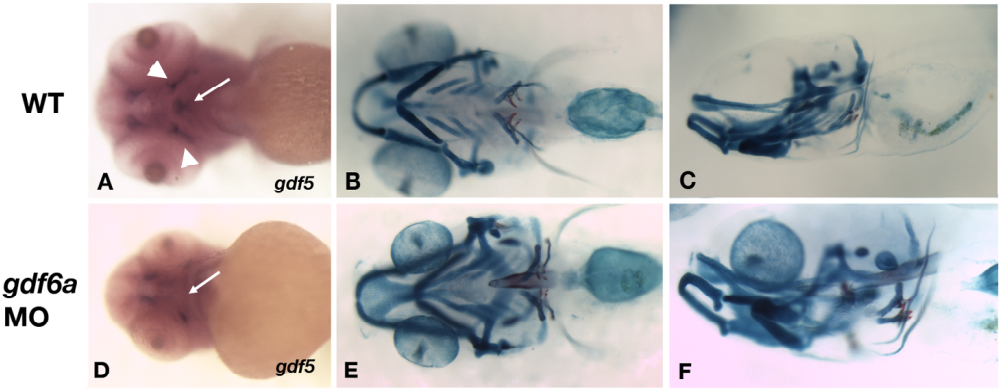

Figure 5-8: Analysis of cartilage and bone development in *gdf6a* morphants. The expression of *gdf5* at 3 dpf is observed at the first pharangeal joint arch (arrowhead in A), and at the midline of the second pharyngeal arch (arrow in A). Although *gdf5* expression is normal at the first joint arch, the expression at the midline of the second joint is lost (B). At 6 dpf, staining of jaw cartilage (blue) and ossification of the notocord (red) is normal in *gdf6a* morphants.

Although the anterior tip of the notochord appears prematurely calcified in *gdf6a* morphants, this process is highly variable and thus we conclude morpholino inhibition of *gdf6a* does not strongly affect jaw cartilage development or bone ossification.

Discussion

Using microarray analysis on whole *gdf6a* morphant embryos, we have identified potential roles for Gdf6a function in addition to those established in the neural retina, including the lens, neural tube, pineal gland, and the skeletal system. *gdf6a* expression is detected in the roof plate of the neural tube at early stages of development and is required for the expression of the proneural gene *atonal homolog 1a* (*atoh1a*). The expression domain of this gene defines a subset of glutamatergic neurons that include the neurons of the tegmental nuclei, the deep cerebellar nuclei, and the granule cells (Machold and Fishell, 2005; Wang et al., 2005; Wilson and Wingate, 2006) within the developing cerebellum. The cerebellum forms in the dorsal anterior hindbrain and plays an important role in the interpretation of sensory input and controls locomotive behavior (Kani et al., 2010). Although *atoh1a* expression is evident at 24 hpf, these neural progenitor cells do not give rise to mature neurons until 3 dpf, thus our microarray analysis does not lend insight as to whether the tegmental nuclei, the deep cerebellar nuclei, or the granule cells develop normally in the absence of Gdf6a function. Analysis at later stages of development using cell type specific markers will be required for this purpose.

In addition to its role in the development of the neural tube, our microarray analysis also identified five genes expressed in the pineal complex at 24 hpf. The pineal complex consists of the midline pineal organ and the left-sided parapineal organ, which together, control circadian rhythm in fish (Kazimi and Cahill, 1999; Whitmore et al., 2000) as well as left-right specific functions of the habenulae in the zebrafish midbrain (Concha et al., 2003; Gamse et al., 2002). One such gene, *tbx2b*, is expressed throughout the pineal anlage, and is required for the production and migration of parapineal cell lineages, as loss of *tbx2b* results in fewer parapineal cells that fail to migrate from the midline (Snelson et al., 2008b). Further analysis, including validation of reduced pineal expression of *tbx2b* is required to make any conclusions about a possible Gdf6a dependent role for *tbx2b* in pineal development.

The expression of *cone-rod homeobox* (*crx*) was also identified by microarray analysis as dependent on Gdf6 for its expression. *crx* has been rigorously studied for its role in photoreceptor development in the neural retina, however this process has not yet begun at 24 hpf when the microarray was conducted. At 24 hpf however, *crx* is expressed robustly in the pineal complex for the development of photoreceptors that control circadian rhythm (Concha et al., 2003). *in situ* hybridization indicates that *crx* is expressed at normal levels in the pineal complex at 24 hpf, however the expression domain is reduced. This phenotype is reiterated by using an antibody that specifically stains pineal photoreceptors, which also highlights a reduced domain of staining. Thus, loss of

Gdf6a may affect organ size due to deceased numbers of photoreceptors within the pineal complex.

In support of this hypothesis, three additional genes that are required for neurogenesis in the pineal complex, including both photoreceptor and projection neurons, were identified as downstream of Gdf6a via microarray analysis. These include the *floating head* (*flh*) homeodomain transcription factor (Masai et al., 1997; Snelson et al., 2008a), and two basic helix loop helix (bHLH) transcription factor encoding genes, *achaete/scute homolog 1a* (*acl1a*) and *neurogenin1* (*ngn1*). Epistatic analysis places *acl1a* and *ngn1* genetically downstream of *flh* in pineal neural progenitor cells for the expression of photoreceptor specific opsin genes (Cau and Wilson, 2003). In *asc1a* or *ngn1* morphants, opsin expression intensity is detected at normal levels, but fewer cells expressing opsins are observed (Cau and Wilson, 2003), similar to what is seen with *crx* expression in *gdf6a* morphants. However further experiments are required to verify that *gdf6a* acts upstream of this transcription factor network to regulate pineal gland neurogenesis, and to determine the nature of neuronal defects in the pineal gland of embryos that lack Gdf6a function.

Although our microarray analysis strongly suggests a role for Gdf6a in pineal development, we do not detect expression of *gdf6a* in the pineal gland at stages ranging from 24 hpf to 4 dpf. *gdf6a* is expressed in anterior structures such as the jaw, roofplate, and retina at these stages, and although Gdf6a exerts in function in a cell non-autonomous fashion (Gosse and Baier, 2009, and this work), it is unlikely that these expression domains regulate pineal development.

In support of this, we do not detect phosphorylation of Smad 1, 5, 8 proteins in the pineal complex, and thus there is no evidence that Bmp signaling is active in this tissue. Alternatively, Bmps have been shown to signal through a non-canonical pathway involving activation of Protein Kinase A (PKA) (Liu et al., 2005). Analysis of PKA activation was not addressed in our study, and thus it is possible that Gdf6a signaling from anterior tissues could regulate pineal development through this non-canonical pathway.

Although cells that give rise to photoreceptors in the zebrafish retina have not exited the cell cycle at 24 hpf when our microarray was conducted, we identified reduced expression of *retinitis pigmentosa homolog 9* (*PAP-1*) in *gdf6a* morphants. Mutation of this gene in humans results in early onset degeneration of both rod and cone photoreceptors (Inglehearn et al., 1993; Keen et al., 2002). *rp9* encodes a ubiquitously expressed spliceosome factor that interacts directly with the tri-snRNP complex to regulate pre-mRNA splicing. Genes encoding numerous other factors that participate either directly or indirectly with pre-mRNA splicing have been identified in Retinitis Pigmentosa patients worldwide (Maubaret and Hamel, 2005), with at least one mechanism involving snRNA unwinding during spliceosome activation and disassembly being described (Zhao et al., 2009). In *gdf6a* morphant embryos, photoreceptors are not present in the ventral most region of the retina (where coloboma is present), indicating that loss of *gdf6a* may affect photoreceptor differentiation or survival, possibly through downstream regulation of *rp9*.

In addition to retinal patterning, Bmp molecules have been implicated in the development of the lens in whole animal and cell culture systems (Boswell et al., 2008; Faber et al., 2002). Our data builds on current knowledge, extending the spectrum of Bmp molecules that can affect lens development to include Gdf6a. Inhibition of Gdf6a results in the absence of Smad 1/5/8 phosphorylation in the lens, and down-regulation of numerous lens specific genes including *cryba2a* and *lim2.3*. Genes of the *crystallin* family are associated with lens fiber differentiation, and mutations in a human ortholog of *lim2* cause lens opacity (Ponnam et al., 2008; Shiels et al., 2007). At 4 dpf, the *gdf6a* morphant lens appears clear and there is no evidence of nuclear retention in the lens fiber cells as seen in many zebrafish models of lens opacity (Goishi et al., 2006; Ponnam et al., 2008). This may be the result of reduced effectiveness of morpholinos at later stages of embryonic development (Evans et al., 2005). However when combined with Dorsomorphin, lens formation is disrupted as evidenced by increased immunoreactivity for differentiating lens fiber cells and nuclear retention. This suggests that although aspects of lens development may proceed normally in *gdf6a* morphants (for example, *efnb2a* is expressed normally and *cryba1b* is only mildly affected) terminal differentiation of lens fiber cells in these embryos is disrupted. Identical phenotypes are observed through knockdown of transcription factors such as *pitx3* and *foxe3* (Shi et al., 2005; Shi et al., 2006), however we have not addressed in this study whether *gdf6a* functions within the same genetic pathway as these molecules.

The expression pattern of *gdf6a*, which includes pharyngeal jaw elements, strongly suggests a role for Gdf6a in the development of jaw cartilages. In support of this, we have demonstrated that Gdf6a controls the expression of *gdf5* in at least one domain within the developing jaw cartilage, and Gdf5 mouse mutants display defects in this tissue (Settle et al., 2003). However analysis of jaw cartilage organization in *gdf6a* morphants does not reveal any overt defects. One possible explanation for this lack of phenotype may be the use of morpholinos to detect phenotypes at late stages of embryonic development, as morpholinos can lose their effectiveness over time (Evans et al., 2005). As *gdf6a* null mutants are now available (but were not at the time of his study), possible late phenotypes involving jaw cartilages should be re-analyzed in a mutant, as opposed to a morphant background.

Further support for a role of *gdf6a* in skeletal development is gained through aberrant expression of *noggin* genes within the scleratome in *gdf6a* morphants at 24 hpf. Although there are no distinct bones in the zebrafish embryo at this stage, the scleratome will eventually give rise to bones including vertebrae. Further analysis will be required at later embryonic/juvenile stages to determine if vertebral development is disrupted in zebrafish lacking Gdf6a function, however it is known that mice and human patients with mutations in *GDF6* display vertebral fusions (Asai-Coakwell et al., 2009; Tassabehji et al., 2008), and thus it is likely that *gdf6a* influences vertebral development in zebrafish as well.

Conclusions

In addition to established roles in retinal patterning, we have identified potential roles for *gdf6a* in the neural tube, lens and skeletal systems. Although these results are preliminary and require further investigation, *gdf6a* appears to be required for lens fiber maturation and axial development in the zebrafish embryo. Possible roles in the development of the pineal complex require clarification as *gdf6a* expression and canonical Bmp signaling are not detected in this tissue. Gdf6a may play a role in the development of Retinitis Pigmentosa, however expression analysis of genes associated with this disease, such as *rp9,* need to be analyzed at later stages of development in order to make definitive conclusions.

Bibliography

Alvarez-Delfin, K., et al., 2009. Tbx2b is required for ultraviolet photoreceptor cell specification during zebrafish retinal development. Proc Natl Acad Sci U S A. 106**,** 2023-8.

Asai-Coakwell, M., et al., 2007. GDF6, a novel locus for a spectrum of ocular developmental anomalies. Am J Hum Genet. 80**,** 306-15.

Asai-Coakwell, M., et al., 2009. Incomplete penetrance and phenotypic variability characterize Gdf6-attributable oculo-skeletal phenotypes. Hum Mol Genet. 18**,** 1110-21.

Bonner, J., et al., 2008. Proliferation and patterning are mediated independently in the dorsal spinal cord downstream of canonical Wnt signaling. Dev Biol. 313**,** 398-407.

Boswell, B. A., et al., 2008. Essential role of BMPs in FGF-induced secondary lens fiber differentiation. Dev Biol. 324**,** 202-12.

Brunet, L. J., et al., 1998. Noggin, cartilage morphogenesis, and joint formation in the mammalian skeleton. Science. 280**,** 1455-7.

Cau, E., Wilson, S. W., 2003. Ash1a and Neurogenin1 function downstream of Floating head to regulate epiphysial neurogenesis. Development. 130**,** 2455-66.

Chaurasia, S. S., et al., 2005. Molecular cloning, localization and circadian expression of chicken melanopsin (Opn4): differential regulation of expression in pineal and retinal cell types. J Neurochem. 92**,** 158-70.

Clement, J. H., et al., 1995. Bone morphogenetic protein 2 in the early development of Xenopus laevis. Mech Dev. 52**,** 357-70.

Concha, M. L., et al., 2003. Local tissue interactions across the dorsal midline of the forebrain establish CNS laterality. Neuron. 39**,** 423-38.

Dahm, R., et al., 2007. Development and adult morphology of the eye lens in the zebrafish. Exp Eye Res. 85**,** 74-89.

Dean, D. B., et al., 2010. Distinct functionalities of bone morphogenetic protein antagonists during fracture healing in mice. J Anat. 216**,** 625-30.

Delot, E., et al., 1999. The BMP-related protein radar: a maintenance factor for dorsal neuroectoderm cells? Mech Dev. 85**,** 15-25.

Evans, T. G., et al., 2005. Zebrafish Hsp70 is required for embryonic lens formation. Cell Stress Chaperones. 10**,** 66-78.

Faber, S. C., et al., 2002. Bmp signaling is required for development of primary lens fiber cells. Development. 129**,** 3727-37.

Furuta, Y., Hogan, B. L., 1998. BMP4 is essential for lens induction in the mouse embryo. Genes Dev. 12**,** 3764-75.

Gamse, J. T., et al., 2002. Otx5 regulates genes that show circadian expression in the zebrafish pineal complex. Nat Genet. 30**,** 117-21.

Goishi, K., et al., 2006. AlphaA-crystallin expression prevents gamma-crystallin insolubility and cataract formation in the zebrafish cloche mutant lens. Development. 133**,** 2585-93.

Gosse, N. J., Baier, H., 2009. An essential role for Radar (Gdf6a) in inducing dorsal fate in the zebrafish retina. Proc Natl Acad Sci U S A. 106**,** 2236-41.

Goutel, C., et al., 2000. The ventralizing activity of Radar, a maternally expressed bone morphogenetic protein, reveals complex bone morphogenetic protein interactions controlling dorso-ventral patterning in zebrafish. Mech Dev. 99**,** 15-27.

Gross, J. M., Dowling, J. E., 2005. Tbx2b is essential for neuronal differentiation along the dorsal/ventral axis of the zebrafish retina. Proc Natl Acad Sci U S A. 102**,** 4371-6.

Hall, C. J., et al., 2002. Radar is required for the establishment of vascular integrity in the zebrafish. Dev Biol. 251**,** 105-17.

Hao, J., et al., 2008. Dorsomorphin, a selective small molecule inhibitor of BMP signaling, promotes cardiomyogenesis in embryonic stem cells. PLoS One. 3**,** e2904.

Inglehearn, C. F., et al., 1993. A new locus for autosomal dominant retinitis pigmentosa on chromosome 7p. Nat Genet. 4**,** 51-3.

Iovine, M. K., et al., 2008. Cx23, a connexin with only four extracellular-loop cysteines, forms functional gap junction channels and hemichannels. FEBS Lett. 582**,** 165-70.

Kani, S., et al., 2010. Proneural gene-linked neurogenesis in zebrafish cerebellum. Dev Biol. 343**,** 1-17.

Katoh, Y., Katoh, M., 2006. Comparative integromics on BMP/GDF family. Int J Mol Med. 17**,** 951-5.

Kazimi, N., Cahill, G. M., 1999. Development of a circadian melatonin rhythm in embryonic zebrafish. Brain Res Dev Brain Res. 117**,** 47-52.

Keen, T. J., et al., 2002. Mutations in a protein target of the Pim-1 kinase associated with the RP9 form of autosomal dominant retinitis pigmentosa. Eur J Hum Genet. 10**,** 245-9.

Knochel, S., et al., 2001. Structure and expression of Xenopus tropicalis BMP-2 and BMP-4 genes. Mech Dev. 109**,** 79-82.

Liu H., et al., 2005. Margiotta JF, Howard MJ. BMP4 supports noradrenergic differentiation by a PKA-dependent mechanism. Dev Biol. 286, 521-36

Machold, R., Fishell, G., 2005. Math1 is expressed in temporally discrete pools of cerebellar rhombic-lip neural progenitors. Neuron. 48**,** 17-24.

Maita, H., et al., 2004. PAP-1, the mutated gene underlying the RP9 form of dominant retinitis pigmentosa, is a splicing factor. Exp Cell Res. 300**,** 283-96.

Masai, I., et al., 1997. floating head and masterblind regulate neuronal patterning in the roof of the forebrain. Neuron. 18**,** 43-57.

Maubaret, C., Hamel, C., 2005. [Genetics of retinitis pigmentosa: metabolic classification and phenotype/genotype correlations]. J Fr Ophtalmol. 28**,** 71-92.

Merino, R., et al., 1999. Expression and function of Gdf-5 during digit skeletogenesis in the embryonic chick leg bud. Dev Biol. 206**,** 33-45.

Miller, C. T., et al., 2003. Two endothelin 1 effectors, hand2 and bapx1, pattern ventral pharyngeal cartilage and the jaw joint. Development. 130**,** 1353-65.

Morozov, V., Wawrousek, E. F., 2006. Caspase-dependent secondary lens fiber cell disintegration in alphaA-/alphaB-crystallin double-knockout mice. Development. 133**,** 813-21.

Ponnam, S. P., et al., 2008. A missense mutation in LIM2 causes autosomal recessive congenital cataract. Mol Vis. 14**,** 1204-8.

Qian, L., et al., 2005. Ethanol disrupts the formation of hypochord and dorsal aorta during the development of embryonic zebrafish. Sci China C Life Sci. 48**,** 608-15.

Quay, W. B., 1963. Circadian Rhythm in Rat Pineal Serotonin and Its Modifications by Estrous Cycle and Photoperiod. Gen Comp Endocrinol. 14**,** 473-9.

Quay, W. B., 1965. Photic relations and experimental dissociation of circadian rhythms in pineal composition and running activity in rats. Photochem Photobiol. 4**,** 425-32.

Quay, W. B., 1966. 24-hour rhythms in pineal 5-hydroxytryptamine and hydroxyindole-o-methyl transferase activity in the macaque. Proc Soc Exp Biol Med. 121**,** 946-8.

Reed, N. P., Mortlock, D. P., 2010. Identification of a distant cis-regulatory element controlling pharyngeal arch-specific expression of zebrafish gdf6a/radar. Dev Dyn. 239**,** 1047-60.

Robu, M. E., et al., 2007. p53 activation by knockdown technologies. PLoS Genet. 3**,** e78.

Settle, S. H., Jr., et al., 2003. Multiple joint and skeletal patterning defects caused by single and double mutations in the mouse Gdf6 and Gdf5 genes. Dev Biol. 254**,** 116-30.

Shi, X., et al., 2005. Zebrafish pitx3 is necessary for normal lens and retinal development. Mech Dev. 122**,** 513-27.

Shi, X., et al., 2006. Zebrafish foxe3: roles in ocular lens morphogenesis through interaction with pitx3. Mech Dev. 123**,** 761-82.

Shiels, A., et al., 2007. Refractive defects and cataracts in mice lacking lens intrinsic membrane protein-2. Invest Ophthalmol Vis Sci. 48**,** 500-8.

Snelson, C. D., et al., 2008a. Formation of the asymmetric pineal complex in zebrafish requires two independently acting transcription factors. Dev Dyn. 237**,** 3538-44.

Snelson, C. D., et al., 2008b. Tbx2b is required for the development of the parapineal organ. Development. 135**,** 1693-702.

Storm, E. E., et al., 1994. Limb alterations in brachypodism mice due to mutations in a new member of the TGF beta-superfamily. Nature. 368**,** 639-43.

Tassabehji, M., et al., 2008. Mutations in GDF6 are associated with vertebral segmentation defects in Klippel-Feil syndrome. Hum Mutat. 29**,** 1017-27.

Urist, M. R., et al., 1979. Solubilized and insolubilized bone morphogenetic protein. Proc Natl Acad Sci U S A. 76**,** 1828-32.

Urist, M. R., et al., 1976. A bone morphogenetic polypeptide. Calcif Tissue Res. 21 Suppl**,** 81-7.

Wang, V. Y., et al., 2005. Math1 expression redefines the rhombic lip derivatives and reveals novel lineages within the brainstem and cerebellum. Neuron. 48**,** 31-43.

Wawersik, S., et al., 1999. BMP7 acts in murine lens placode development. Dev Biol. 207**,** 176-88.

Whitmore, D., et al., 2000. A clockwork organ. Biol Chem. 381**,** 793-800.

Wilson, L. J., Wingate, R. J., 2006. Temporal identity transition in the avian cerebellar rhombic lip. Dev Biol. 297**,** 508-21.

Zhao, C., et al., 2009. Autosomal-dominant retinitis pigmentosa caused by a mutation in SNRNP200, a gene required for unwinding of U4/U6 snRNAs. Am J Hum Genet. 85**,** 617-27.

Ziv, L., et al., 2005. Functional development of the zebrafish pineal gland: light-induced expression of period2 is required for onset of the circadian clock. J Neuroendocrinol. 17**,** 314-20.

Chapter 6

Toward defining a mechanism for the development of microphthalmia in *gdf6a* mutant embryos

Introduction

Microphthalmia, or the presence of a small eye, is found in up to 11 % of blind children worldwide (Verma and Fitzpatrick, 2007). Microphthalmia and anophthalmia (complete lack of eye tissue), are proposed to represent mild and severe cases of a phenotypic continuum (Verma and Fitzpatrick, 2007), and together can be found with a birth prevalence of 30 in 100,000 in some populations (Campbell et al., 2002; Morrison et al., 2002). Clinically, microphthalmia/anophthalmia cases can be divided into two classes: (1) primary, meaning the eye does not reach the correct size during embryogenesis (or does not form at all in the case of anophthalmia); and (2) secondary, where the eye degenerates subsequent to formation.

Primary microphthalmia or anophthalmia can be caused by disruption of many developmental processes. Failure of retinal differentiation, decreased proliferation, increased rates of cell death, as well as failure of lens induction have all been associated with microphthalmic or anophthalmic phenotypes. For example, mutations in (*OTX2*) cause anophthalmia or bilateral microphthalmia (Ragge et al., 2005a; Schilter et al., 2010), and have been associated with the development of retinal pigmented epithelium (Martinez-Morales et al., 2003; Westenskow et al., 2009) as well as in the control of proliferation and apoptosis in the developing eye (Martinez-Morales et al., 2001). Mutations in SRY-Box 2 (SOX2) which account for up to 20% of microphthalmia (Ragge et al., 2005b; Schneider et al., 2009), have been implicated in the development of both neural retina and lens tissues, suggesting that aberrant development of either tissue can

lead to microphthalmia/anophthalmia. Although it is not clear how aberrant lens development leads to microphthalmia, mutations in the Forkhead transcription factor *FOXE3* results in aphakia (lack of lens) and microphthalmia, and in these patients, microphthalmia was thought to be secondary to lens agenesis (Valleix et al., 2006). Lastly, mutations in the *visual system homoebox gene 2* (*vsx2*, also known as *CHX10*) have also been demonstrated in patients with microphthalmia (Ferda Percin et al., 2000), and is believed to play a role in proliferation of early retinal progenitor cells based on its expression pattern (Schmitt et al., 2009).

Of critical importance to the development of microphthalmia is the Bmp signaling pathway, as mutations in Bmp ligands have been associated with microphthalmia in human patients and animal models. For example, frameshift and missense mutations in *Bone Morphogenetic Protein* (*BMP4*) have been shown to segregate with microphthalmia and anophthalmia in two independent families (Bakrania et al., 2008). Sequence variants in *Growth and Differentiation Factor 3* (*GDF3*) have been found in microphthalmic patients, and *in vitro* analysis demonstrates that such variants may be causative (Ye et al., 2010). Furthermore, we and others have demonstrated that chromosomal rearrangements, as well as point mutations in *GDF6* results in microphthalmia, (Asai-Coakwell et al., 2007; Asai-Coakwell et al., 2009; Gonzalez-Rodriguez et al., 2010), and that this phenotype is recapitulated in animal models (Gosse and Baier, 2009; Hanel and Hensey, 2006, and this thesis). Similarly, in a chick model system, over-expression of the Bmp antagonist *gremlin* results in small eyes (Huillard et al.,

2005), further supporting a role for Bmp signaling in the development of microphthalmia.

Unlike mammalian systems, the zebrafish eye continues to grow throughout the life of the animal, and thus a population of multipotent stem cells is maintained (in the ciliary marginal zone, CMZ) so that additional retinal neurons can differentiate and contribute to the overall growth of the eye. Although most vertebrate eyes, including humans (Bhatia et al., 2009), maintain a stem cell population, the function of this population remains unclear as most vertebrates add only very few (if any) additional retinal neurons postnatally, and the ability of this stem cell population to respond to injury is limited (Bhatia et al., 2009; Haynes et al., 2007). Thus the zebrafish presents an additional mechanism by which microphthalmia can occur (in addition to the mechanisms described earlier in this chapter), whereby failure to maintain stem cell populations in the CMZ leads to reduced rates of retinal neurogenesis during the life of juvenile or adult fish.

There is evidence to suggest that Bmp signaling is required for adult retinal neurogenesis. In chicken embryos, one of the few vertebrate models in which retinal stem cells respond to ocular injury, regeneration of retinal neurons requires the actions of Bmp signaling through the canonical Smad 1/5/8 pathway (Haynes et al., 2007). Thus, there is precedent that Bmps can control the activation of retinal stem cells to produce new retinal neurons in an adult animal.

In this chapter, we investigate the mechanism by which loss of *gdf6a* results in microphthalmia in a newly available *gdf6a* null mutant zebrafish line

(*dark half*). We have conducted a microarray screen on dissected eye tissue from homozygous *gdf6a* mutant embryos, and have found that Gdf6a is required for a large set of genes that are specifically expressed in the ciliary marginal zone (CMZ), at a time when retinal progenitors are exiting the cell cycle to differentiate into neurons. Although increased apoptosis has been documented in *gdf6a* mutant eyes (Gosse et al., 2009), we propose that Gdf6a may also be required for maintenance of retinal stem cell populations and thus microphthalmia in these animals may result, in part, due to failure to add additional retinal neurons to the growing eye.

Results

Gdf6a is expressed in the CMZ and homozygous mutants display microphthalmia

To gain insight into the mechanism of *gdf6a* induced microphthalmia, we assessed *gdf6a* homozygous mutants to determine when this phenotype occurs during development. At 24 hpf, eyes of *gdf6a* mutants are of normal size, indicating that proliferation or cell death prior to this stage are unlikely to contribute to the microphthalmic phenotype. At 2 dpf, *gdf6a* mutants have noticeably smaller eyes (65 +/- 2.7 % of WT eye size, Figure 6-1 A, B), which is even more evident by 4dpf (44% +/- 3.4 % of WT eye size Figure 6-1 C, D). *gdf6a* is expressed specifically in the CMZ (and a small subset of retinal ganglion cells) during these stages (Figure 6-1 E-H), suggesting that regulation of stem cell populations by Gdf6a may be critical for normal eye size in zebrafish.

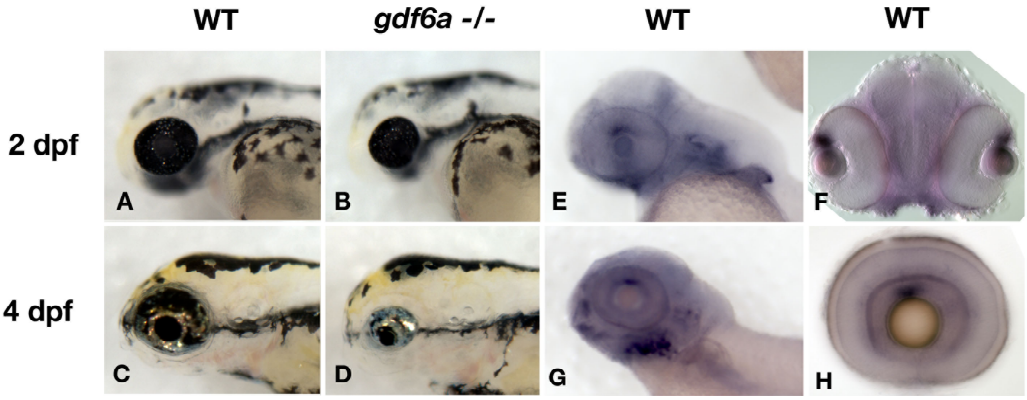

Figure 6-1: Analysis of *gdf6a* expression (in wildtype embryos) and eye size in *gdf6a* homozygous null embryos. The zebrafish *dark half* mutant line contains a null mutation if *gdf6a*, and results in small eyes which is evident by 2dpf (A, B), and even more so by 4 dpf (C, D). At 2dpf, *gdf6a* expression in the eye is confined to a small patch of cells in the dorsal retina (E). When viewed in cross-section this expression domain appears to include the dorsal ciliary marginal zone and dorsal ganglion cell layer (F). Expression in the dorsal retina is also evident a 4 dpf (G), although low levels of expression are detected throughout the ganglion cell layer (H).

Microarray analysis of gdf6a -/- eyes at 2 dpf

Our microarray screen was conducted using RNA isolated from dissected eyes at 2 dpf. 169 genes were found to be down-regulated in *gdf6a* mutants by 2 fold, while approximately 600 genes were down-regulated by 1.5 fold (See appendix C for a list of all genes down-regulated 2 fold). 52 genes were found to be up-regulated in *gdf6a* mutant eyes by 2 fold, while approximately 400 were found to be up-regulated 1.5 fold (See appendix D for a list of all genes up-regulated by 2-fold). These Gdf6a responsive genes are involved in almost all known retinal processes, including, but not limited to, axial patterning, differentiation of specific retinal neuron cell types, and cell cycle regulation. A subset of these genes are displayed in Table 6-1.

Validation of Gdf6a responsive genes by in situ hybridization

A number of microarray targets were chosen, based on known annotations and expression patterns, for validation by *in situ* hybridization. The expression of *atoh7*, a gene required for retinal neurogenesis, and *tbx2b,* which is required for photoreceptor differentiation, are expressed throughout the retina at 2 dpf (Figure 6-2 A, C), and expression is greatly attenuated in *gdf6a* mutant embryos (Figure 6-2 B, D). The expression of *foxn4*, required for differentiation of the inner nuclear layer in mice (Li et al., 2004), is expressed throughout the retina at 2 dpf (Figure 6-2 E), and is down-regulated in *gdf6a* mutants (Figure 6-2 F), although residual expression remains. *tbx4* is found in the exclusively in the dorsal retina (Figure 6-2 G), and is absent in *gdf6a* mutants (Figure 6-2, H). The expression of

Table 6-1: Regulation of genes involved in patterning and differentiation in *gdf6a* mutant eyes, identified by microarray analysis

Gene		Ontology	Fold Change	Validation
tbx4	*T-box transcription factor 4*	unknown	16.7	ISH
atoh7	*atonal homolog 7*	differentiation, GCL	5.60	ISH
ndrg1l	*N-myc downregulated gene 1 like*	differentiation, PRL	3.34	None
myoc	*myocilin*	fluid balance, IOP	3.10	None
fpgs	*folylpolyglutamate Synthetase*	Cancer progression	2.93	ISH
foxi1	*forkhead-box transcription factor i1*	ear, jaw development	2.20	ISH
foxn4	*forkhead-box transcription factor 4*	differentiation, INL	2.17	ISH
tbx2a	*T-box transcription factor 2a*	unknown	2.00	None
tbx2b	*T-box transcription factor 2b*	differentiation, PRL	1.73	ISH
hmx1	*H6 homeobox 1*	axial patterning	1.70	ISH
hmx4	*H6 homeobox 4*	axial patterning	1.70	None
pax2a	*paired box 2a*	axial patterning	0.61	None
foxi2	*forkhead-box transciption factor i2*	craniofacial development	0.51	None
crabp1b	*cellular retinoic acid binding protein 1b*	phototransduction	0.55	None

Fold change WT/*gdf6a -/-*

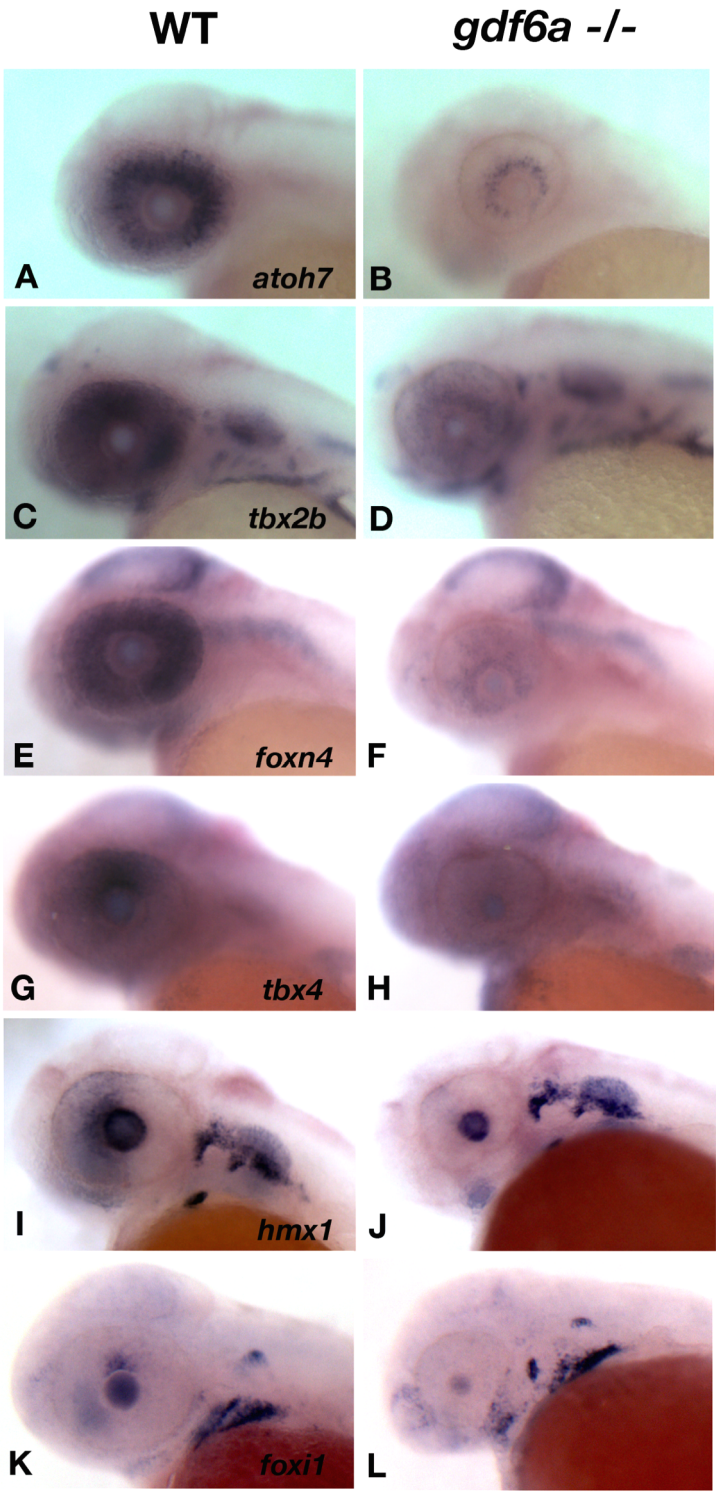
WT
gdf6a -/-
A
atoh7
B
C
tbx2b
D
E
foxn4
F
G
tbx4
H
I
hmx1
J
K
foxi1
L

Figure 6-2: Validation of Gdf6a responsive genes via *in situ* hybridization. The Expression of *atoh7* (A), *tbx2b* (C) and *foxn4* (E) are expressed throughout the neural retina at 2 dpf. Expression is reduced in *gdf6a* mutant embryos (B, D, F). Expression of *tbx4* is observed throughout the dorsal retina (G), and is lost in *gdf6a* mutants (H). *hmx1* is expressed in the lens and nasal retina (I), and while expression in the nasal retina is lost in *gdf6a* mutants, expression in the lens is unaffected (J). Expression of *foxi1* is detected in the lens and a small patch of cells in the dorsal retina (K). In *gdf6a* mutants, expression in the dorsal retina is lost (L), while expression in the lens appears down-regulated.

hmx1, a gene required to pattern the nasal-temporal retinal axis in chickens (Schulte and Cepko, 2000; Takahashi et al., 2003), is found in the lens and nasal retina in wildtype animals (Figure 6-2 I). Expression in the nasal retina is eliminated in *gdf6a* mutants (Figure 6-2 J), while expression in the lens persists. Another forkhead transcription factor, *foxi1*, is expressed in a small subset of cells in the dorsal ciliary marginal zone (Figure 6-2 K), as well as in the lens. *gdf6a* mutants still display expression in the lens, but retinal expression is lost (Figure 6-2 L). *tbx2b*, *hmx1*, and *foxi1* also are expressed in the ear at 2dpf, but no difference is seen between wildtype and *gdf6a* mutant animals. Similarly, *foxi1* and *tbx2b* are expressed in pharyngeal jaw elements, but are not affected in *gdf6a* mutant embryos. *foxn4* expression can be detected in the proliferative zone of the optic tectum, however no difference is seen between wildtype animals and *gdf6a* mutants.

Gdf6a is required for expression of cell cycle regulators in the CMZ

Our microarray analysis identified a number of genes with known functions in regulating cell cycle progression (Table 6-2), and that have expression specifically in the ciliary marginal zone (Figure 6-3). The expression of *carbamoyl-phosphate synthetase2-aspartate transcarbamylase-dihydroorotase* (*cad*) is found in the CMZ and dorsal retina in wildtype embryos (Figure 6-3, A, B), and is down-regulated in both domains in *gdf6a* mutants (Figure 6-3 C, D). Expression in the tectal proliferative zone is unaffected. The expression of *ubiquitin-like protein containing PHD and ring finger domains-1*, *(uhrf1)* is also

Table 6-2: Reduced expression of genes involved in cycle regulation in *gdf6a* mutant eyes, identified by microarray analysis

Gene		Ontology	Fold change	Validation
rx1	*retinal homeobox 1*	Proliferation, CMZ	3.72	ISH
wnt2	*wingless-type MMTV integration site M2*	Proliferation, CMZ	2.70	None
mcm3	*mini-chromosome maintenance protein*	DNA replication	2.00	None
chaf1b	*chromatin assembly factor 1b*	DNA replication	1.90	None
cad	*carbamoyl-phosphate synthetase2-aspartate transcarbamylase-dihydroorotase*	cell cycle regulation, pyrimidine synthesis	1.74	ISH
myca	*myelocytomatosis oncogene a*	transcription, proliferation	1.70	ISH
cnot7	*CCR4-NOT transcription complex, subunit 7*	proliferation	1.70	None
uhrf1	*ubiquitin-like, containing PHD and RING finger domains 1*	growth, proliferation	1.60	ISH
ccnf	*cyclin F*	cell cycle regulation	1.50	None
mycn	*myelocytomatosis viral related oncogene, neuroblastoma*	transcription, proliferation	1.40	ISH
mcm5	*mini-chromosome maintenance protein*	DNA replication	1.40	None

Fold change WT/*gdf6a* -/-

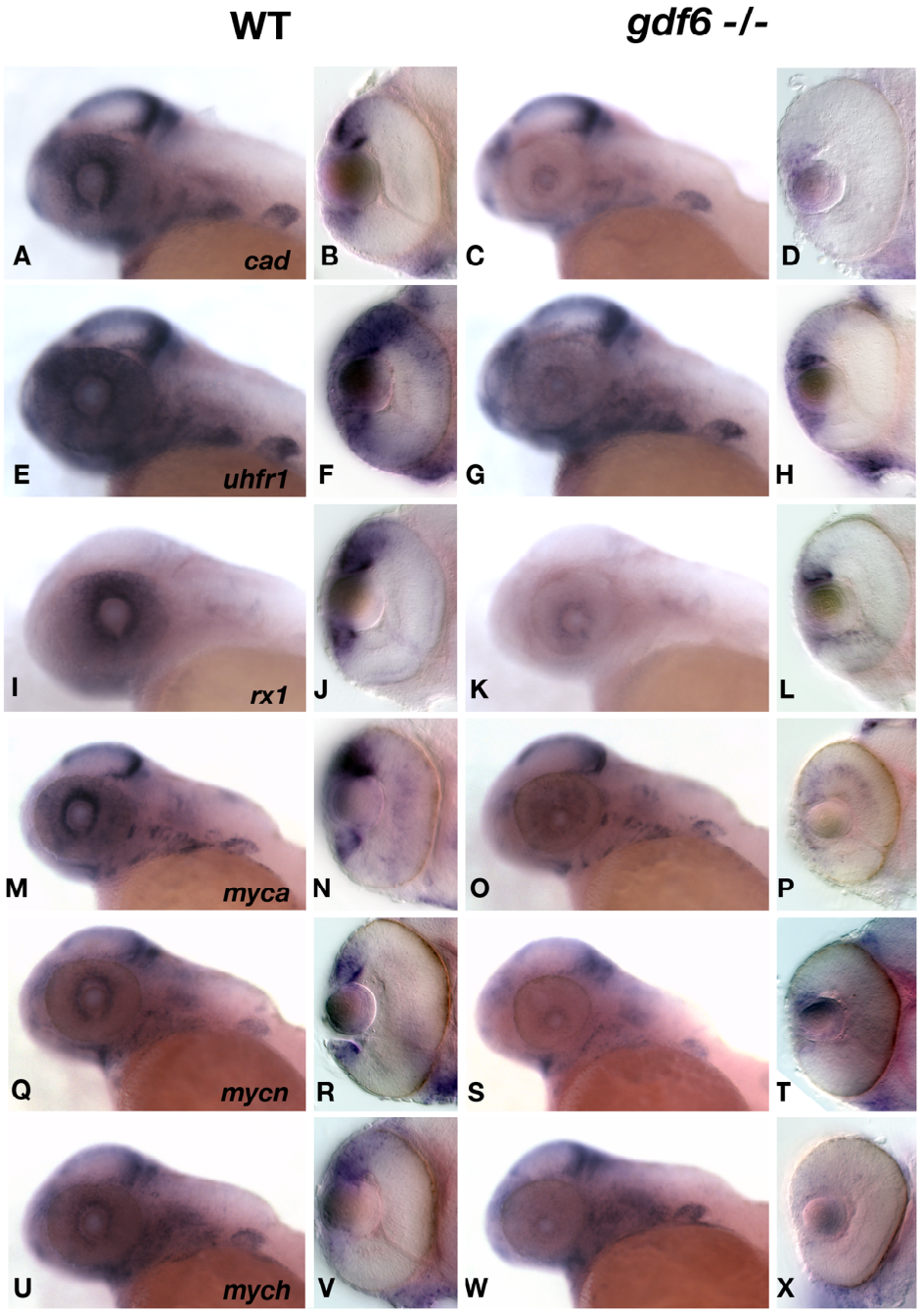
WT
gdf6 -/-
A
cad
B
C
D
E
uhfr1
F
G
H
I
rx1
J
K
L
M
myca
N
O
P
Q
mycn
R
S
T
U
mych
V
W
X

Figure 6-3: Validation of Gdf6a responsive gene with known roles in cell cycle progression. Expression of *cad,* found in the dorsal retina, CMZ and tectum (A, B), is highly down-regulated in *gdf6a* mutants in both the retina and CMZ, but unchanged in the tectum (C, D). Expression of *uhrf1* is found in the same domains, although more widespread throughout the retina (E, F), and is also down-regulated in *gdf6a* mutants. *rx1*, whose expression overlaps with *cad* in the CMZ and dorsal retina (I, J) is down-regulated, although more so in the retina than the CMZ (K, L). Expression of three *myc* paralogs, *myca*, *mycn*, and *mych*, is found in the CMZ and proliferative zones of the optic tectum (M, N, Q, R, U, V). Loss of *gdf6a* results in reduced expression of *myca* (O, P), *mycn* (S, T), while expression of *mych* is eliminated in the CMZ (W, X). Expression in the tectum remains unaffected.

detected in the CMZ and dorsal retina (Figure 6-3 E, F), and like *cad*, expression is reduced in *gdf6a* mutants, although the reduction of expression in the CMZ is subtle. Expression of *uhrf1* in the tectum of *gdf6a* mutants in normal. Similarly, the expression of *retinal homeobox 1* (*rx1*) in both the CMZ and dorsal retina is reduced in *gdf6a* mutants (compare Figure 6-3 K, L with I, J).

The zebrafish genome contains four *myelocytomatosis oncogene homolog* (*myc*) paralogs, three of which were represented on our microarray. Two *myc* genes, *myca* and *mycn,* are responsive to Gdf6a signaling (Table 6-2), while *mycb* expression was unchanged. The fourth *myc* paralog, *mych*, was not represented on our microarray. We thus analyzed the expression of three *myc* genes, including *myca* (Figure 6-3 M, N), *mycn* (Figure 6-3 Q, R), and *mych* (Figure 6-3 U, V). Expression of *myca* and *mycn* is reduced in the CMZ of *gdf6a* mutant eyes (Figure 6-3 O, P, S, T), while *mych* expression is lost completely (Figure 6-3 W, X), indicating that control of cell proliferation by all three *myc* paralogs in zebrafish may influence the microphthalmic phenotype observed in *gdf6a* mutants. Expression of all three *myc* genes is detected in the tectal proliferative zone, and remains unaffected in *gdf6a* mutants.

Over-expression of gdf6a induces secondary microphthalmia/anophthalmia

To complement our loss of function studies, we over-expressed *gdf6a*, under the control of the *heat shock 70* (*hsp70*) promoter. Injection of this construct causes no observable eye defects (Figure 6-4 A), nor does the heat shock protocol in wildtype embryos (Figure 6-4 B). Over-expression of *gdf6a,*

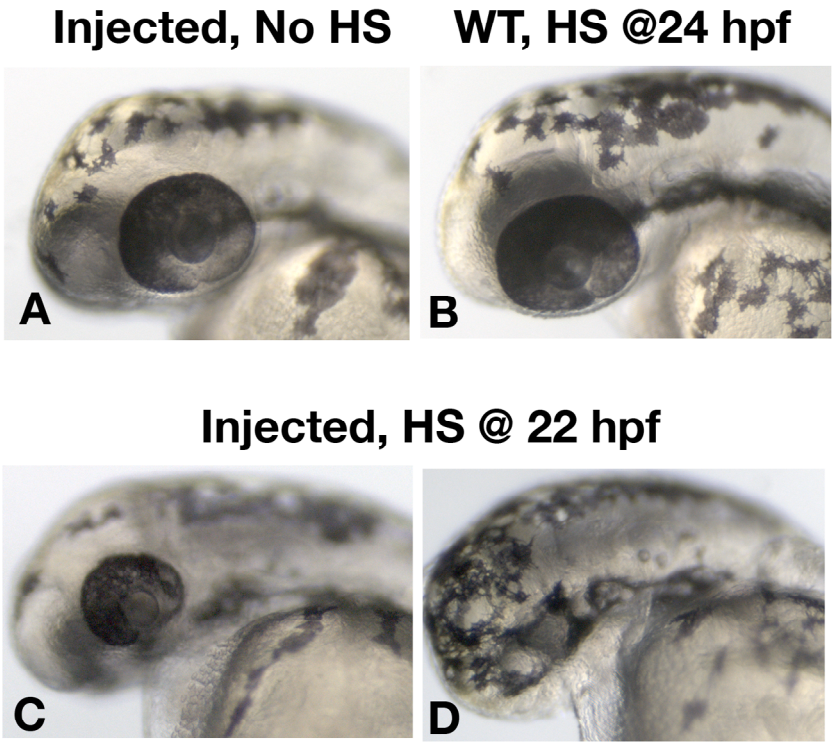

Figure 6-4: Over-expression of *gdf6a* results in microphthalmia/anophthalmia. Over-expression of *gdf6a* via the *hsp70* promoter induced microphthalmia and coloboma in previously wild type embryos. A small number of embryos displayed complete loss of eye tissue subsequent to heat shock induced *gdf6a* expression (D). Neither injection of the heat shock inducible *gdf6a* construct (A), nor the heat shocking protocol, affects eye size (B).

induced by heat shock at 22 hpf, results in secondary microphthalmia (Figure 6-4 C, n=18/28, 64%). Secondary anophthalmia was observed, but at a much lower prevalence (Figure 6-4 D, n=2/28, 7%). As induction of *gdf6a* expression did not take place until 22 hpf, these data suggest that Gdf6a can control eye growth, and degeneration after the eyecup is developed.

Discussion

In this chapter, we have conducted an analysis of gene expression in *gdf6a* homozygous mutant eyes via microarray and *in situ* analysis. Although *gdf6a* is expressed throughout the dorsal retina at early stages of development (see chapters 3 and 4), expression is confined to a small patch of cells in the dorsal retina by 2 dpf, when our microarray was conducted. This expression is specific to the ciliary marginal zone. It is therefore plausible that Gdf6a signaling is required for maintenance of stem cell populations within the CMZ, as well as differentiation of specific neuronal cell types within retina. These hypotheses require further testing to determine if proliferation in the CMZ is aberrant in *gdf6a* mutants, or if there is evidence of a lack of differentiation of specific cell types within the retina.

We have identified a number of genes, necessary for the differentiation of specific neural cell types in the eye, to be responsive to Gdf6a signaling. For example, *atoh7* has been identified as a key gene for retinal neurogenesis in general (Le et al., 2006), and null mutations result in the complete failure of the earliest born neurons of the retina, the retinal ganglion cells (Kay et al., 2001).

Furthermore, studies show that loss of *atoh7* leads to the accumulation of later born neurons, such as amacrine (Kay et al., 2001), or müller glia (Le et al., 2006). Thus, it is hypothesized that *atoh7* is required to define the earliest competency state in retinal differentiation, and without this gene product, progenitor cells in the inner retina continue to proliferate instead of exiting the cell cycle and differentiating into retinal ganglion cells. In *gdf6a* mutant embryos, residual *atoh7* expression persists, and is unclear what the ramifications of having reduced (as opposed to absent) *atoh7* expression might be for the competency state of retinal progenitors and the progression of the first wave of neurogenesis.

We have also defined *foxn4* as genetically downstream of *gdf6a*, as expression is highly down-regulated in *gdf6a* mutants. In mice, targeted disruption of this gene eliminates amacrine neurons and reduces horizontal cell number, while over-expression of *Foxn4* strongly promotes an amacrine cell fate (Li et al., 2004). This indicates that *Foxn4* is necessary for commitment to the amacrine cell fate and is required for the genesis of horizontal cells. It has been suggested that *foxn4* may function in regulating proliferation and neural differentiation in the zebrafish eye based on its expression pattern, but loss or gain of function studies in zebrafish have not been undertaken, and thus it is not known *foxn4* is required for the differentiation of amacrine or horizontal cells specifically in this model system.

Outside the eye, Foxn4 function is required for development of the atrioventricular (AV) canal that divides the zebrafish heart into two distinct chambers. Furthermore, Foxn4 was found to bind a highly conserved Tbx2b

enhancer domain element, and drive *tbx2b* expression in this tissue (Chi et al., 2008). We have also identified *tbx2b* as highly down-regulated in *gdf6a* mutant eyes, although it remains to be determined if *tbx2b* and *foxn4* directly interact during neurogenesis in the eye, as they do during heart chamber formation. Loss of *tbx2b* in zebrafish results in aberrant neuronal differentiation along the dorsal-ventral retinal axis (Gross and Dowling, 2005) as well a fate switch from ultraviolet (uv) sensitive cones to rod photoreceptor cells (Alvarez-Delfin et al., 2009). Furthermore, we detected reduced expression of a second *tbx2* paralog (*tbx2a,* Table 6-1) in *gdf6a* mutant eye, however there is no report detailing whether or not *tbx2a* functions redundantly with *tbx2b* for retinal patterning and differentiation. Further testing will be required to determine if neuronal differentiation is impaired in *gdf6a* mutant eyes, whether there is any switch of cell fate, and whether there is a direct interaction between *tbx2b* and *foxn4,* in order to produce such phenotypes.

Two other dorsal specific genes, *tbx4* and *foxi1* are lost in *gdf6a* mutant eyes upon *in situ* analysis. Tbx4 is known to regulate muscle and tendon patterning during limb development (Minguillon et al., 2009), while *foxi2* is required for proper ear and jaw patterning (Solomon et al., 2003), but again there is no report detailing the function of either in the developing eye. *rx1* expression is also detected in the dorsal retina, and has been implicated in the differentiation of photoreceptor cells (Nelson et al., 2009). It is possible *gdf6a* mutants have aberrant photoreceptor differentiation although again, this was not tested in our study. Thus, further analysis is required to determine if neurogenesis is disrupted

along the dorsal-ventral axis of *gdf6a* mutants, or whether there is a fate switch of any specific cell type.

With respect to microphthalmia, *gdf6a* expression in the dorsal ciliary marginal zone is required for the proper expression of a subset of cells in this domain, many of which have known roles in cell cycle regulation. This zone of multipotent stem cells is essential for the addition of retinal neurons to the zebrafish eye as the animal continues to grow (Wehman et al., 2005). Genes such as *cad*, which is mutated in the zebrafish *perplexed* mutant (Willer et al., 2005), are required for cell cycle progression through maintenance of adequate rates of DNA synthesis. *cad* mutants have smaller eyes, resulting from cells spending roughly double the normal time in S phase and subsequent apoptosis of these cells (Link et al., 2001). As *cad* expression is highly down-regulated in *gdf6a* mutants, it is possible that DNA synthesis rates and thus cell cycle progression are altered, although this remains to be tested directly.

Although we detected *rx1* expression in the CMZ of wild type eyes, its role in maintaining this specific stem cell population is unclear. *rx1* has been shown to be required to maintain early retinal cells in a proliferating, progenitor-like state (Zaghloul and Moody, 2007), but this analysis was conducted much earlier than 2 dpf (when our analysis was conducted), and thus its role in the CMZ remains untested. Another important cell cycle regulator, *uhrf1* (also known as ICBP90 in humans), is down regulated in the retina and CMZ in *gdf6a* mutants. *uhrf1* has been shown to regulate cell cycle progression and tumor cell growth in mammalian tissue culture systems (Jeanblanc et al., 2005; Jenkins et al., 2005),

and is required for liver growth and regeneration in zebrafish (Sadler et al., 2007). Thus, it is plausible that *uhfr1* regulates cell proliferation in the eye, and that this contributes to the microphthalmic phenotype seen in *gdf6a* mutants.

The *myc* oncogenes have long been known to regulate cell proliferation in animals, and are a major causative factor in many cancers (Reviewed by Ruggero, 2009). Moreover, in the mouse genome, *Myc* promoters contain Smad1 consensus binding sites, and binding of Smad1 to such sequences stimulates *Myc* transcription in dysplastic tissues (Hu and Rosenblum, 2005). These data support a direct relationship between Bmp signaling and *Myc* transcription. We have detected expression of 3 *myc* paralogs specifically within the CMZ of zebrafish eyes, and thus these genes may play a key role in maintaining stem cell proliferation in this domain. In support of this hypothesis, *mych* morphants are microphthalmic (Hong et al., 2008), and thus the combined loss of expression of three *myc* genes in the CMZ could play a causative role in the microphthalmic phenotype observed in *gdf6a* mutants. Further analysis, such as attempted rescue of the small eye phenotype in *gdf6a* mutants via over-expression of *myc* genes, will be required to gain supporting data for this hypothesis.

To complement our analysis of microphthalmic phenotypes in *gdf6a* mutants, we over-expressed *gdf6a* at a time when retinal progenitors are proliferating in the eyecup. Surprisingly, over-expression of *gdf6a* also induced microphthalmia, and in rare cases, anophthalmia. Although numerous human patients with mutations in *GDF6*, or chromosomal deletions encompassing *GDF6* have been described (Asai-Coakwell et al., 2007; Asai-Coakwell et al., 2009), no

patients have been identified with gain of function mutations or chromosomal duplications involving the *GDF6*, and thus it is unknown if *GDF6* gain of function would lead to microphthalmia/anophthalmia humans. Currently, our lab and collaborating labs have uncovered sequence variants in the *bambi* gene in microphthalmic/anophthalmic patients, although it remains to be determined if these variants are causative. Decreased Bambi function would presumably result in increased Bmp signaling during eye development, and thus microphthalmia in these patients may result due to increased Bmp signaling. We hypothesize that over-expression of *gdf6a* increases the rate of cell death in the retina possibly via aberrant control of cell proliferation. Further testing including BrdU incorporation (to detect cell proliferation), and TUNEL or activated Caspase staining (to detect cell death) will be conducted in the future to determine whether this hypothesis is correct.

Conclusions

We have shown that *gdf6a* mutants recapitulate the microphthalmic phenotype previously observed *gdf6a* morphant embryos. Expression of cell cycle regulating genes in both the retina and the ciliary marginal zone is dependent on Gdf6a function and thus likely contributes to the development of microphthalmia in these embryos.

Bibliography

Alvarez-Delfin, K., et al., 2009. Tbx2b is required for ultraviolet photoreceptor cell specification during zebrafish retinal development. Proc Natl Acad Sci U S A. 106**,** 2023-8.

Asai-Coakwell, M., et al., 2007. GDF6, a novel locus for a spectrum of ocular developmental anomalies. Am J Hum Genet. 80**,** 306-15.

Asai-Coakwell, M., et al., 2009. Incomplete penetrance and phenotypic variability characterize Gdf6-attributable oculo-skeletal phenotypes. Hum Mol Genet. 18**,** 1110-21.

Bakrania, P., et al., 2008. Mutations in BMP4 cause eye, brain, and digit developmental anomalies: overlap between the BMP4 and hedgehog signaling pathways. Am J Hum Genet. 82**,** 304-19.

Bhatia, B., et al., 2009. Distribution of Muller stem cells within the neural retina: evidence for the existence of a ciliary margin-like zone in the adult human eye. Exp Eye Res. 89**,** 373-82.

Campbell, H., et al., 2002. A capture-recapture model to estimate prevalence of children born in Scotland with developmental eye defects. J Cancer Epidemiol Prev. 7**,** 21-8.

Chi, N. C., et al., 2008. Foxn4 directly regulates tbx2b expression and atrioventricular canal formation. Genes Dev. 22**,** 734-9.

Ferda Percin, E., et al., 2000. Human microphthalmia associated with mutations in the retinal homeobox gene CHX10. Nat Genet. 25**,** 397-401.

Gonzalez-Rodriguez, J., et al., 2010. Mutational screening of CHX10, GDF6, OTX2, RAX and SOX2 genes in 50 unrelated microphthalmia-anophthalmia-coloboma (MAC) spectrum cases. Br J Ophthalmol.

Gosse, N. J., Baier, H., 2009. An essential role for Radar (Gdf6a) in inducing dorsal fate in the zebrafish retina. Proc Natl Acad Sci U S A. 106**,** 2236-41.

Gross, J. M., Dowling, J. E., 2005. Tbx2b is essential for neuronal differentiation along the dorsal/ventral axis of the zebrafish retina. Proc Natl Acad Sci U S A. 102**,** 4371-6.

Hanel, M. L., Hensey, C., 2006. Eye and neural defects associated with loss of GDF6. BMC Dev Biol. 6**,** 43.

Haynes, T., et al., 2007. BMP signaling mediates stem/progenitor cell-induced retina regeneration. Proc Natl Acad Sci U S A. 104**,** 20380-5.

Hong, S. K., et al., 2008. The mych gene is required for neural crest survival during zebrafish development. PLoS One. 3**,** e2029.

Hu, M. C., Rosenblum, N. D., 2005. Smad1, beta-catenin and Tcf4 associate in a molecular complex with the Myc promoter in dysplastic renal tissue and cooperate to control Myc transcription. Development. 132**,** 215-25.

Huillard, E., et al., 2005. Defects in chicken neuroretina misexpressing the BMP antagonist Drm/Gremlin. Dev Biol. 283**,** 335-44.

Jeanblanc, M., et al., 2005. The retinoblastoma gene and its product are targeted by ICBP90: a key mechanism in the G1/S transition during the cell cycle. Oncogene. 24**,** 7337-45.

Jenkins, Y., et al., 2005. Critical role of the ubiquitin ligase activity of UHRF1, a nuclear RING finger protein, in tumor cell growth. Mol Biol Cell. 16**,** 5621-9.

Kay, J. N., et al., 2001. Retinal ganglion cell genesis requires lakritz, a Zebrafish atonal Homolog. Neuron. 30**,** 725-36.

Le, T. T., et al., 2006. Math5 is required for both early retinal neuron differentiation and cell cycle progression. Dev Biol. 295**,** 764-78.

Li, S., et al., 2004. Foxn4 controls the genesis of amacrine and horizontal cells by retinal progenitors. Neuron. 43**,** 795-807.

Link, B. A., et al., 2001. The perplexed and confused mutations affect distinct stages during the transition from proliferating to post-mitotic cells within the zebrafish retina. Dev Biol. 236**,** 436-53.

Martinez-Morales, J. R., et al., 2003. OTX2 activates the molecular network underlying retina pigment epithelium differentiation. J Biol Chem. 278**,** 21721-31.

Martinez-Morales, J. R., et al., 2001. Otx genes are required for tissue specification in the developing eye. Development. 128**,** 2019-30.

Minguillon, C., et al., 2009. Tbx4/5 gene duplication and the origin of vertebrate paired appendages. Proc Natl Acad Sci U S A. 106**,** 21726-30.

Morrison, D., et al., 2002. National study of microphthalmia, anophthalmia, and coloboma (MAC) in Scotland: investigation of genetic aetiology. J Med Genet. 39**,** 16-22.

Nelson, S. M., et al., 2009. Retinal homeobox 1 is required for retinal neurogenesis and photoreceptor differentiation in embryonic zebrafish. Dev Biol. 328**,** 24-39.

Ragge, N. K., et al., 2005a. Heterozygous mutations of OTX2 cause severe ocular malformations. Am J Hum Genet. 76**,** 1008-22.

Ragge, N. K., et al., 2005b. SOX2 anophthalmia syndrome. Am J Med Genet A. 135**,** 1-7; discussion 8.

Ruggero, D., 2009. The role of Myc-induced protein synthesis in cancer. Cancer Res. 69**,** 8839-43.

Sadler, K. C., et al., 2007. Liver growth in the embryo and during liver regeneration in zebrafish requires the cell cycle regulator, uhrf1. Proc Natl Acad Sci U S A. 104**,** 1570-5.

Schilter, K. F., et al., 2010. OTX2 microphthalmia syndrome: four novel mutations and delineation of a phenotype. Clin Genet.

Schmitt, S., et al., 2009. Molecular characterization of human retinal progenitor cells. Invest Ophthalmol Vis Sci. 50**,** 5901-8.

Schneider, A., et al., 2009. Novel SOX2 mutations and genotype-phenotype correlation in anophthalmia and microphthalmia. Am J Med Genet A. 149A**,** 2706-15.

Schulte, D., Cepko, C. L., 2000. Two homeobox genes define the domain of EphA3 expression in the developing chick retina. Development. 127**,** 5033-45.

Solomon, K. S., et al., 2003. Zebrafish foxi1 mediates otic placode formation and jaw development. Development. 130**,** 929-40.

Takahashi, H., et al., 2003. CBF1 controls the retinotectal topographical map along the anteroposterior axis through multiple mechanisms. Development. 130**,** 5203-15.

Valleix, S., et al., 2006. Homozygous nonsense mutation in the FOXE3 gene as a cause of congenital primary aphakia in humans. Am J Hum Genet. 79**,** 358-64.

Verma, A. S., Fitzpatrick, D. R., 2007. Anophthalmia and microphthalmia. Orphanet J Rare Dis. 2**,** 47.

Wehman, A. M., et al., 2005. Genetic dissection of the zebrafish retinal stem-cell compartment. Dev Biol. 281**,** 53-65.

Westenskow, P., et al., 2009. Beta-catenin controls differentiation of the retinal pigment epithelium in the mouse optic cup by regulating Mitf and Otx2 expression. Development. 136**,** 2505-10.

Willer, G. B., et al., 2005. Analysis of the Zebrafish perplexed mutation reveals tissue-specific roles for de novo pyrimidine synthesis during development. Genetics. 170**,** 1827-37.

Ye, M., et al., 2010. Mutation of the bone morphogenetic protein GDF3 causes ocular and skeletal anomalies. Hum Mol Genet. 19**,** 287-98.

Zaghloul, N. A., Moody, S. A., 2007. Alterations of rx1 and pax6 expression levels at neural plate stages differentially affect the production of retinal cell types and maintenance of retinal stem cell qualities. Dev Biol. 306**,** 222-40.

Chapter 7

General Discussion and Conclusions

In this thesis, I have defined critical roles for two homeodomain transcription factor families, Pbx and Meis, in patterning the zebrafish dorsal retina. Inhibition of Pbx2/4 and Meis family members leads to a loss of dorsal identity, which may be mediated, at least in part, to transcriptional regulation of a downstream growth factor *gdf6a*. Further analysis in *gdf6a* mutants identifies topographic errors suggesting that incorrect patterning of the optic vesicle profoundly changes the connectivity between the eye and tectum at later stages in development. I have further defined roles for *gdf6a* in lens and skeletal development, and have begun to define a mechanism for the role this critical growth factor plays in the development of microphthalmia.

Insights into Pbx and Meis mediated retinal-tectal patterning

Initial studies using *pbx2/4* loss of function define a clear role for regulation of dorsal patterning genes such as *tbx5* and *aldh1a2*. These phenotypes is observed early (18 hpf), but becomes subtle later in development (24 hpf). At these later stages, other pbx genes, such as *pbx1*, and *pbx3.1* (Waskiewicz et al., 2002), are transcriptionally active and thus may be at least partially responsible for recovery of observed phenotypes. Using a *meis* dominant negative approach that inhibits all Meis family members, we can recapitulate dorsal pattering phenotypes, which in these embryos, are observed at later stages of development. This suggests that Pbx2/4 and Meis family members cooperatively pattern the dorsal retina as they do other embryonic tissues (Choe et al., 2009; Choe et al., 2002; Pillay et al., 2010; Waskiewicz et al., 2001; Zhang et al., 2006). It is not yet

known how Pbx2 and Pbx4, which are ubiquitously expressed (Waskiewicz et al., 2002), or Meis family members, which have more restricted expression patterns but are ubiquitous throughout the eye (Choe et al., 2002), act to exert influence on a specific domain within the retina. It is possible that spatially restricted transcription factors in the dorsal retina may be required to form complexes with Pbx and Meis proteins, thereby adding specificity to their transcription promoting activity.

Analysis of the retinal contribution to topographic mapping is difficult in *pbx2/4* null embryos, as loss of these genes influences tectal development and patterning. Indeed, we have shown that tectal patterning genes such as *efna2* and *efnA5a* have altered expression patterns in *pbx2/4* null embryos, and that the tectum is morphologically disrupted. In these embryos, retinal ganglion cells exhibit outgrowth errors where axons stall prior to entry onto the optic tectum, thus preventing analysis of topographic mapping. Similarly, it has been reported that *meis1.1* morphants have tectal patterning defects, and although a small proportion of embryos display topographic mapping errors on the optic tectum, most embryos show an axon outgrowth defect (Erickson *et al.*, in press) similar to what is observed in *pbx2/4* null embryos. Although it is likely that RGC outgrowth phenotypes result from aberrant tectal development, we cannot rule out the possibility that loss of dorsal identity plays a role in producing this phenotype. This could be resolved through transplantation experiments, allowing for analysis of mutant or morphant retinal ganglion cell outgrowth and mapping in a wildtype

embryo (and thus tectum), while similarly assaying the outgrowth and mapping of a wildtype retinal ganglion cell in a mutant or morphant embryo.

Retinal patterning and topographic mapping requires gdf6a

The dorsal patterning defects seen in *pbx2/4* null, or *meis* dominant negative embryos may be mediated in part by transcriptional regulation of a downstream growth factor, *gdf6a*, as expression of *gdf6a* in the dorsal retina is highly down-regulated in embryos lacking Pbx2/4 or Meis function (Chapter 3). Morpholino inhibition of *gdf6a* leads to a complete loss of dorsal patterning genes such as *tbx5* and *aldh1a2*, and furthermore, the retina is re-specified to a ventral state, as ventral specific genes such as *vax2* are found throughout the eye. We further show that the expression of *ephb2* in no longer confined to the ventral retina, and expression of the dorsal specific *efnb2a* is lost, which likely have a direct influence on topographic mapping. Although similar phenotypes are observed in the dorsal retina in *pbx2/4* null embryos and *gdf6a* morphants, we cannot conclude unequivocally that Pbx2/4 patterns the dorsal retina via regulation of *gdf6a* expression, as direct regulation of dorsal patterning genes such as *tbx5* is possible. This can be tested via over-expression of *gdf6a* in *pbx2/4* null backgrounds. A rescue of dorsal patterning defects should be observed if indeed Pbx2/4 regulates dorsal retinal patterning through regulation of *gdf6a.*

Unlike *pbx2/4* null or *meis* DN embryos, tectal development does not appear to be affected in *gdf6a* mutants (see chapter 6), thereby allowing for analysis of topographic mapping in response to aberrant eye patterning. In these

embryos, topographic mapping is altered, whereby ganglion cells from the dorsal retina map to a more medial position on the optic tectum, an area normally occupied by ganglion cells from the ventral retina only (Gosse and Baier, 2009 and chapter 4). Our data thus firmly supports a model whereby Gdf6a regulates the expression of spatially restricted transcription factors, such as *tbx5* and *vax2*, that in turn regulate dorsal and ventral specific transcription of *efnb2a* and *ephb2* and thus proper topographic mapping along the medial-lateral tectal axis.

Although it is clear that *gdf6a* is required for dorsal retina specification, Bmps are known to signal as heterodimers (Butler and Dodd, 2003; Little and Mullins, 2009) and thus the relative contributions of other Bmp ligands warrant further investigation. In zebrafish, both *bmp4* and *bmp2b* are expressed in the dorsal retina (Gosse and Baier, 2009; Veien et al., 2008). Over-expression of *ventroptin*, a Bmp4 inhibitor, alters topographic mapping in chicken embryos (Sakuta et al., 2001) while over-expression of *Bmp2* induces similar phenotypes in transgenic mice (Plas et al., 2008).

Our over-expression analysis demonstrates that *gdf6a* alone is sufficient to induce dorsal cell fate highlighting the possibility that Gdf6a may function as a homodimer. Such manipulations result in expanded Smad 1/5/8 phosphorylation and *tbx5* expression in the presumptive ventral domain of the retina. As other Bmp ligands are not expressed in the ventral retina, two possibilities exist for Bmp receptor activation; 1) Gdf6a homodimers are sufficient to activate Bmp receptor complexes to wild type levels or 2) low levels of Gdf6a homodimer signaling are sufficient to activate expression of other *bmps*, thereby allowing for

heterodimer formation and thus wildtype levels of Smad phosphorylation. The latter hypothesis is attractive as Bmp homodimers have been shown to elicit much lower levels of Bmp receptor activation than heterodimers (Little and Mullins, 2009), and Gdf6a signaling can regulate the expression of other Bmp ligands (Gosse and Baier, 2009; Veien et al., 2008, and this work).

We have demonstrated that although *bmp4* is transcriptionally regulated by Gdf6a, it is dispensable for dorsal retina specification as no changes of *tbx5* expression or Smad phosphorylation are observed in Bmp4 morphants. These data do not support a role for Bmp4 in heterodimer formation with Gdf6a. We have not tested the contribution of *bmp2* in dorsal retinal specification, however it has been shown that Xenopus Gdf6 can form heterodimers with Bmp2 when over-expressed in vivo (Chang and Hemmati-Brivanlou, 1999). Analysis of dorsal retinal patterning in zebrafish *bmp2* mutants (Mullins et al., 1996) could add clarification, as similar dorsal retinal patterning phenotypes should be observed.

gdf6a initiates dorsal cell identity

In zebrafish, spatially restricted transcription factors can be observed in the eye vesicle as early as the 6 somite stage, when expression of *tbx5* is induced in the presumptive dorsal retina. The Wingless-type MMTV integration site (Wnt) signaling pathway has been shown to be required for dorsal retinal specification, however Wnt signaling is not active in the retina prior to 10 somites, and thus loss of *tbx5* expression is only observed at later stages (Veien et al., 2008). These observations suggest that patterning the dorsal-ventral retinal axis occurs in at

least two phases; First, an initiation phase at 6 somites, where the expression of *tbx5* and other dorsal determinants are induced, and second, a maintenance phase (beginning between 10 somites and 24 hpf) where discrete signaling pathways ensure that dorsal cell identity persists over time.

We clearly demonstrate that *gdf6a* acts during the initiation stage of dorsal retinal patterning, as the expression of *tbx5* is not induced at the 6 somite stage in *gdf6a* morphants. *gdf6a* is expressed adjacent to the presumptive dorsal retina just prior to initiation of *tbx5* expression, and is thus positioned to act at the earliest stages of dorsal patterning. Using a gain of function approach that is mosaic in nature, we have shown that Gdf6a acts in a non-cell autonomous manner, as cells expressing the *gdf6a* construct induce Smad 1/5/8 phosphorylation in surrounding cells. Thus, this extraocular source of Gdf6a ligand is certainly capable of inducing dorsal retinal patterning. Although not directly tested, it is likely that maintenance of dorsal cell identity by the Wnt signaling pathway requires Gdf6a function. *gdf6a* expression is initiated but not maintained in embryos lacking Wnt function (Veien et al., 2008) suggesting that the Wnt pathway functions to maintain Gdf6a signaling at later stages of development, ensuring that dorsal retinal identity persists. Definitive testing of this hypothesis could be accomplished by over-expressing *gdf6a* in a Wnt inhibited background, which would rescue Wnt induced patterning defects if our hypothesis is correct.

Coloboma and dorsal-ventral retinal patterning

Coloboma, or failure to close optic fissure during development, is known to occur as the result of mis-pattering the dorsal-ventral retinal axis (Gregory-Evans et al., 2004). Both *gdf6a* morphant and mutant embryos present with coloboma, which could result from the inability to express *tbx5* and *vax2* in their spatially restricted domains, as manipulation of both genes can result in coloboma (Barbieri et al., 2002; Zhou et al., 2008). In addition, we have also demonstrated that the expression of retinoic acid (RA) synthesis genes are altered in *gdf6a* morphant embryos. There is suggestive evidence that aberrant RA signaling can cause coloboma in humans (Hornby et al., 2003; Seeliger et al., 1999), while implantation of RA soaked beads can induce ectopic fissure formation in animal models (Hyatt et al., 1996). Ectopic fissure formation is seen if *gdf6a* morphant and mutant embryos in addition to coloboma, further implicating Gdf6a dependent RA signaling in regulating optic fissure formation and closure.

Two genes are responsible for retinoic acid synthesis in the zebrafish retina, the dorsal specific *aldh1a2*, and the ventral specific *aldh1a3*. RA is hypothesized to signal in a ventral high/dorsal low gradient, as the ventral specific *aldh1a3* is much more efficient at synthesizing RA as its dorsal counterpart, *aldh1a2* (Hyatt et al., 1996). We observe a loss of *aldh1a2* in *gdf6a* morphants, while *aldh1a3* is moderately up-regulated, which would presumably exaggerate a ventral high/dorsal low gradient. Thus, altered RA signaling may also be responsible, at least in part, for the development of coloboma and ectopic fissure formation in eyes lacking Gdf6a function. Furthermore, the expression of RA

synthesizing genes in the eye is controlled by both Tbx*5* and Vax2 (Golz et al., 2008), suggesting a linear pathway for closure of the optic fissure, whereby *gdf6a* regulates polarized expression of *tbx5* and *vax2*, which in turn regulate the expression of *aldh1a2* and *aldh1a3* in the dorsal and ventral retina, respectively.

pbx2/4 and gdf6a loss of function results in microphthalmia

Microphthalmia is observed in *pbx2/4* null embryos, however the mechanism by which this results is not known. Loss of *rx3* in Medaka inhibits retinal progenitor cell proliferation in the optic vesicles subsequent to their envagination, and over-expression of *rx3* leads to enlarged optic vesicles (Loosli et al., 2001). We detect increased expression of *rx3* at later stages in *pbx2/4* null eyes, which obviously does not lead to enlarged optic vesicles. Thus, the effect of increased *rx3* expression in *pbx2/4* null embryos remains unclear. Although we have demonstrated decreased expression of *rx2* in *pbx2/4* null eyes, possible effects on progenitor cell proliferation have not been tested as part of this study. Over-expression of *rx2* can lead to ectopic eye formation, but this results from a fate switch of forebrain cells into retinal progenitors (Chuang and Raymond, 2001). It is possible that reduced expression of *rx2* in *pbx2/4* null embryos may result in a fate switch, meaning that some retinal progenitors may be specified to a forebrain cell fate, leading to reduced numbers of retinal progenitors and thus smaller eyes. Analysis of forebrain specific markers in *pbx2/4* null embryos will be required to test this hypothesis.

As Meis proteins are known to bind Pbx proteins and cooperatively pattern numerous embryonic tissues, recent reports concerning small eye phenotypes in *meis1* morphant zebrafish may shed light on the mechanism by which loss of Pbx2/4 induces microphthalmia. Meis1 is required ubiquitously in early proliferating cells in the zebrafish eye, and inhibition using morpholinos result in a specific delay in the G1-to-S phase transition, and thus smaller eye size (Bessa et al., 2008). Furthermore, it was shown that Meis1 regulated the expression of both *cyclinD1* (Bessa et al., 2008; Heine et al., 2008) and *myca* (Bessa et al., 2008), two known G1 regulators of the cell cycle in vertebrates (Levine and Green, 2004). Interestingly, as the neurogenic wave sweeps across the retina, *meis1* expression becomes confined to the ciliary marginal zone, indicating that Meis1 may also regulate proliferation in stem cell populations that are required for growth of the eye after neurogenesis is complete.

Although we have not tested the expression of these cell cycle genes in *pbx2/4* null embryos, microphthalmia is also observed in *gdf6a* mutants, and we have demonstrated reduced expression of critical cell cycle regulators in the ciliary marginal zone of these embryos. These include reduced expression of *cyclinF*, as well as three *myc* orthologs, phenotypes that are very similar to that of *meis1* morphants. Although increased cell death has been documented in *gdf6a* mutant eyes, *gdf6a* expression becomes confined to the CMZ after retinal neurogenesis (Chapter 6), similar to that of Meis1 morphants (Bessa et al., 2008), and thus aberrant regulation of proliferation in these stem cell populations may lead to the microphthalmic phenotype in *gdf6a* mutants.

Gdf6a signaling is required for lens and skeletal development

The induction of lens tissue, and subsequent differentiation of lens fibers may also be dependent of Gdf6a function. We have demonstrated Smad 1/5/8 phosphorylation in the lens, which is lost upon inhibition of *gdf6a*, as well as reduced expression of genes that are required for lens fiber cell differentiation. Lens fibers must degrade their nucleus upon terminal differentiation in order to produce an optically clear fiber (Bassnett and Beebe, 1992). We observe nuclei within concentric rings of elongated fiber cells in *gdf6a* morphant embryos (when incubated with Dorsomorphin, a Bmp inhibitor), suggesting that terminal differentiation of lens fibers is blocked. However we also observe increased staining of ZL-1 in the lens of *gdf6a* morphants (incubated with Dorsomorphin). This antibody highlights differentiated lens fibers, and thus increased staining contradicts the nuclear retention phenotype. Thus, further analysis is required to determine the exact nature of lens defects observed through inhibition of Gdf6a. These analyses should also be repeated in *gdf6a* mutant embryos, as *gdf6a* morpholino inhibition alone did not result in altered ZL-1 staining or nuclear retention. These phenotypes were only observed when *gdf6a* morpholinos were used in combination with a general Bmp inhibitor, and therefore we cannot rule out the possibility that other Bmps, such as Bmp2/4/7 which have been implicated in lens development in mice (Boswell et al., 2008), may also influence zebrafish lens development in addition to Gdf6a.

Outside of the eye, studies have indicated a role for Gdf6 in bone development, as Gdf6 knockout mice display skeletal defects such a vertebral

fusions (Asai-Coakwell et al., 2009; Settle et al., 2003). At 24 hpf, we observe axial defects and reduced expression of *noggin1* and *noggin2,* which are required for development of the axial skeleton (Oxley et al., 2008; Wijgerde et al., 2005). However osteogenic bone formation has not begun in zebrafish at this time (Inohaya et al., 2007), making it difficult to speculate whether these gene expression phenotypes lead to aberrant development of the axial skeleton at later developmental stages. Analysis of jaw cartilage organization at 6 dpf does not reveal any overt phenotype, which may be the result of reduced morpholino effectiveness. Indeed we observe reduced expression of *gdf5* in pharyngeal jaw elements at 3 dpf, suggesting that jaw cartilage development does not proceed normally in these embryos. These discrepancies can be resolved by repeating our analysis of cartilage and bone staining in *gdf6a* mutant embryos, which survive up to 5 weeks post fertilization (Gosse and Baier, 2009), thus facilitating analysis at later stages of development and eliminating the need for morpholino induced *gdf6a* inhibition.

Clinical relevance of GDF6 function

The increasing wealth of knowledge concerning the function of Gdf6a in regulating developmental processes required for eye and skeletal development has made this gene an attractive candidate for mutational analysis in patients with ocular and skeletal phenotypes. During the course of this work, numerous mutations in the *GDF6* coding sequence were defined in human patients who suffer from combined ocular and skeletal defects.

An analysis using a large panel of MAC (microphtmalmia, anaphthalmia, or coloboma) patients found a number of missense mutations in the propeptide domain of the immature ligand that result in reduced GDF6 protein secretion in cell culture assays (Asai-Coakwell et al., 2009). This process is important for Gdf6 function as we have shown that in zebrafish, Gdf6a exerts its effects in a cell non-autonomous manner (Chapter 4). Patients displayed both eye (microphthalmia or coloboma, or both) as well as vertebral fusions consistent with the Killppel-Feil syndrome (Asai-Coakwell et al., 2009). These data were further confirmed through the study of MAC patients of Mexican Mestizo origin, where three recurrent *GDF6* mutations were found (Gonzalez-Rodriguez et al., 2010), as well as one novel mutation in the exonic sequence. In collaboration with the laboratories of Dr. Ordan Lehmann (University of Alberta) and Dr. T. Michael Underhill (University of British Colombia), we have demonstrated reduced functionality of human *GDF6* mutations when over-expressed in both zebrafish and cell culture reporter assays (Asai-Coakwell et al., 2009) highlighting the importance of understanding *gdf6a* function in animal models. These analyses are reported in appendix E.

Conclusions

Understanding the basic fundamental processes regulated by Gdf6a in zebrafish has lead to a wealth of knowledge with respect to eye development. I have clearly shown that *gdf6a* is required for eye patterning along the dorsal-ventral axis. My data also suggests that homeodomain transcription factors of the

Pbx and Meis families act upstream of *gdf6a* for dorsal retinal specification. Furthermore, I have provided preliminary evidence that Gdf6a has vital role in other embryonic tissues, including the lens, pineal complex, and skeletal systems. Manipulation of *gdf6a* in zebrafish leads to many of the same ocular and skeletal phenotypes observed in human patients with *GDF6* mutations, such as microphthalmia and coloboma, making our loss of function zebrafish model an invaluable tool for better understanding of these human conditions.

Bibliography

Asai-Coakwell, M., et al., 2009. Incomplete penetrance and phenotypic variability characterize Gdf6-attributable oculo-skeletal phenotypes. Hum Mol Genet. 18**,** 1110-21.

Barbieri, A. M., et al., 2002. Vax2 inactivation in mouse determines alteration of the eye dorsal-ventral axis, misrouting of the optic fibres and eye coloboma. Development. 129**,** 805-13.

Bassnett, S., Beebe, D. C., 1992. Coincident loss of mitochondria and nuclei during lens fiber cell differentiation. Dev Dyn. 194**,** 85-93.

Bessa, J., et al., 2008. meis1 regulates cyclin D1 and c-myc expression, and controls the proliferation of the multipotent cells in the early developing zebrafish eye. Development. 135**,** 799-803.

Boswell, B. A., et al., 2008. Essential role of BMPs in FGF-induced secondary lens fiber differentiation. Dev Biol. 324**,** 202-12.

Butler, S. J., Dodd, J., 2003. A role for BMP heterodimers in roof plate-mediated repulsion of commissural axons. Neuron. 38**,** 389-401.

Chang, C., Hemmati-Brivanlou, A., 1999. Xenopus GDF6, a new antagonist of noggin and a partner of BMPs. Development. 126**,** 3347-57.

Choe, S. K., et al., 2009. Meis cofactors control HDAC and CBP accessibility at Hox-regulated promoters during zebrafish embryogenesis. Dev Cell. 17**,** 561-7.

Choe, S. K., et al., 2002. Meis family proteins are required for hindbrain development in the zebrafish. Development. 129**,** 585-95.

Chuang, J. C., Raymond, P. A., 2001. Zebrafish genes rx1 and rx2 help define the region of forebrain that gives rise to retina. Dev Biol. 231**,** 13-30.

Erickson T. Meis1 specifies positional information in the retina and tectum to organize the zebrafish visual system. Neural Development, in press.

Golz, S., et al., 2008. Regulation of RALDH-1, RALDH-3 and CYP26A1 by transcription factors cVax/Vax2 and Tbx5 in the embryonic chick retina. Int J Dev Neurosci. 26**,** 435-45.

Gonzalez-Rodriguez, J., et al., 2010. Mutational screening of CHX10, GDF6, OTX2, RAX and SOX2 genes in 50 unrelated microphthalmia-anophthalmia-coloboma (MAC) spectrum cases. Br J Ophthalmol.

Gosse, N. J., Baier, H., 2009. An essential role for Radar (Gdf6a) in inducing dorsal fate in the zebrafish retina. Proc Natl Acad Sci U S A. 106**,** 2236-41.

Gregory-Evans, C. Y., et al., 2004. Ocular coloboma: a reassessment in the age of molecular neuroscience. J Med Genet. 41**,** 881-91.

Heine, P., et al., 2008. Evidence for an evolutionary conserved role of homothorax/Meis1/2 during vertebrate retina development. Development. 135**,** 805-11.

Hornby, S. J., et al., 2003. Eye birth defects in humans may be caused by a recessively-inherited genetic predisposition to the effects of maternal vitamin A deficiency during pregnancy. Med Sci Monit. 9**,** HY23-6.

Hyatt, G. A., et al., 1996. Retinoic acid establishes ventral retinal characteristics. Development. 122**,** 195-204.

Inohaya, K., et al., 2007. The teleost intervertebral region acts as a growth center of the centrum: in vivo visualization of osteoblasts and their progenitors in transgenic fish. Dev Dyn. 236**,** 3031-46.

Levine, E. M., Green, E. S., 2004. Cell-intrinsic regulators of proliferation in vertebrate retinal progenitors. Semin Cell Dev Biol. 15**,** 63-74.

Little, S. C., Mullins, M. C., 2009. Bone morphogenetic protein heterodimers assemble heteromeric type I receptor complexes to pattern the dorsoventral axis. Nat Cell Biol. 11**,** 637-43.

Loosli, F., et al., 2001. Medaka eyeless is the key factor linking retinal determination and eye growth. Development. 128**,** 4035-44.

Mullins, M. C., et al., 1996. Genes establishing dorsoventral pattern formation in the zebrafish embryo: the ventral specifying genes. Development. 123**,** 81-93.

Oxley, C. D., et al., 2008. Growth and skeletal development in families with NOGGIN gene mutations. Horm Res. 69**,** 221-6.

Pillay, L. M., et al., 2010. The Hox cofactors Meis1 and Pbx act upstream of gata1 to regulate primitive hematopoiesis. Dev Biol. 340**,** 306-17.

Plas, D. T., et al., 2008. Bone morphogenetic proteins, eye patterning, and retinocollicular map formation in the mouse. J Neurosci. 28**,** 7057-67.

Sakuta, H., et al., 2001. Ventroptin: a BMP-4 antagonist expressed in a double-gradient pattern in the retina. Science. 293**,** 111-5.

Seeliger, M. W., et al., 1999. Phenotype in retinol deficiency due to a hereditary defect in retinol binding protein synthesis. Invest Ophthalmol Vis Sci. 40**,** 3-11.

Settle, S. H., Jr., et al., 2003. Multiple joint and skeletal patterning defects caused by single and double mutations in the mouse Gdf6 and Gdf5 genes. Dev Biol. 254**,** 116-30.

Veien, E. S., et al., 2008. Canonical Wnt signaling is required for the maintenance of dorsal retinal identity. Development. 135**,** 4101-11.

Waskiewicz, A. J., et al., 2001. Zebrafish Meis functions to stabilize Pbx proteins and regulate hindbrain patterning. Development. 128**,** 4139-51.

Waskiewicz, A. J., et al., 2002. Eliminating zebrafish pbx proteins reveals a hindbrain ground state. Dev Cell. 3**,** 723-33.

Wijgerde, M., et al., 2005. Noggin antagonism of BMP4 signaling controls development of the axial skeleton in the mouse. Dev Biol. 286**,** 149-57.

Zhang, X., et al., 2006. Pax6 is regulated by Meis and Pbx homeoproteins during pancreatic development. Dev Biol. 300**,** 748-57.

Zhou, C. J., et al., 2008. Ocular coloboma and dorsoventral neuroretinal patterning defects in Lrp6 mutant eyes. Dev Dyn. 237**,** 3681-9.

Appendix A

List of genes down-regulated in *gdf6a* morphant embryos by at least 2-fold, identified by microarray analysis at 24 hpf.

Rank	Gene Name	Systematic Name	Avg ratio
1	vtn	BC055570	7.92
2	vtn	BC055570	6.69
3	ENSDART00000009171	ENSDART00000009171	6.24
4	cryba1b	NM_001002586	5.41
5	cryba2a	NM_001002049	4.87
6	CK869940	zgc:163013	4.28
7	LOC402925	BC076260	4.05
8	zgc:103655	NM_001005949	4.01
9	TC291342	TC291342	3.96
10	BF717570	BF717570	3.78
11	TC279019	TC279019	3.54
12	atoh1a	NM_131091	3.53
13	crybb1	NM_173231	3.42
14	tnnt3b	NM_181653	3.39
15	tnnt3b	NM_181653	3.35
16	TC283683	TC283683	3.34
17	TC291238	TC291238	3.32
18	TC269328	TC269328	3.32
19	tnnt3b	NM_181653	3.31
20	TC291242	TC291242	3.29
21	zgc:77591	NM_214702	3.18
22	zgc:100893 (tyrp1b)	NM_001002749	3.16
23	zgc:103767	NM_001006006	3.12
24	zgc:91968	NM_001002167	3.09
25	zgc:103767	NM_001006006	3.02
26	zgc:77591	NM_214702	3.00
27	zgc:103767	NM_001006006	2.96
28	zgc:103448	NM_001007353	2.88
29	BC076207	BC076207	2.81
30	zgc:92334	NM_001002454	2.80
31	zgc:103448	NM_001007353	2.80
32	igfbp1	NM_173283	2.77
33	tnnt3b	NM_181653	2.76
34	ENSDART00000030830	ENSDART00000030830	2.76
35	zgc:103408	NM_001004618	2.74
36	sb:cb890	NM_198824	2.73
37	tnnt3b	NM_181653	2.71
38	zgc:103448	NM_001007353	2.68
39	ENSDART00000020861	ENSDART00000020861	2.68
40	mdka	NM_131070	2.59
41	zgc:85969	NM_212914	2.58
42	wu:fb55f05	CK027604	2.56

43	CN501939	CN501939	2.55
44	ENSDART00000004535	ENSDART00000004535	2.53
45	myhz2	NM_152982	2.51
46	slc4a1	NM_198338	2.48
47	zgc:56217	NM_200212	2.48
48	myhz2	NM_152982	2.46
49	TC290346	TC290346	2.45
50	BC078372	BC078372	2.44
51	tpbgl	NM_194392	2.43
52	zgc:92368	NM_001003512	2.42
53	ENSDART00000047556	ENSDART00000047556	2.42
54	TC279875	TC279875	2.42
55	TC299194	TC299194	2.41
56	CA476762	CA476762	2.38
57	hbae1	NM_182940	2.34
58	TC290061	TC290061	2.30
59	TC289947	TC289947	2.29
60	TC274669	TC274669	2.29
61	zgc:103664	NM_001008585	2.28
62	mdm4	NM_212732	2.27
63	zgc:77778	NM_213203	2.24
64	zgc:92719	CN513136	2.24
65	zgc:92434	NM_001002173	2.24
66	TC297904	TC297904	2.23
67	angptl3	NM_131818	2.22
68	bf	NM_131338	2.21
69	zgc:55610	NM_200256	2.17
70	zgc:92368	NM_001003512	2.17
71	zgc:76922 (sult1st4)	NM_205620	2.15
72	pax9	NM_131298	2.14
73	ENSDART00000033914	ENSDART00000033914	2.13
74	zgc:92719 (lim2.3)	NM_001002587	2.11
75	mdm4	NM_212732	2.11
76	zgc:55673	NM_200171	2.11
77	cry1b	NM_131790	2.11
78	wu:fe11h12	AY192988	2.08
79	TC292184	TC292184	2.08
80	zgc:55610 (slc25a32a)	NM_200256	2.08
81	ENSDART00000050282	ENSDART00000050282	2.07
82	zgc:66117	NM_199560	2.07
83	TC295371	TC295371	2.06
84	TC290310	TC290310	2.04
85	TC268919	TC268919	2.04
86	per4	NM_212439	2.04
87	TC292060	TC292060	2.03
88	AL714971	AL714971	2.03
89	cx23	BC091468	2.02
90	zgc:66117	NM_199560	2.02
91	lyz	ENSDART00000041575	2.02

92	BC078368 (aspn)	BC078368	2.02
93	TC295131	TC295131	2.00
94	zgc:66329	TC296853	1.99
95	TC300415	TC300415	1.99
96	TC290877	TC290877	1.99
97	CO354277	CO354277	1.99
98	wu:fe36g06	AW128734	1.99
99	rx2	NM_131226	1.98
100	TC295598	TC295598	1.97
101	ENSDART00000002347	ENSDART00000002347	1.97
102	zgc:77284	NM_213234	1.97
103	BC090471	BC090471	1.96
104	zgc:77004	NM_213316	1.96
105	TC272598	TC272598	1.96
106	zgc:85890	NM_207059	1.96
107	vangl2	BC065983	1.95
108	TC280202	TC280202	1.95
109	zgc:92278	NM_001002610	1.95

Fold change: WT/*gdf6a* MO

Appendix B

List of genes up-regulated in *gdf6a* morphant embryos by at least 2-fold, identified by microarray analysis at 24 hpf.

Rank	Gene name	Systematic name	Avg ratio
1	tp53	NM_131327	5.35
2	tp53	NM_131327	5.27
3	ccng1	NM_199481	4.82
4	casp8	NM_131510	4.65
5	gadd45al	NM_200576	4.23
6	CN504773	CN504773	3.95
7	gtpbp1l	BC056806	3.87
8	zgc:92605	NM_001002708	3.87
9	AL728695	AL728695	3.83
10	zgc:56246 (tm9sf3)	NM_213389	3.82
11	TC280849	TC280849	3.75
12	mdm2	NM_131364	3.72
13	foxo5	NM_131085	3.69
14	ldb3	NM_201505	3.53
15	hsp47	NM_131204	3.38
16	zgc:92830	NM_001002506 (lyrm1)	3.09
17	zgc:66126	NM_199891 (ecd)	3.08
18	vrk2	NM_201170	3.07
19	hsp47	NM_131204	2.97
20	BC074098	BC074098	2.96
21	hsp47	NM_131204	2.93
22	zgc:55750 (rasl11b)	NM_200140	2.93
23	gadd45al	NM_200576	2.91
24	hsp47	BC071301	2.90
25	TC291802	TC291802	2.79
26	ldb3	NM_201505	2.76
27	mmp2	NM_198067	2.72
28	TC278959	TC278959	2.72
29	TC270856	TC270856	2.66
30	ENSDART00000042381	ENSDART00000042381	2.63
31	TC293311	TC293311	2.57
32	ENSDART00000012038	ENSDART00000012038	2.46
33	zgc:56722	NM_213519	2.45
34	lsm7	NM_200011	2.44
35	TC281840	TC281840	2.37
36	snrpd3	NM_001002081	2.36
37	strap	NM_200304	2.34
38	zgc:66214	BC055550 (eftud2)	2.30
39	TC280328	TC280328	2.30
40	zgc:92287	NM_001002606	2.28
41	zgc:66214	BC055550 (eftud2)	2.27
42	hsp90b	ENSDART00000023550	2.24

43	slc31a1	NM_205717	2.22
44	mmp9	NM_213123	2.21
45	BM316955	BM316955	2.19
46	rdh1	NM_198069	2.17
47	upb1	NM_199616	2.17
48	zgc:101832	NM_001007383	2.14
49	CN019163	CN019163	2.14
50	zgc:85882	NM_212942	2.13
51	slc31a1	NM_205717	2.12
52	zgc:92267	NM_001008578	2.11
53	hsp90b	ENSDART00000018715	2.11
54	snrpd1	NM_173252	2.11
55	hccs	NM_201451	2.09
56	CK027840	CK027840	2.08
57	slc31a1	NM_205717	2.07
58	ENSDART00000047336	ENSDART00000047336	2.07
59	CO354313	CO354313	2.06
60	zgc:92753	NM_001002568	2.06
61	fhit	NM_200740	2.04
62	TC292008	TC292008	2.03
63	zgc:77806	NM_205691	2.03
64	TC298316	TC298316	2.03
65	mmp9	NM_213123	2.02
66	ENSDART00000046923	ENSDART00000046923	2.02
67	ENSDART00000027366	ENSDART00000027366	2.01
68	ENSDART00000041243	ENSDART00000041243	1.99
69	zgc:91878	NM_001003464	1.99
70	igf2	NM_131433	1.98
71	zgc:56585	BC066622	1.98
72	zgc:77538	NM_212897 (clic5)	1.98

Fold change: *gdf6a* MO/WT

Appendix C

List of all genes down-regulated by at least 2-fold in *gdf6a* mutant eyes, identified by microarray analysis at 2 dpf.

Rank	Gene Name	Systematic Name	Avg ratio
1	tbx4	NM_130914	16.66
2	LOC100004247	ENSDART00000100857	6.49
3	DN857529	DN857529	5.52
4	LOC557409	NM_001098246	5.00
5	DN860828	DN860828	4.58
6	ENSDART00000084735	ENSDART00000084735	4.31
7	LOC564004	XM_687364	4.03
8	rx1	NM_131225	3.72
9	BM154215	BM154215	3.55
10	ENSDART00000091472	ENSDART00000091472	3.41
11	ENSDART00000063704	ENSDART00000063704	3.40
12	acox3	NM_213147	3.37
13	CO357677	CO357677	3.37
14	LOC556554	ENSDART00000079363	3.37
15	ndrg1l	NM_200692	3.34
16	EE210955	EE210955	3.33
17	LOC561911	XM_685313	3.28
18	ENSDART00000088360	ENSDART00000088360	3.23
19	zgc:92109	NM_001007294	3.17
20	zgc:56565	NM_200298	3.15
21	LOC795575	ENSDART00000091013	3.01
22	zgc:113449	NM_001014334	2.96
23	LOC569583	EH998613	2.95
24	fpgs	ENSDART00000065858	2.93
25	TC333563	TC333563	2.93
26	TC358048	TC358048	2.90
27	TC351716	TC351716	2.82
28	atoh7	NM_131632	2.77
29	lim2.5	NM_001013522	2.73
30	si:ch211-108c6.2	NM_001030130	2.72
31	zgc:101716	NM_001007425	2.70
32	wnt2	NM_130950	2.70
33	LOC553217	ENSDART00000081918	2.70
34	ENSDART00000018235	ENSDART00000018235	2.68
35	CV110355	CV110355	2.67
36	LOC568846	XM_692202	2.67
37	mcm3	NM_212567	2.66
38	DY570760	DY570760	2.64
39	CT699980	CT699980	2.63
40	zgc:165605	NM_001098768	2.63
41	AL914638	AL914638	2.61
42	zgc:56565	NM_200298	2.61

43	zgc:103489	NM_001008609	2.55
44	zgc:85969	NM_212914	2.53
45	zgc:63690	NM_200483	2.52
46	LOC100000579	CT607160	2.51
47	zgc:112374	NM_001024417	2.51
48	TC328254	TC328254	2.48
49	TC356269	TC356269	2.47
50	LOC563353	NM_001045014	2.47
51	LOC796900	XM_001337271	2.46
52	pdc2	NM_001025464	2.46
53	TC342677	TC342677	2.46
54	ENSDART00000051756	ENSDART00000051756	2.44
55	EH497033	EH497033	2.44
56	LOC797503	BC154566	2.44
57	egln3	NM_213310	2.43
58	ENSDART00000064985	ENSDART00000064985	2.43
59	LOC100000459	XM_001340626	2.42
60	LOC795055	NM_001103195	2.40
61	LOC795275	ENSDART00000059498	2.39
62	zgc:162164	NM_001089535	2.39
63	zgc:103750	NM_001008633	2.38
64	atoh7	NM_131632	2.37
65	LOC566148	XM_689421	2.37
66	ENSDART00000062780	ENSDART00000062780	2.36
67	TC309312	TC309312	2.35
68	TC328955	TC328955	2.34
69	zgc:92621	NM_001002701	2.33
70	zgc:136604	NM_001031674	2.32
71	TC327847	TC327847	2.32
72	ENSDART00000059609	ENSDART00000059609	2.32
73	klf7l	NM_001044766	2.31
74	vox	NM_131698	2.31
75	TC332046	TC332046	2.31
76	TC341305	TC341305	2.31
77	zgc:92715	NM_001002590	2.31
78	arl3l2	NM_200719	2.30
79	oprd1b	NM_212755	2.30
80	ENSDART00000073684	ENSDART00000073684	2.29
81	AL920897	AL920897	2.28
82	LOC100007704	XM_001344060	2.26
83	pah	NM_200551	2.26
84	TC349575	TC349575	2.24
85	LOC563030	ENSDART00000084069	2.24
86	foxn4	NM_131099	2.24
87	BC152295	BC152295	2.24
88	zgc:63663	NM_200614	2.24
89	crygm2b	NM_001020783	2.23
90	TC341659	TC341659	2.22
91	zgc:153398	NM_001045353	2.22

92	ENSDART00000066213	ENSDART00000066213	2.22
93	EH552369	EH552369	2.22
94	CN175259	CN175259	2.21
95	E1A_r60_a135	E1A_r60_a135	2.21
96	six7	NM_131354	2.21
97	zgc:162699	NM_001089562	2.21
98	foxi1	NM_181735	2.20
99	LOC569550	NM_001045185	2.20
100	ctgf	NM_001015041	2.20
101	lama1	NM_001034986	2.19
102	TC352609	TC352609	2.18
103	ahrra	NM_001035265	2.18
104	ENSDART00000104442	ENSDART00000104442	2.17
105	foxn4	NM_131099	2.17
106	elmod2	BC083488	2.17
107	TC362708	TC362708	2.16
108	ucp4	NM_199523	2.15
109	zgc:66268	NM_200512	2.15
110	zgc:101102	NM_001002735	2.15
111	LOC570516	ENSDART00000101569	2.15
112	LOC569604	ENSDART00000065956	2.14
113	EB985774	EB985774	2.14
114	LOC567619	XM_690920	2.13
115	AW232027	AW232027	2.13
116	LOC100008034	XM_001346314	2.12
117	CT646656	CT646656	2.12
118	crygM2a	NM_001018121	2.12
119	MGC172241	NM_001110106	2.12
120	TC330158	TC330158	2.12
121	mybpc1	NM_001007322	2.11
122	LOC796123	XM_001336392	2.11
123	LOC556383	ENSDART00000086195	2.11
124	ENSDART00000098540	ENSDART00000098540	2.11
125	LOC567236	XM_690528	2.10
126	wu:fi33f01	DR714691	2.10
127	foxn4	NM_131099	2.09
128	si:ch211-181p13.2	BI883225	2.08
129	LOC571493	ENSDART00000086094	2.07
130	TC360106	TC360106	2.07
131	mcfd2	NM_001005939	2.07
132	TC345451	TC345451	2.07
133	CT584599	CT584599	2.06
134	LOC561004	XM_684402	2.06
135	BC097065	BC097065	2.06
136	zgc:76877	NM_207083	2.06
137	bag2	NM_201000	2.05
138	tbx2a	NM_001102384	2.04
139	ck2a1	NM_131252	2.04
140	TC353105	TC353105	2.04

141	e2f4	NM_213432	2.03
142	CA588064	CA588064	2.03
143	cxcr4b	NM_131834	2.03
144	EH513933	EH513933	2.03
145	dnase1l3l	NM_001002403	2.02
146	zgc:110620	NM_001013546	2.02
147	clic5	NM_212897	2.02
148	LOC555947	NM_001098244	2.01
149	rbm24	NM_212865	2.00
150	LOC567535	ENSDART00000098441	2.00
151	csf1r	NM_131672	2.00
152	EH524434	EH524434	2.00
153	LOC553527	BC093317	2.00
154	zgc:109932	NM_001020530	1.99
155	TC328117	TC328117	1.99
156	LOC100000603	ENSDART00000052235	1.99
157	zgc:152691	NM_001076737	1.99
158	zgc:101113	NM_001003560	1.99
159	zgc:110021	NM_001024427	1.99
160	LOC568707	NM_001045488	1.98
161	TC362086	TC362086	1.98
162	TC341928	TC341928	1.98
163	CO933078	CO933078	1.97
164	TC334280	TC334280	1.97
165	zgc:162210	NM_001089456	1.96
166	TC320185	TC320185	1.96
167	LOC100000853	ENSDART00000075730	1.96
168	CT721957	CT721957	1.96
169	CF550486	CF550486	1.95

Fold change: WT/*gdf6a* mutant

Appendix D

List of all genes up-regulated in *gdf6a* mutant eyes by at least 2-fold, identified by microarray analysis at 2dpf.

Rank	Gene Name	Systematic Name	Avg Ratio
1	crygs1	NM_001013276	3.97
2	crygs1	ENSDART00000063127	3.47
3	LOC569018	NM_001045174	2.99
4	LOC795519	ENSDART00000098973	2.95
5	LOC795519	XM_001333422	2.83
6	CH73-138E16.2	NM_001100096	2.74
7	nxph1	NM_001002733	2.64
8	egr2a	NM_183341	2.55
9	gdap1	NM_001020675	2.41
10	ENSDART00000038740	ENSDART00000038740	2.41
11	zgc:113405	ENSDART00000076979	2.40
12	drgx	NM_001037105	2.39
13	ENSDART00000092783	ENSDART00000092783	2.38
14	ism1	NM_001012376	2.35
15	LOC794362	NM_001111214	2.32
16	zgc:153082	NM_001080002	2.29
17	BI865717	BI865717	2.25
18	LOC565454	XM_688733	2.24
19	LOC100002258	ENSDART00000101488	2.17
20	LOC557900	ENSDART00000086058	2.14
21	gnb3l	NM_001002437	2.14
22	TC316711	TC316711	2.12
23	si:ch211-147d7.6	NM_001025522	2.11
24	hmox1	NM_199678	2.10
25	ctsk	NM_001017778	2.10
26	pla1a	NM_207056	2.08
27	TC343896	TC343896	2.08
28	znf703	NM_131822	2.08
29	cth	NM_212604	2.07
30	zgc:114158	NM_001025185	2.05
31	LOC100003999	XM_001343386	2.05
32	tdh	NM_213245	2.04
33	ENSDART00000062738	ENSDART00000062738	2.04
34	mylz2	NM_131188	2.03
35	si:dkey-240a12.3	NM_001082923	2.03
36	hmox1	NM_199678	2.03
37	CT667687	CT667687	2.02
38	LOC100000596	XM_001340721	2.02
39	zgc:77752	NM_200888	2.02

40	LOC569467	EE310093	2.02
41	oaz2	NM_194432	2.01
42	ENSDART00000089035	ENSDART00000089035	2.01
43	LOC566849	XM_690136	2.01
44	ENSDART00000026492	ENSDART00000026492	2.01
45	ENSDART00000075926	ENSDART00000075926	2.00
46	TC363371	TC363371	1.99
47	pvalb6	NM_205573	1.97
48	foxi2	NM_198916	1.97
49	sox21b	NM_001009888	1.97
50	aldh1a3	NM_001044745	1.96
51	TC331551	TC331551	1.95
52	zgc:153767	NM_001080022	1.95

Fold change: *gdf6a* mutant/WT

Appendix E

For functional analysis of mutations in GDF6 patients, two approaches were taken. First, mutant sequences (A249E and K424R, 19129173), and wildtype *GDF6* mRNA were injected into zebrafish at the one cell stage for subsequent phenotypic analysis at 24 hpf. Capped, Poly-adenylated mRNA was synthesized using mMachine kit (Ambion). Injection of zebrafish *gdf6a* RNA is known to cause severely ventralized phenotypes (Goutel et al., 2000). We found that injection of human wildtype *GDF6* mRNA produced the same ventralized phenotypes, which range from embryos displaying smaller heads and enlarged tails, to a complete lack of head formation (Hammerschmidt et al., 1996). 2 pg of *GDF6* RNA was sufficient to induce ventralized phenotypes in approximately 50% of the embryos.

For cell culture reporter assays, PLM cells were harvested from embryonic age (E) 11.5 CD-1 mouse embryos as previously described (Hoffman et al., 2006; Weston et al., 2002). Transfections were carried out with Effectene (Qiagen, Mississauga, ON, CAN) according to the manufacturer's instructions in 384-well plates. Briefly, DNA-transfection mixtures were aliquoted into wells followed by the addition of approximately 100,000 PLM cells, and wells were topped-up to a total volume of 100 µl. Media was replenished 24 h post-transfection, and lysates were collected 48 h post-transfection. Luciferase activity was measured using the Dual Luciferase Kit (Promega, Madison, WI, USA) and

firefly luciferase was normalized to an internal Renilla luciferase control. Luciferase assays were performed in quadruplicate and repeated three times.

Analysis in zebrafish reveals a small, but significant reduction in the proportion of embryos showing ventralized phenotypes (Figure 1), when injected with either mutant mRNA (44.8% n=76, for K424R, 47.1%, n=52 for A294E), when compared to embryos injected with wildytpe GDF6 mRNA (54.5% n=55) $p<0.05$, X^2 analysis). All analysis were repeated in triplicate.

Similarly, a small but consistent reduction in GDF6 activity was observed in for both mutations in our cell culture luciferase Performed in the lab of T. Michael Underhill (Figure 2). Expression of wild-type GDF6 led to 3.4-fold increased reporter activity. In contrast, expression of GDF6–A249E and GDF6–K424R constructs resulted in 2.9-fold and 2.4-fold increases in reporter gene activity ($P < 0.034$ and $P < 0.002$; t-test) These data indicate that both K424R and A294E mutations are hypomorphic and may be causative in producing oculo-skeletal phenotypes in patients.

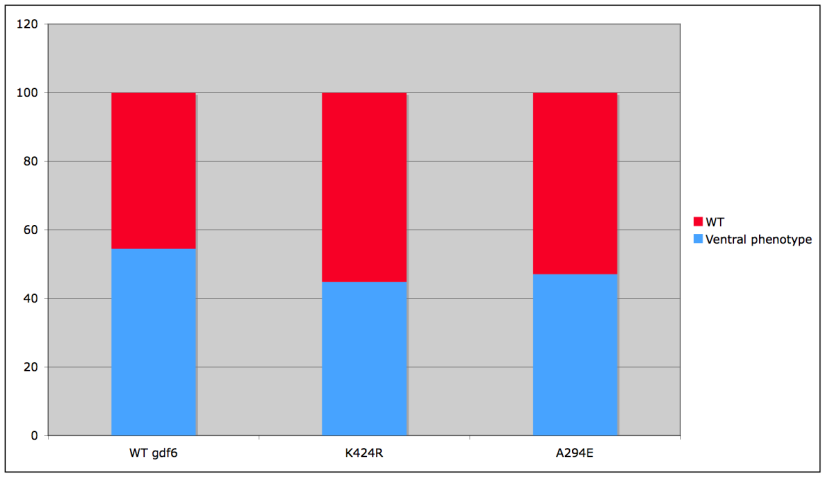

Figure 1: Analysis of phenotypes of zebrafish injected with human mutant *GDF6* mRNA (WT, K424R and A294E). Injection of wildtype *GDF6* mRNA induced ventralized phenotypes in 54.5% of embryos, while injection of 2 pg of K424R mRNA resulted in 44.8% of embryos displaying a ventralized phenotype. Injection of 2 pg of A294E mRNA resulted in 47.1% of embryos displaying a ventralized phenotype.

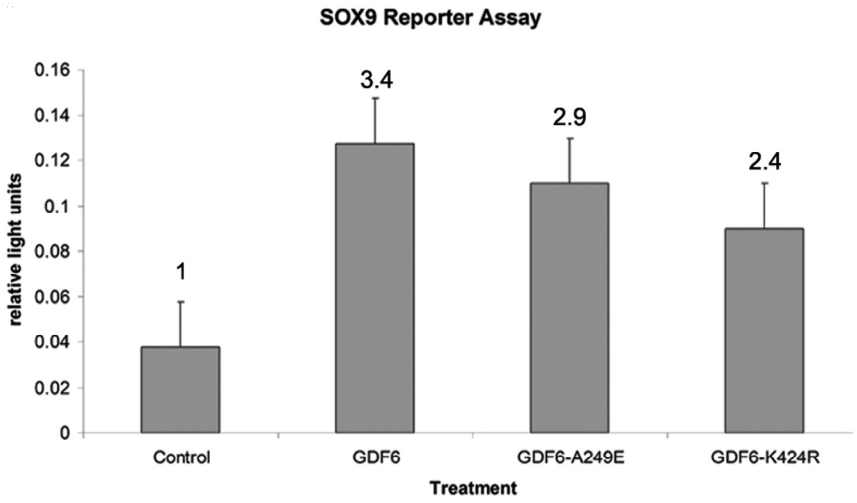

Figure 2: Functional analyses of GDF6 mutants in cell culture. (A) Significant differences in activity of A249E and K424R-containing mutants in the SOX9-reporter luciferase assay were observed, compared with wildtype. Reporter gene activity expressed in relative light units, normalized to the control; the percentage reduction compared with wild-type are: A249E = 14% (0.1098), K424R = 30% (0.0897); wild-type = 0.1273]. Figure and legend from (Asai-Coakwell et al., 2009).

Bibliography

Asai-Coakwell, M., et al., 2009. Incomplete penetrance and phenotypic variability characterize Gdf6-attributable oculo-skeletal phenotypes. Hum Mol Genet. 18**,** 1110-21.

Goutel, C., et al., 2000. The ventralizing activity of Radar, a maternally expressed bone morphogenetic protein, reveals complex bone morphogenetic protein interactions controlling dorso-ventral patterning in zebrafish. Mech Dev. 99**,** 15-27.

Hammerschmidt, M., et al., 1996. dino and mercedes, two genes regulating dorsal development in the zebrafish embryo. Development. 123**,** 95-102.

Hoffman, L. M., et al., 2006. BMP action in skeletogenesis involves attenuation of retinoid signaling. J Cell Biol. 174**,** 101-13.

Weston, A. D., et al., 2002. Requirement for RAR-mediated gene repression in skeletal progenitor differentiation. J Cell Biol. 158**,** 39-51.